REPORT OF APOLLO 13 REVIEW BOARD

APPENDIX F - SPECIAL TESTS AND ANALYSES

APPENDIX G - BOARD ADMINISTRATIVE PROCEDURES

APPENDIX H - BOARD RELEASES AND PRESS STATEMENTS

NATIONAL AERONAUTICS AND SPACE ADMINISTRATION

APPENDIX F

SPECIAL TESTS AND ANALYSES

CONTENTS

This page left blank intentionally.

PART F1

INTRODUCTION

An integral part of the Apollo 13 Review Board's effort included an extensive test and analysis program to evaluate in detail postulated modes of failure. The majority of these tests and analyses were conducted at the Manned Spacecraft Center (MSC) and five other NASA centers--Langley Research Center (LRC), Ames Research Center (ARC), Lewis Research Center (LeRC), Marshall Space Flight Center (MSFC), and Kennedy Space Center (KSC). Some tests at White Sands Test Facility (WSTF), North American Rockwell, Beech Aircraft, Parker Aircraft, and Boeing were also conducted. The results of this intensive test and analysis program formed, to a large extent, the basis for the development of many of the Board's findings, determinations, and recommendations.

During the review, the requests for tests and analyses were channeled through the MSC Apollo Program Office, which maintained a master file. The selection of individual tests and analyses was made after a preliminary study by Review Board specialists. In each case the request was approved by the Board Chairman or a specially designated Board monitor. In many instances the preparation and execution of tests were observed by Apollo 13 Review Board representatives.

Nearly a hundred separate tests and analyses have been conducted. The level of effort expended on this test and analysis program included a total of several hundred people over a period of about 6 weeks.

The first portion of this Appendix is a summary of those tests and analyses which most precisely support the sequence of events during this accident. This is followed by a more detailed description of these tests and analyses. This Appendix concludes with a test and analyses master list and a fault tree analysis.

It should be noted that an attempt has been made to include all tests that have been carried out in support of this review in the master list. As a result, the list includes a number of early tests which were exploratory, and in some cases inconclusive, and may not appear to lend substantive information. For each effort, there is summary information which includes identification, a statement of the objective, and a brief statement of results. More complete data on studies and tests can be found in the official files of the Apollo 13 Review Board.

This page left blank intentionally.

PART F2

SUMMARY OF TESTS AND ANALYSES

To assist the reader, a summary of the most significant tests and analyses is included in this part. The summary consists of a series of concise statements which are based on the results from one or more test or analysis. The summaries are presented in chronological order of the events as they occurred in the spacecraft.

DETANKING AT KENNEDY SPACE CENTER

A test simulating the conditions of the special detanking operations during the countdown demonstration test (CDDT) revealed that the thermal switches were overloaded and failed in the "closed" position. The failure of the thermostats caused very high temperatures (700° to 1000° F) inside the heater tubes. Damage to the wire insultation resulted from this overheating. Subsequent tests showed that under the conditions existing in the tank, the wire insulation would seriously degrade at temperatures between 700° F and 1000° F, thus exposing bare wire.

QUANTITY GAGE DROPOUT

Tests to determine the signal characteristics of the quantity probe under various fault conditions showed that a short between the concentric tubes would cause an off-scale high reading which would then go to zero when the short is removed, remain there for about 1/2 second, and then return to the correct indication in about 1-1/2 seconds. These are the characteristics that were observed in flight. It is not established that the failure of the quantity gage was related to the combustion that occurred in the oxygen tank no. 2.

IGNITION AND COMBUSTION PROPAGATION

The energy required to achieve the pressure rise from 887 psia to 1008 psia observed in oxygen tank no. 2 (10 to 130 Btu) can be supplied by the combustion of the Teflon wire insulation in the tank and conduit (260 Btu). Tests have also indicated that other Teflon elements and certain aluminum components inside the tank may also be ignited and thus contribute to the available energy.

Experiments show that the Teflon insulation on the actual wires in oxygen tank no. 2 can be ignited by an energy pulse which is less than the energy estimated to be available from the observed flight data.

Test of fuses in the motor power leads showed that sufficient energy to ignite Teflon insulation could be drawn through the fuses before they would blow.

The flame propagation rate experiments in supercritical oxygen indicate a rather slow burning rate along Teflon wire insulation (about 0.25 in/sec downward in one-g). Propagation rates as low as 0.12 in/sec were measured under zero-g conditions. These measurements are consistent with the slow rate of pressure rise observed in the spacecraft.

Under one-g conditions, Teflon wire insulation flames will propagate along the wire through apertures fitted with Teflon grommets.

TANK FAILURE

Several combustion tests confirmed that burning of Teflon and possibly aluminum could reach high enough temperatures to cause either the tank or the conduits into the tank to fail. Oxygen pressure was very likely lost due to the failure of the conduit.

A test in one-g in which the actual bundled Teflon insulated wire was ignited within the conduit leading from an oxygen tank and filled with supercritical oxygen resulted in bursting the heat-weakened conduit wall.

A test which contained an upper portion of the quantity probe and conduit showed that ignition of the motor lead bundle in supercritical oxygen results in flame propagation through the quantity probe insulator and into the conduit. Posttest examination showed an approximately 2-inch diameter hole had been burned out of a 3/8-inch thick stainless steel simulated tank closure plate.

PANEL LOSS

Tests with 1/2-scale honeycomb panel models in vacuum produced complete panel separation with a rapid band loaded pressure pulse in the oxygen tank shelf space. Peak pressures in the simulated tunnel volume with scaled venting were considerably lower (about 1/5) than that of the oxygen tank shelf space. These tests are consistent with the information obtained from the photographs of the service module taken by the Apollo 13 crew.

PART F3

SELECTED TESTS AND ANALYSES

This page left blank intentionally.

PART F3.1

THERMAL SWITCH TESTS

Objective

Determine the behavior of the thermostatic switches in the oxygen tank no. 2 under the conditions experienced during the abnormal detanking experienced at KSC. During the KSC tests, heater currents of 6.5 amperes at 65 V dc were used.

Approach and Results

Subsequent to discovering that the heater thermostatic switches most likely fused in the closed position during the KSC detanking procedures, tests were conducted to determine the power handling capabilities of these switches.

Batteries were used as a power source to test the switches. They were initially supplied with 31 V dc at currents up to 3.5 amperes. No contact degradation was observed under these conditions. When the voltage was raised to 65 V dc, some increase in contact resistance (up to about 3 ohms from a few milliohms) was noted at 1.25 amperes, although the switch continued to operate. The current was then increased to 1.5 amperes at 65 V dc; and when the switch attempted to open, it fused closed. The body of the switch was removed and the condition of the contact can be seen in figure F3.1-1.

Conclusions

Thermostatic switches similar to those in oxygen tank no. 2 will fuse closed when they attempt to open with a 65 V dc potential and currents in excess of 1.5 ampere.

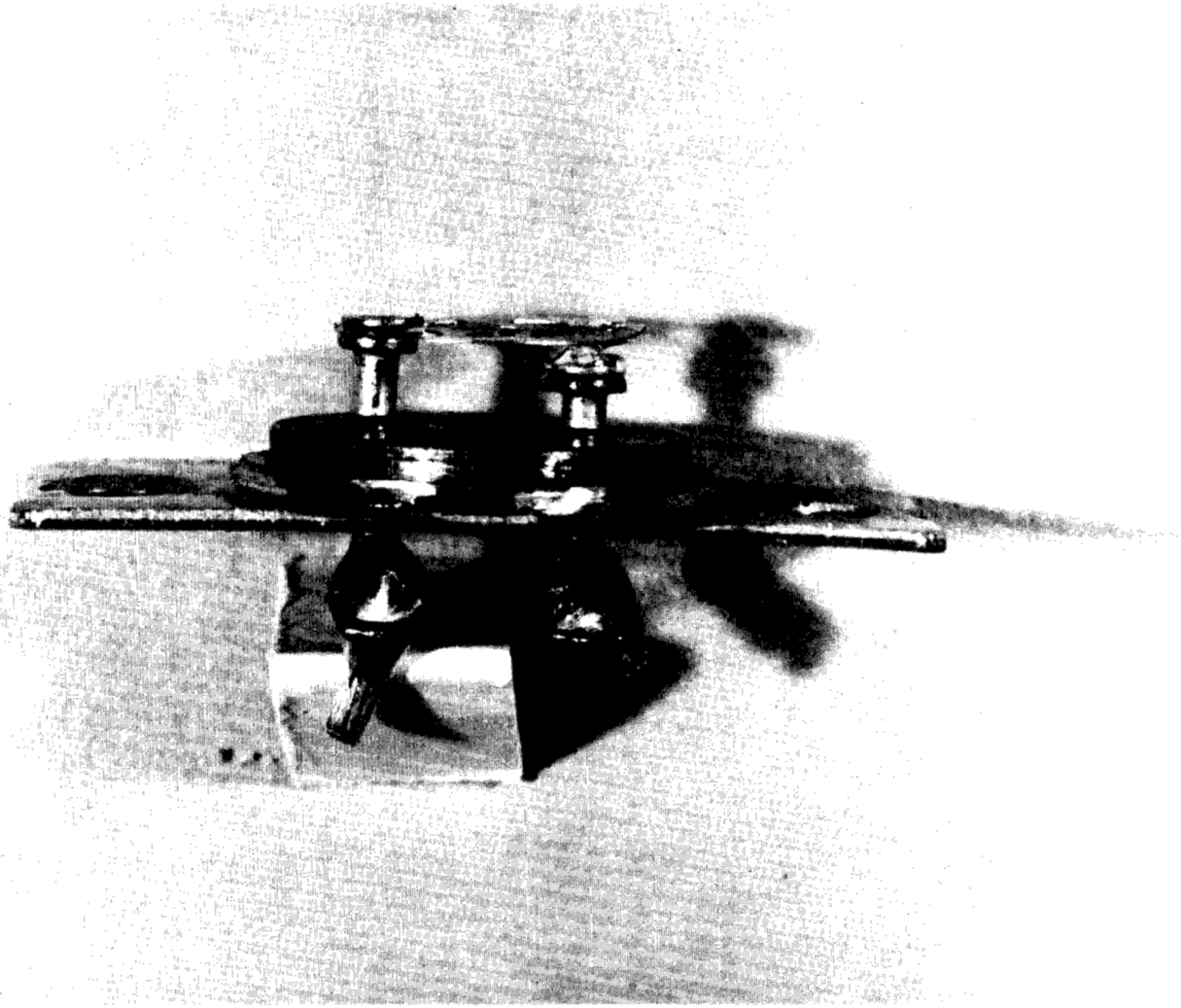

Figure F3.1-1.- Fused thermal switch control.

PART F3.2

TEFLON INSULATION DAMAGE DUE TO OVERHEATING

Objective

These tests were conducted to determine the damage that could have been done to the Teflon wire insulation during the abnormal detanking operation at Cape Kennedy.

Approach and Results

The likelihood that the equipment inside the oxygen tank was subjected to high temperatures for several hours prompted tests to reveal any changes in the thermochemistry of the remaining material. Four samples were treated in a heated oxygen flow system. The flow rate was 259 cc/sec. These samples were compared with an unbaked control sample. A typical sample of wire is shown in figure F3.2-1. The mass-loss results are given in table F3.2-I.

The relative values of heats of reaction in subsequent DTA tests in oxygen show that the degraded material is slightly more energetic per unit mass than the virgin material when oxidized.

Conclusions

The tests reveal that severe damage could have resulted to the wire insulation during the abnormal detanking procedure. In several places along the leads, bare wire was exposed which could have led to the short circuits that initiated the accident.

Figure F3.2-1.- Damaged Teflon insulation.

TABLE F3.2-I.- INSULATION DEGRADATION TESTS

Sample	Baking		
	Temperature, °F	Time, hr	Weight loss, percent insulation
1	77		0
2	572	2.75	+0.15
3	752	1.0	-0.08
4	860	0.5	-34.
5	932	0.5	-102.

PART F3.3

THERMODYNAMICS AND COMBUSTION ANALYSIS OF OXYGEN TANK PROCESSES

Since there is strong evidence that the failure centered around an abnormal energy addition to oxygen tank no. 2, it seems appropriate to include a special discussion of the analysis of the thermodynamics and combustion processes that may have occurred in this tank. Consideration is given here to (1) the energy required to account for the measured pressure rise, (2) the energy available in potentially combustible materials in the tank, and (3) potential ignition energy.

Energy Required to Account for Measured Pressure Rise

The measured abnormal pressure rise in oxygen tank no. 2 is presented in figure B5-3 of Appendix B. Calculations can be made for two limiting thermodynamic processes to account for this pressure rise. One process assumes that the pressure rise results from an isentropic compression of the supercritical oxygen by an expanding "bubble" of combustion products. This corresponds to the minimum amount of energy required to achieve the measured pressure rise. Another limiting process assumes that the energy addition is accompanied by complete mixing which results in homogeneous fluid properties.

Figure F3.3-1 is a pressure-enthalpy diagram for oxygen whereon point "A" is the thermodynamic state just prior to the abnormal energy addition, approximately -190° F and 887 psia. The path of the isentropic compression (minimum energy) from this state to the maximum pressure measured of 1008 psia is represented by line AB. Thermodynamic properties of oxygen presented by Weber (ref. 1) and Steward (ref. 2) were used to compute the increase in the internal energy of the oxygen. This internal energy increase of the oxygen (242 lb_m) amounts to about 10 Btu. The temperature increase associated with this process is about 1.8° F.

Figure F3.3-1 also shows the constant density path along line AC from 887 psia to 1008 psia. This process could be achieved by complete mixing of the tank contents. The internal energy increase for this case (maximum energy) is about 130 Btu. The temperature increase for this process is 2.6° F. It should be noted that this energy addition is to the oxygen in the tank. It does not include energy that might be added to other tank components such as metal parts.

The measured temperature rise of 38° F (indicated by figure B5-3 in Appendix B) during the pressure rise to 1008 psia cannot be explained by

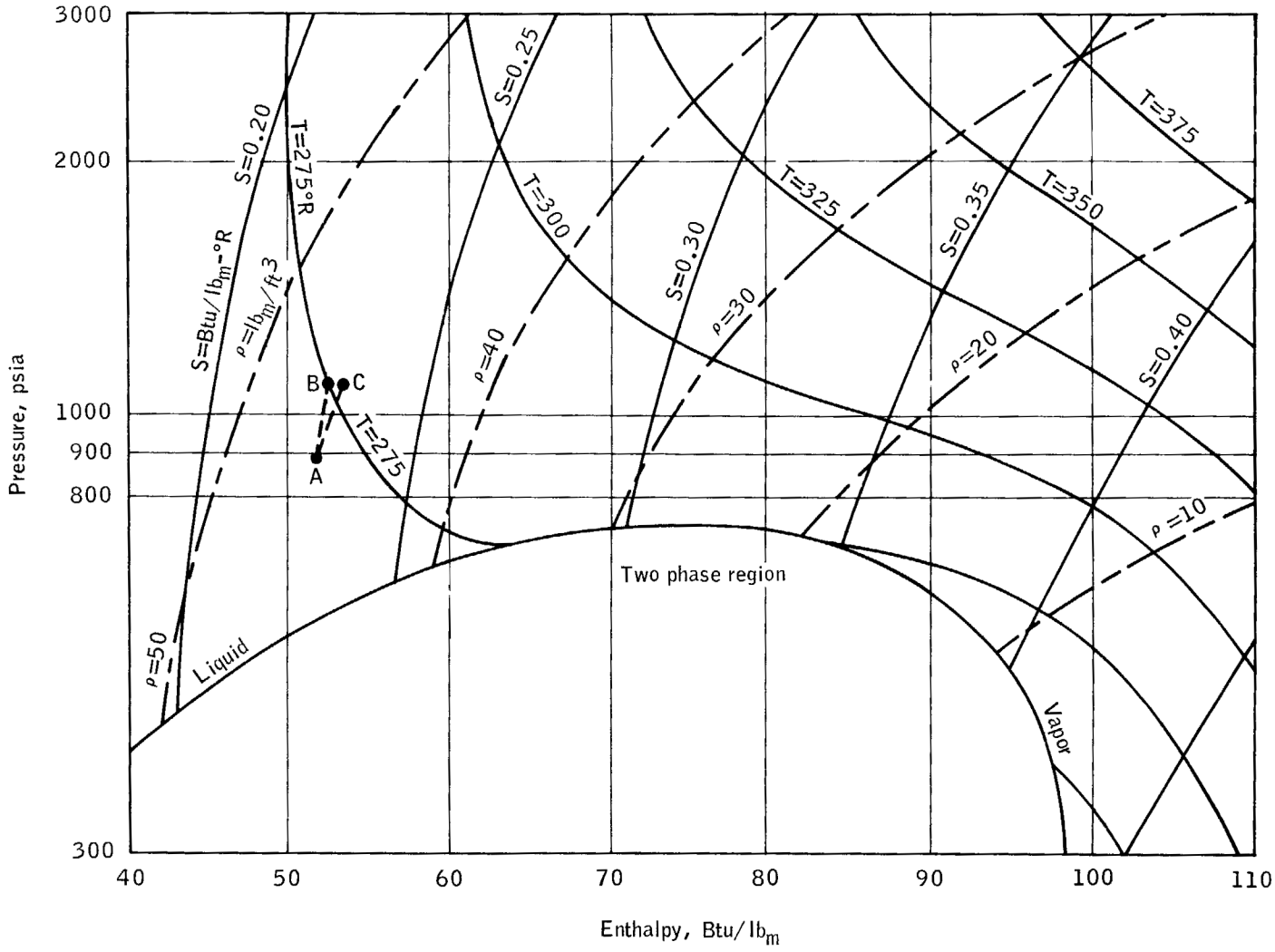

Figure F3.3-1.- Thermodynamic processes on pressure-enthalpy diagram.

either of the above-mentioned thermodynamic processes because they give a rise of only 1.8° and 2.6° F. As figure B5-3 shows, the measured temperature rise lagged the pressure rise. Both this lag and the magnitude of the temperature rise can be explained by the passage of a combustion front near the temperature sensor.

Energy Available in the Potentially Combustible Materials in the Tank

Many materials can of course react with oxygen if an ignition source is provided. Here only Teflon is considered in any detail while aluminum is mentioned briefly.

Teflon (polytetrafluoroethylene) can react with oxygen to form largely a mixture of carbonyl-fluoride, carbon tetrafluoride, carbon dioxide, and other species in small quantity, such as fluorine, depending on the stoichometry and flame temperature. The overall chemical reactions which produce these combustion products include:

$$\frac{1}{n}(C_2F_4)_n + O_2 \rightarrow 2\ COF_2\ ;\quad \Delta H_c = -1910\ \text{Btu/lb}_m\ \text{Teflon}$$

$$\frac{1}{n}(C_2F_4)_n + O_2 \rightarrow CO_2 + CF_4\ ;\quad \Delta H_c = -2130\ \text{Btu/lb}_m\ \text{Teflon}$$

where the heat of combustion for these reactions is also given. For the purpose of this discussion, the heat of combustion of Teflon is taken to be -2000 Btu/lb_m Teflon. The internal energy of combustion ΔE_c is about 99 percent of ΔH_c. The amount of Teflon wire insulation in the system is about 0.13 lb_m, so that the energy available from combustion of Teflon wire insulation alone is about 260 Btu. This amount of energy is therefore more than sufficient to account for the measured pressure rise from 887 to 1008 psia.

If aluminum combustion occurs, or other tank components, the quantity of energy available is many times greater than the energy released by Teflon combustion. Experiments show that once ignited, aluminum burns readily with supercritical oxygen.

Potential Ignition Energy

Several experiments have shown that Teflon insulated wire can be ignited under the conditions that existed in the tank. A series of tests

has shown that the energy required to ignite Teflon in supercritical oxygen is 8 joules or less. It was also determined that ignition was geometry dependant and in one favorable configuration combustion was the fault initiated with an estimated energy as low as 0.45 joule. In any case, the value of 8 joules is less than energy deduced from the telemetry data, as will be shown below.

The fan motors were turned on just before the event occurred. There are clear indications of short circuiting in the fan motor circuitry immediately prior to the observed pressure rise. For the moment, we will consider ignition mechanisms by electrical arcing originating in the fan circuits as being the most probable cause of the fire.

An analysis has been made of the telemetry data that permits an estimate of the total energy that could have been dissipated in a postulated short circuit which ignited the Teflon. A summary of the analysis is presented here.

The following telemetry data were used in the analysis:

1. SCS thrust vector control commands. One hundred samples per second at 10-millisecond intervals. This channel provides, in effect, a time differentiated and filtered indication of phase C of ac bus no. 2 voltage.

2. Bus no. 2 ac phase A voltage. Ten samples per second at 100-millisecond intervals.

3. Fuel cell no. 3 dc voltage at 10 samples per second.

4. Total fuel cell current at 10 samples per second.

The 115-volt fan motor circuit is shown in figure D3-5 of Appendix D. The power for the motor comes from an inverter producing three-phase, 400-cycle, 115-volt power. The motors are operated in parallel, each phase to each motor being separately fused with a 1-ampere fuse (there are a total of six fuses in the circuit). The important portions of the telemetry traces are shown in figure F3.3-2. The sequence of events postulated is as follows:

1. Fan turnon occurs at 55:53:20 g.e.t. and the phase A voltage drops from 116.3 to 115.7 volts. This is normal. The telemetry granularity is ±0.3 volt.

2. At 55:53:23, an ac voltage drop from 115.7 to 114.5 volts is observed, coincident with a fuel cell current increase of 11 amperes. This is the first short circuit that occurred after fan turnon. Since the ac voltage rose from 115.7 to 116.0 volts (as indicated by "toggling"

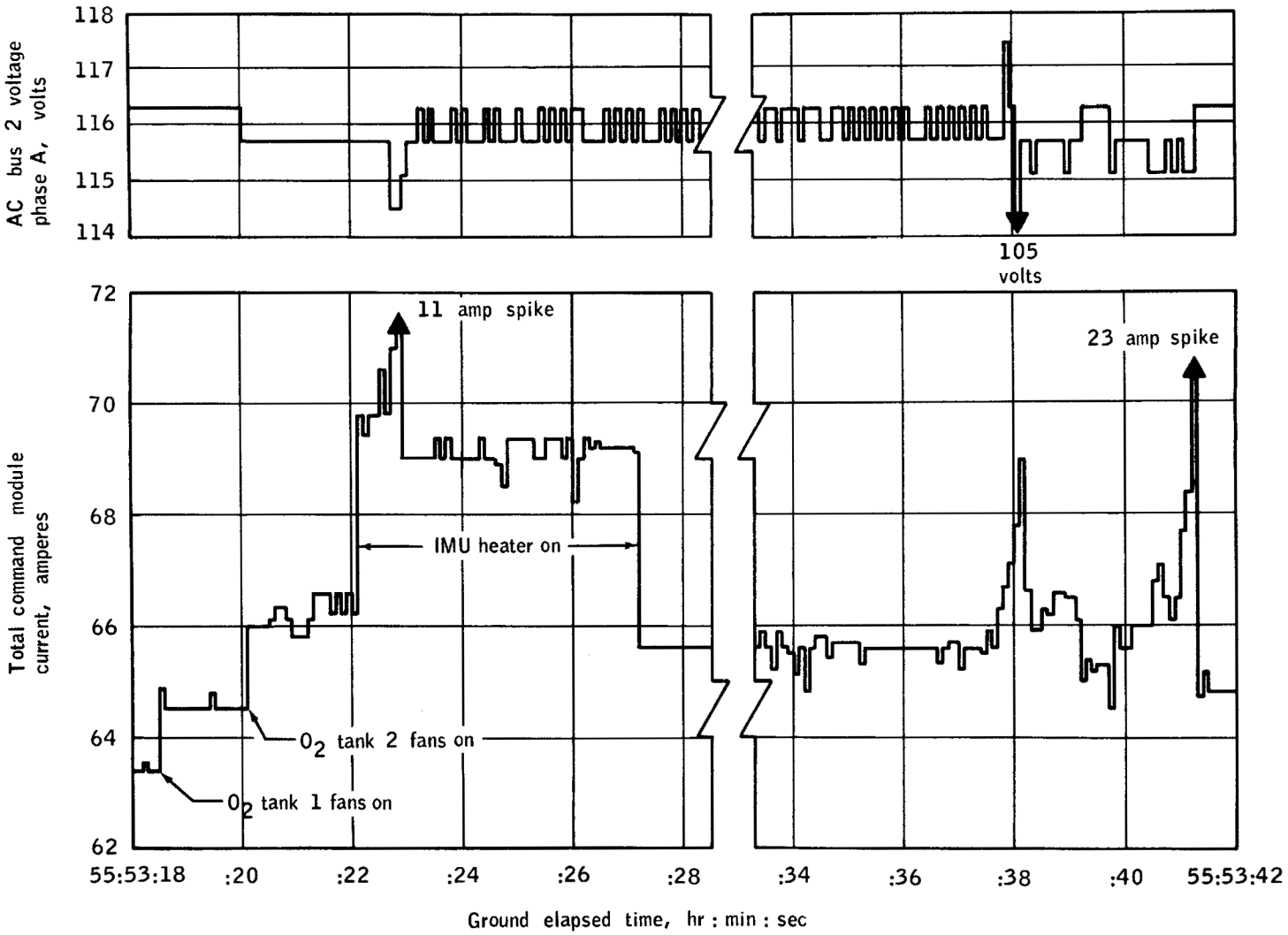

Figure F3.3-2.- Telemetry data for ac bus 2 voltage phase A and total CM current.

between 115.7 and 116.3 volts) after the event, it is probable that the short circuit involved phase A of the motor drive circuit, and all power may have been lost to one of the two fan motors at this time. This hypothesis is further supported by the coincident decrease in fuel cell current of 0.7 ampere, approximately half of the 1.5 amperes drawn by both motors.

3. At 55:53:38 another short circuit occurred, causing an ac voltage rise to 117.5 volts followed by a drop to 105 volts. The voltage rise indicates a short circuit in phase B or C as the regulator tries to bring up the voltage in a nonshorted phase. The 4-ampere dc current spike that occurs concurrently with this ac voltage rise and fall was probably much greater at some time between telemetry samples. The resultant decrease in phase A voltage may indicate an open circuit in one of the other phases of the second motor, causing phase A to draw more than normal current. The pressure in the tank starts to rise at 55:53:36 so that this short probably occurred after some combustion had commenced.

4. A final short circuit occurs at 55:53:41 as indicated by the 22.9-ampere spike on the dc current telemetry. No voltage drop is observed on the ac bus, probably because the short was of such short duration that it was not picked up by the telemetry samples. All the remaining fuses are blown (or the leads open-circuited) by this short circuit since the ac bus voltage and dc current return to the levels observed prior to initial energizing of the fans in oxygen tank no. 2.

The approximate total energy in the short circuit (arcing) can be estimated from the telemetry data. The voltage spikes indicate that the shorts were less than 100 milliseconds (the telemetry sampling interval) in duration. The fact that all the voltage and current "glitches" consisted of essentially one data point (sometimes none) means that the time of the short was very likely 50 milliseconds or less. An independent piece of evidence that bears on the time interval during which the short circuit condition exists comes from the signal on the SCS telemetry. A signal appeared on the SCS telemetry line each time a short circuit occurred on ac bus no. 2. These signals have a data rate 10 times larger than the signals from the ac and dc busses. The initial excursion of each of these SCS signals was 20 to 40 milliseconds long, and was then followed by one or two swings which are due to the SCS circuit filter characteristics. Thus, 30 milliseconds will be taken as an approximate value for the duration of the short circuits.

The current drawn during the short circuit can be estimated from the properties of the fuses used to protect the motor fan circuits. From April 18 to April 20, tests were conducted by MSC personnel to measure failure currents and failure times of the fuses using the same type inverter and fuses that were in the spacecraft. The following are the results of these measurements for a single-phase short circuit (data

taken from a preliminary report of table III of the MSC Apollo 13 Investigation Team):

Volts, ac	Amperes, ac	Duration, milliseconds	Fault energy, joules
107	3.0	120	39
105	4.0	31	13
102	5.0	20	10
95	7.0	10	7
75	9.0	8	5

From these results, the most probable range of ac current in the short circuit that occurred is 3 to 5 amperes. The total energy in the short circuit is therefore between 10 and 16 joules, since it is considered unlikely that the fault persisted for more than 50 milliseconds. Thus, a most probable energy of 13 joules and a most probable ac current of 4 amperes is reasonable for those faults which blew fuses.

These values are applicable to single-phase faults to ground. For two-phase faults, the current in each phase remains the same, while the available ignition energy doubles to 26 joules.

PART F3.4

TEFLON INSULATION IGNITION ENERGY TEST

Objective

To determine the energy required to ignite the Teflon insulation by 115 volt, 60 cycle sparks on flight-qualified wire which had been subjected to the type of heating which could have occurred during the KSC detanking procedure. The spark-generating circuit was fused so that it could deliver no more energy than could have been delivered by the fan motor circuit.

Approach

Sample sections of Teflon-insulated conductors obtained from Beech Aircraft Corporation through MSC were baked in oxygen for 5 hours at 572° F, held overnight at room temperature in oxygen, and baked further for 2 hours at 842° F. The Teflon lost its pliability, cracked, and flaked off as shown in figure F3.4-1.

The test specimen consisted of four strands of degraded-insulation wires, as shown schematically below.

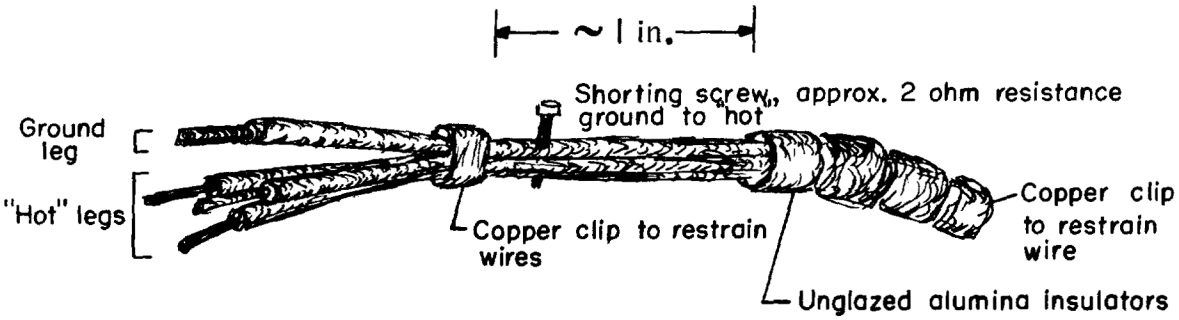

An adjustable short was provided by a number 80 screw driven between the strands of the "ground" wire and then adjusted so that a low-resistance short was established to one of the "hot" legs near some remaining Teflon. A replica of the test harness, made of virgin wire, is also shown in figure F3.4-1. The shorting screw and the standoff loop, installed to hold the screwhead away from the test-chamber walls, are seen in this photograph. The low resistance short was installed in series with a 1-ampere slow-blow fuse. In an independent test series, the current-carrying ability of this fuse was determined by inserting (in series) dummy resistors of various values to replace the shorted

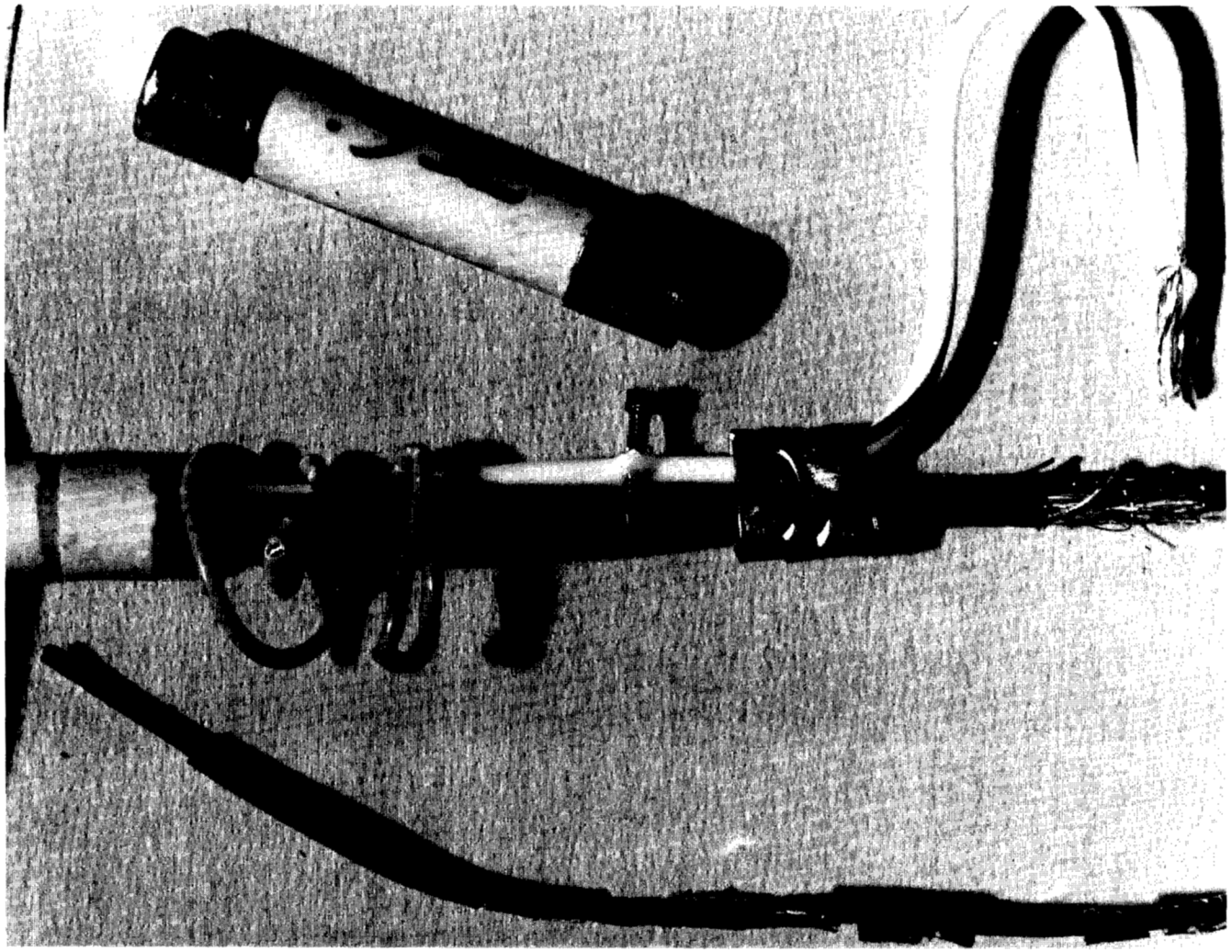

Figure F3.4-1.- Heat degraded wire and test harness replica.

test harness, and a 0.1-ohm resistor across which the voltage drop was measured. Repeated tests showed about 3.5 to 7.5 joules were required to destroy the fuse. Depending on the resistance of the remaining circuit, 10 to 90 percent of the line voltage might appear across the arc. The fault energy of the ignition tests, where the arc resistance is less than 2 ohms, is in the same range (i.e., from 3.5 to 7.5 joules).

The specimen was immersed in liquid oxygen (as before) inside the stainless steel tubing test rig shown in figure F3.4-2. The initial pressure was 920 psi.

Results

The test assembly withstood three firing pulses, 115 volts, 60 cycles, before igniting on the fourth. The 1-ampere fuse was blown each time. The short resistance was measured after each trial and was found to reduce progressively from about 5 ohms to 2 ohms, at which level ignition occurred on the next try. Approximately 1/2 second later the pressure gage showed the start of a 7-1/2 second pressure rise from 920 to 1300 psi. A thermocouple placed about 1 to 2 inches from the ignition point showed a small rise about 1 second after ignition and a large rise about 1/2 second later as the flame swept by. Much of the main conductor wire was consumed; all of the small thermocouple wire was gone. Virtually all of the Teflon was burned--Teflon residue was found only in the upper fitting where the electrical leads are brought into the test chamber. All but one of the alumina insulators vanished.

Conclusion

From the fuse energy tests and these ignition tests, it is clear that from 3.5 to 7.5 joules are adequate to initiate combustion of heat-degraded Teflon insulation. This is essentially the same as is required for unheated wire.

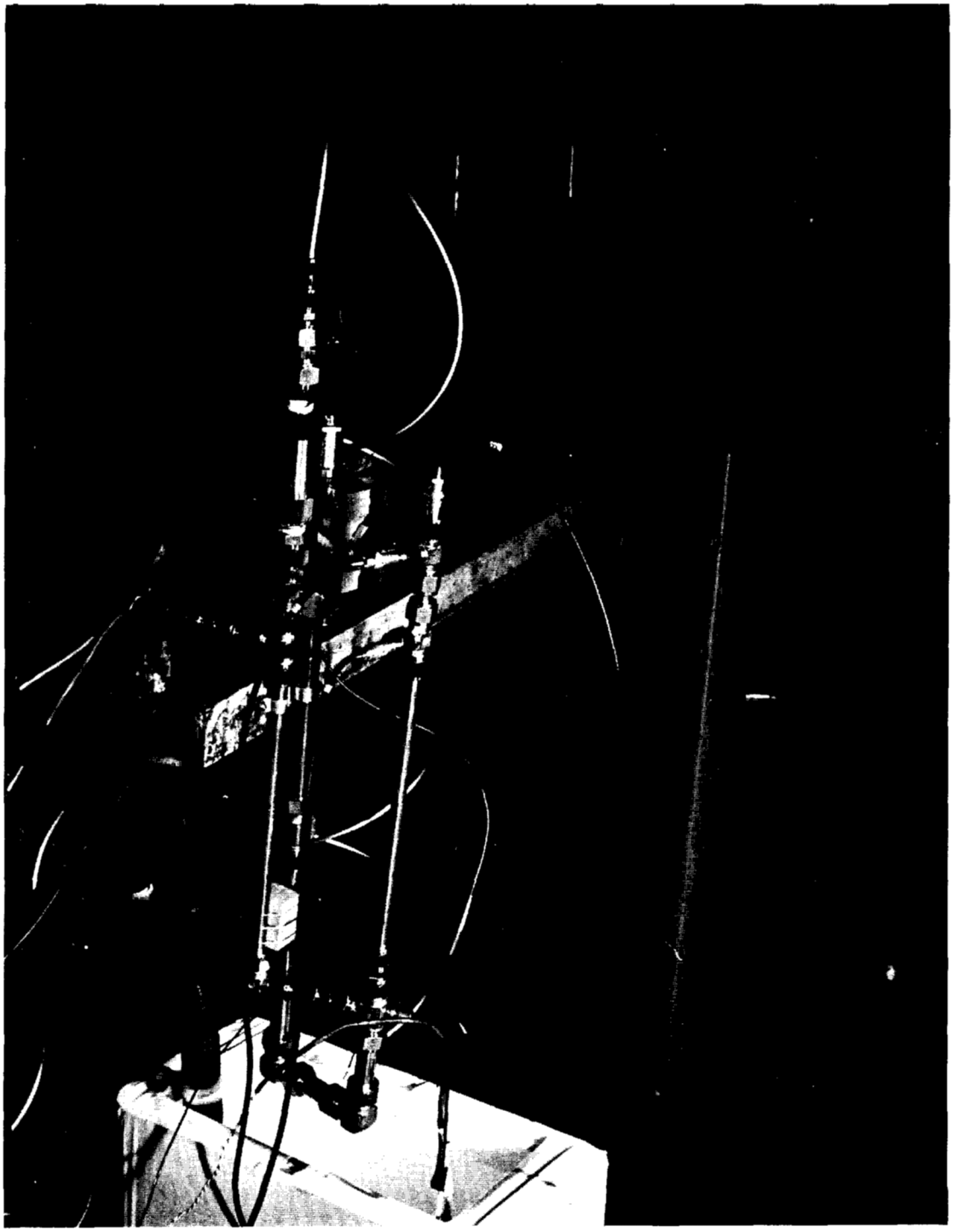

Figure F3.4-2.- Stainless steel test rig.

PART F3.5

IGNITION AND PROPAGATION THROUGH QUANTITY PROBE SLEEVE AND CONDUIT*

Objective

The purpose of this test was to determine if burning wire insulation would propagate through the upper quantity probe insulator. Another objective was to determine the failure mode of the conduit which results from the combustion of the polytetrafluoroethylene insulation.

Experimental

The chamber used for this test consisted of a schedule 80 weld-neck tee equipped with three flanges to provide a viewport, electrical and hard line feedthroughs, and conduit to quantity probe interface. The chamber, which is shown in figure F3.5-1, had a volume of approximately one-third cubic foot. A pressure relief valve was provided to maintain chamber pressure at 1050 psia during test; and, in addition, the chamber contained a rupture disc to prevent chamber failure. Supercritical conditions inside the chamber were obtained by filling with gaseous oxygen to a pressure of 940 psia and cooling externally with liquid nitrogen, using insulating foam covered with thermal blankets. Five thermocouple penetrations were provided through the chamber wall. Chamber pressure was monitored by a pressure transducer. Color motion pictures were taken through the chamber viewport at a speed of 24 frames a second. An additional camera provided external color motion pictures of the conduit-chamber interface.

The test item consisted of an upper portion of the quantity probe interfaced with a conduit assembly shown in figure F3.5-2. The quantity probe used was Block I hardware which had been sectioned for demonstration purposes. An additional hole was drilled in the probe insulator to modify it to Block II and wire was routed through it and the conduit assembly to represent the Apollo 13 configuration. Stainless steel sections were welded onto the probe to close the demonstration ports. Wiring with insulation was allowed to extend beyond the Teflon insulator approximately 4 inches. This wiring was also routed through the conduit and connected to the feedthrough pins through which power, 115 volts at 400 cycles, was supplied to both fan motor bundles by a system which had been

---

*Extracted from "Fuel Quantity Probe Sleeve and Conduit Assembly Flammability Report," prepared by the Manned Spacecraft Center for the Apollo 13 Review Board under TPS 13-T-06, June 5, 1970.

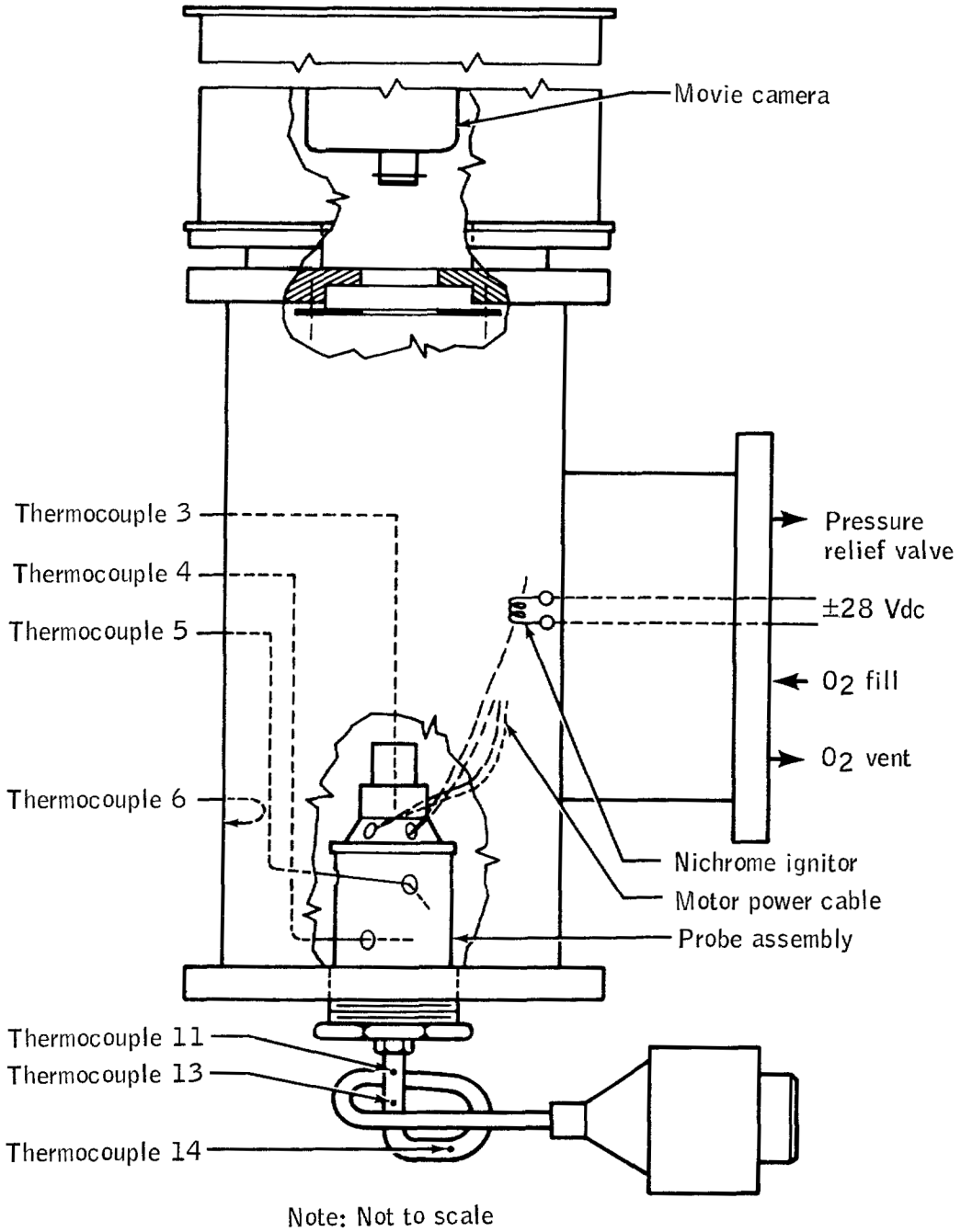

Figure F3.5-1.- Quantity probe and conduit assembly apparatus.

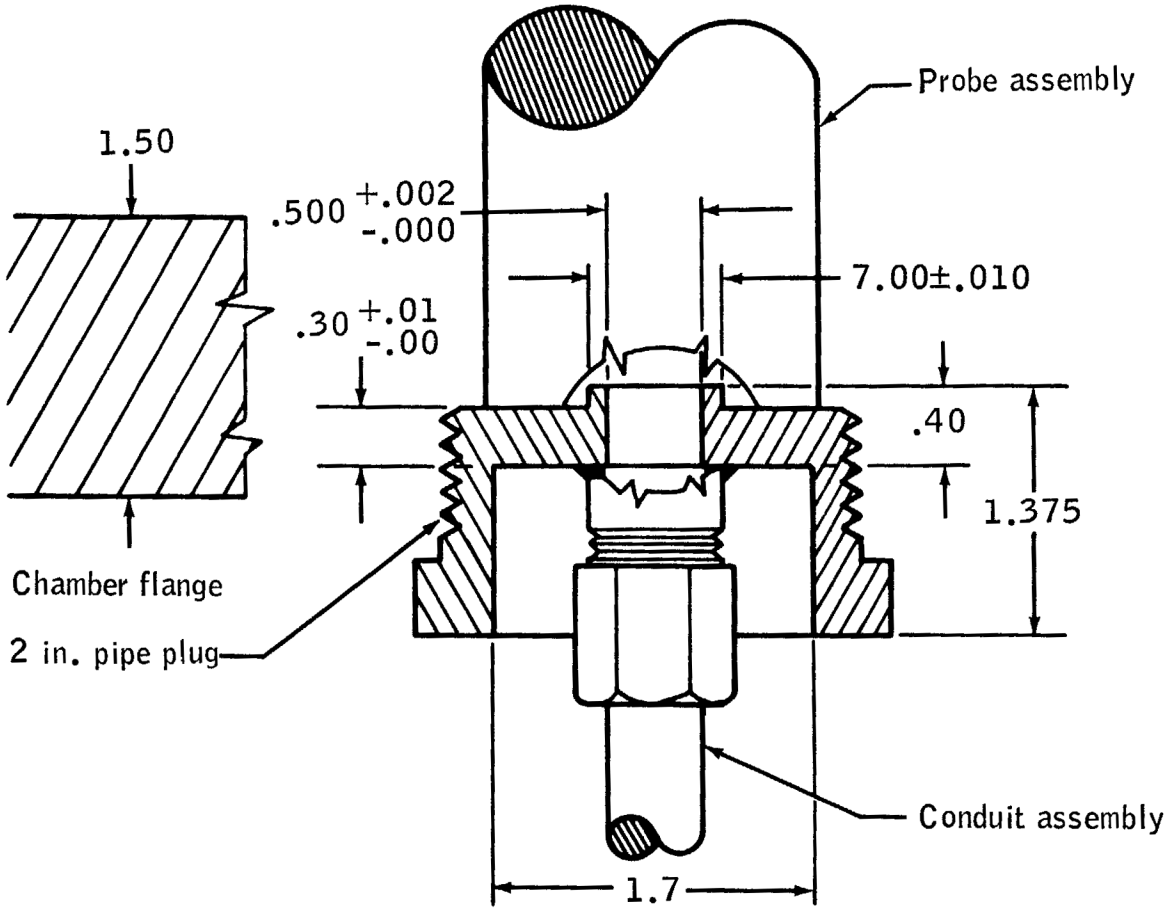

Figure F3.5-2.- Upper quantity probe - conduit interface.

fused using 1-amp fuses. One of the fan motor bundles was allowed to extend beyond the other wiring inside the test chamber and a nichrome ignitor was installed on it.

The probe conduit interface consisted of a stainless steel 2-inch pipe plug machined to the dimensions shown in figure F3.5-2. The interface was mounted on the bottom flange of the chamber so that flame propagation would be downward.

Three thermocouples were located in the region of the quantity probe as shown in figure F3.5-1. Two thermocouples were installed to measure internal chamber wall temperatures. Three thermocouples were installed on the external surface of the conduit as shown in figure F3.5-1.

After filling the chamber to 925 psia with gaseous oxygen, the chamber was cooled until thermocouple 3 shown on figure F3.5-1 indicated -138° F. Twenty-eight volts dc was applied at 5 amps to the ignitor for approximately 3 seconds. The current was increased to 10 amps for 2 seconds at which time fusion of the ignitor occurred.

Results

Pressure history of the chamber is shown in figure F3.5-3. The first relief valve opening occurred at approximately 28 seconds. It subsequently reopened 15 times before failure occurred. Fusion of the ignitor is shown on the graph to indicate ignition of the insulation.

Temperature histories of both internal and external portions of the test apparatus are shown in figures F3.5-4 and F3.5-5. Thermocouple placements in each of these areas are included in the legend figures of each of these graphs. It should be noted that two types of thermocouples were used, one with good sensitivity at low temperatures, copper-constantan, and one with good sensitivity at high temperatures, chromel-alumel. These two types are also indicated in figures F3.5-4 and F3.5-5.

The propagation observed in the color motion picture coverage internally proceeded from the ignition site (fig. F3.5-6) vertically downward. Figure F3.5-7 shows burning of the insulation on the fan motor wire bundle just before reaching the other wire bundles. Figure F3.5-8 shows the burning of several of the wire bundles. Figure F3.5-9 shows the burning of the wire bundles just prior to reaching the Teflon insulator, and figure F3.5-10 shows the more subdued fire after the propagation had progressed further into the upper probe region. Figure F3.5-11 shows the dense smoke after propagation of the burning into the insulator.

Figure F3.5-12 shows the conduit and chamber interface burnthrough scenes taken from the external movie coverage. The time for this sequence (24 frames) is 1 second. The small amount of external burning resulted

from ignition of the Mylar film used to insulate the test chamber.

Visual observation of the failure of the conduit through a test cell window revealed that a flame front resulted as far away as 3 or 4 feet from the chamber.

After the test, the section of conduit was found approximately 8 feet from the chamber. Several pieces of the Teflon insulator, two pieces of the conduit swedgelock nut, and one piece of conduit tubing were gathered from a 20-foot radius around the test area (fig. F3.5-13). The only item remaining in the test chamber was a portion of the Inconel section of the capacitance probe (fig. F3.5-14). The stainless steel portion was completely gone and a portion of the Inconel was burned. No remains of the aluminum portion of the probe could be found. The conduit-chamber interface was torched out to a maximum diameter of 1-7/8 inches (see figs. F3.5-15 and F3.5-16).

Conclusions

It is quite evident from the results of this test that the insulation burning on the electrical conductors did propagate through the probe insulator even in downward burning and proceeded into the conduit. It is difficult to determine if the insulator was ignited and what time was required for the burning to propagate through the insulator. However, failure of the conduit occurred in approximately 10 seconds after burning had proceeded to the insulator-wire bundle interface. After the initial failure of the conduit, the contents of the tank (1/3 cubic foot) were vented in approximately 0.5 second with a major portion of the burning of metal occurring in 0.25 second. Venting of larger amounts of oxygen would not necessarily take longer since continued oxygen flow should produce considerably larger "torched out" sections. In order to produce the heat necessary for the effects observed here, metal burning must have occurred.

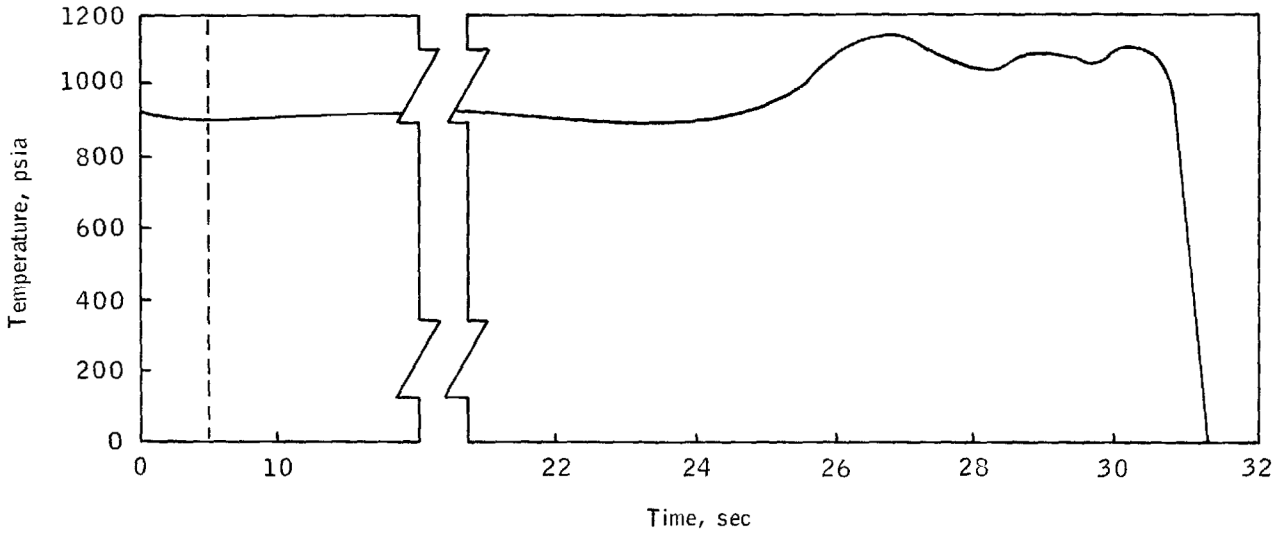

Figure F3.5-3.- Quantity probe and conduit assembly test pressure history.

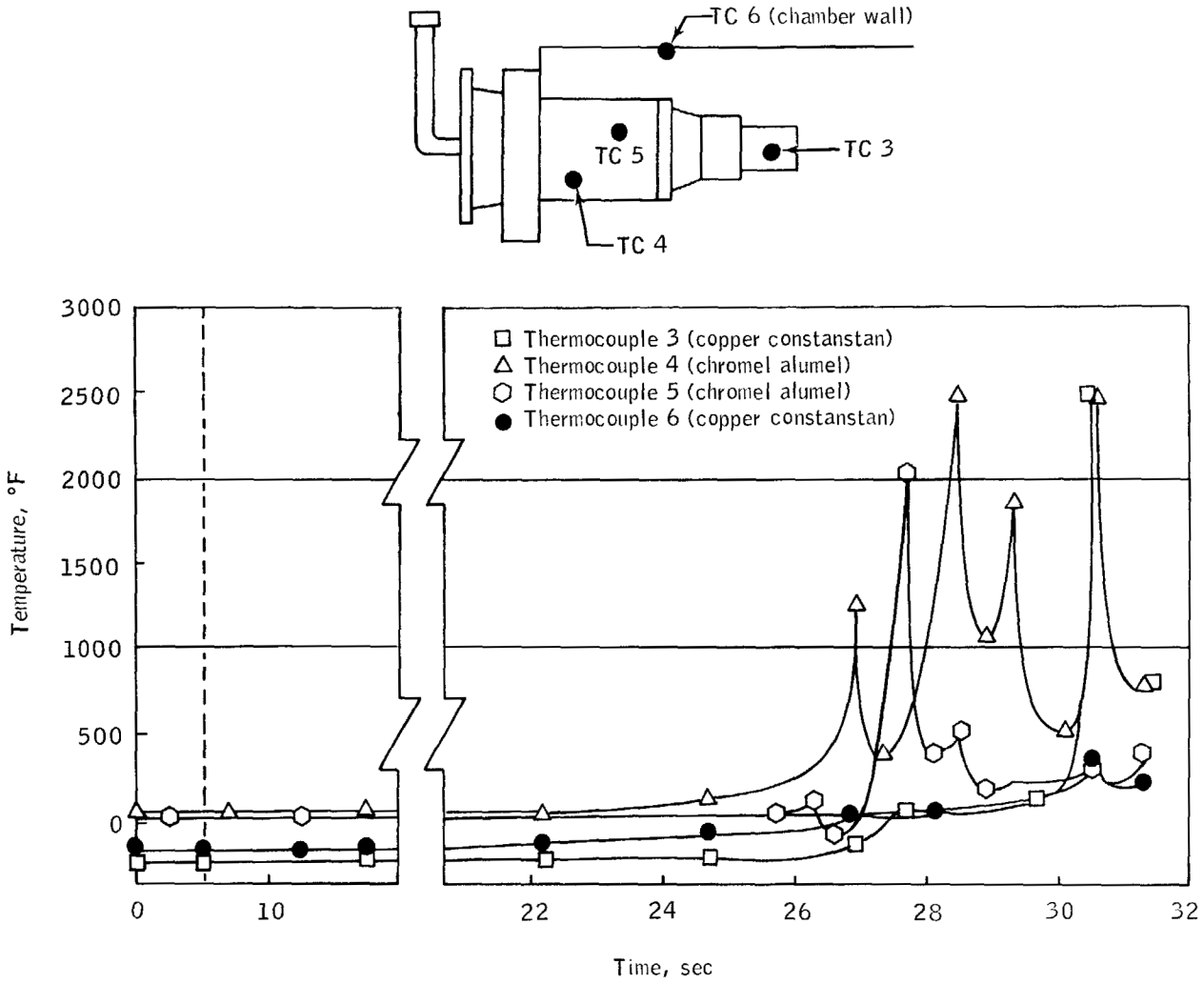

Figure F3.5-4.- Temperature history of quantity probe and chamber wall.

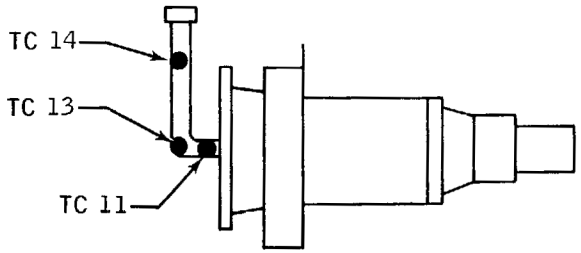

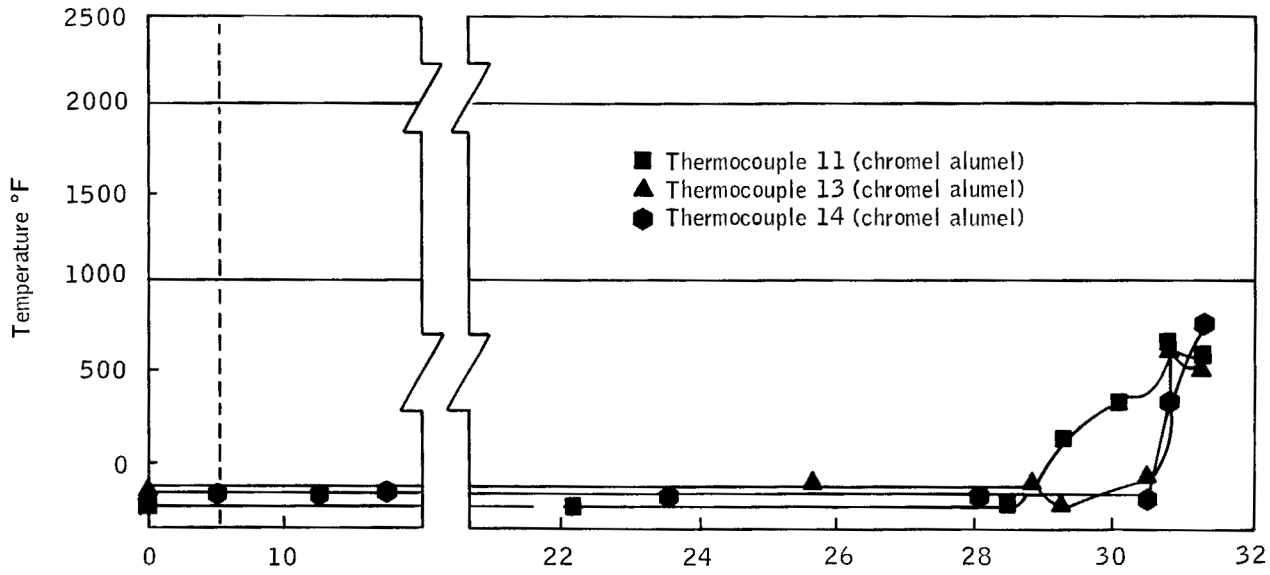

Figure F3.5-5.- Temperature history of conduit.

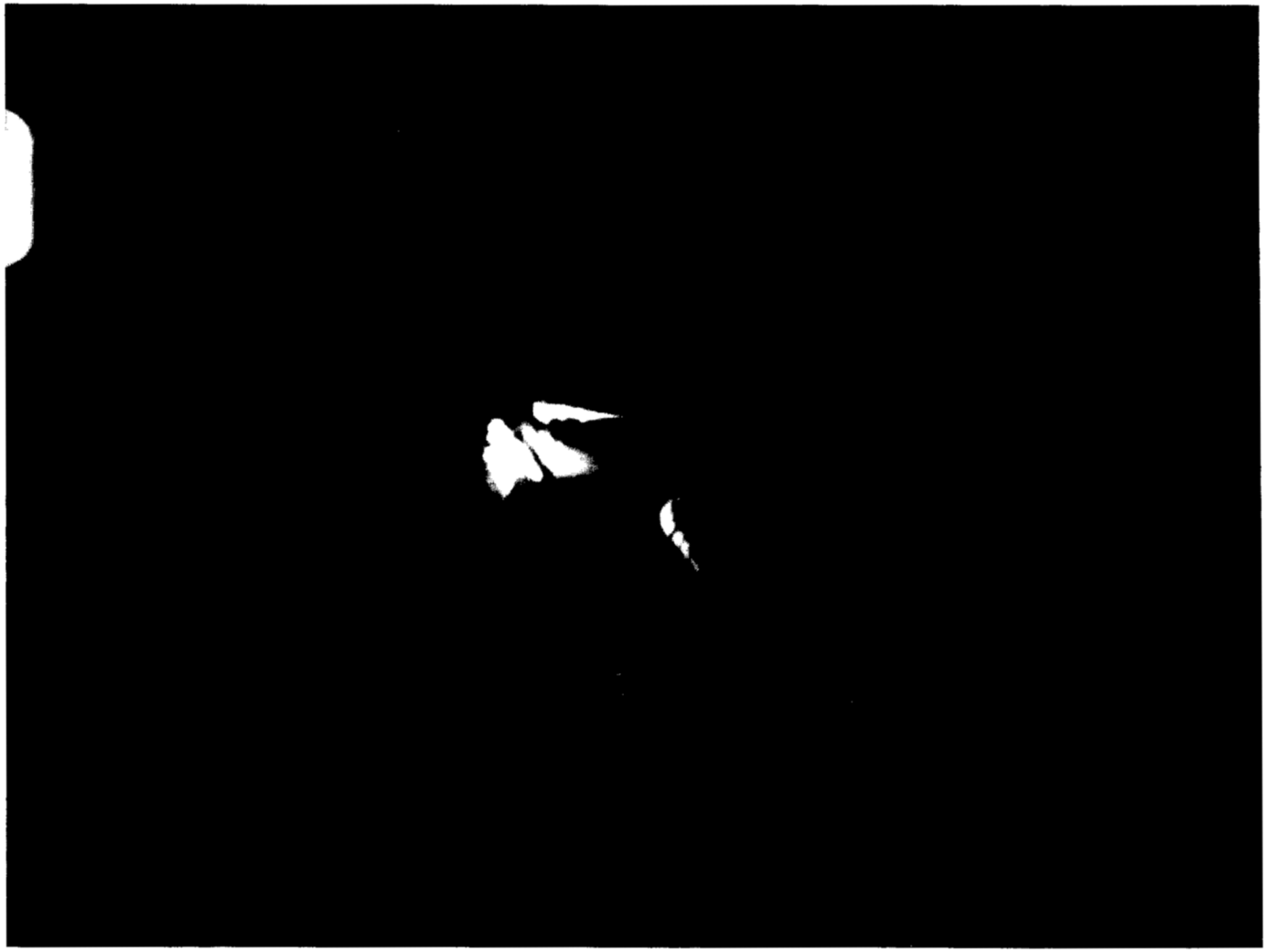

Figure F3.5-6.- Internal chamber view shortly after ignition.

Figure F3.5-7.- Burning along fan motor wire bundle.

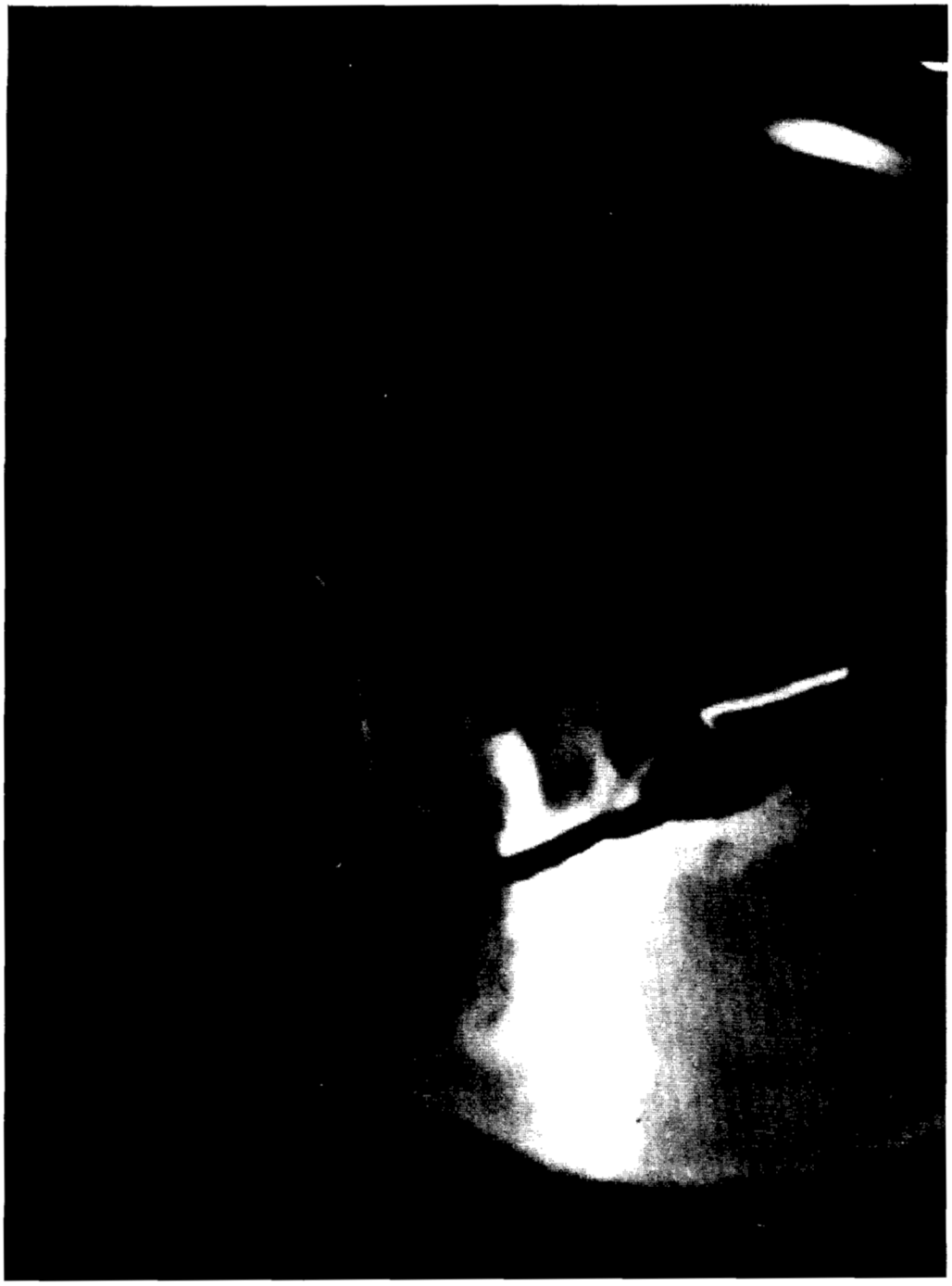

Figure F3.5-8.- Burning of adjacent wire bundles.

Figure F3.5-9.- Burning bundles prior to reaching probe insulator.

Figure F3.5-10.- Burning progressed into insulator.

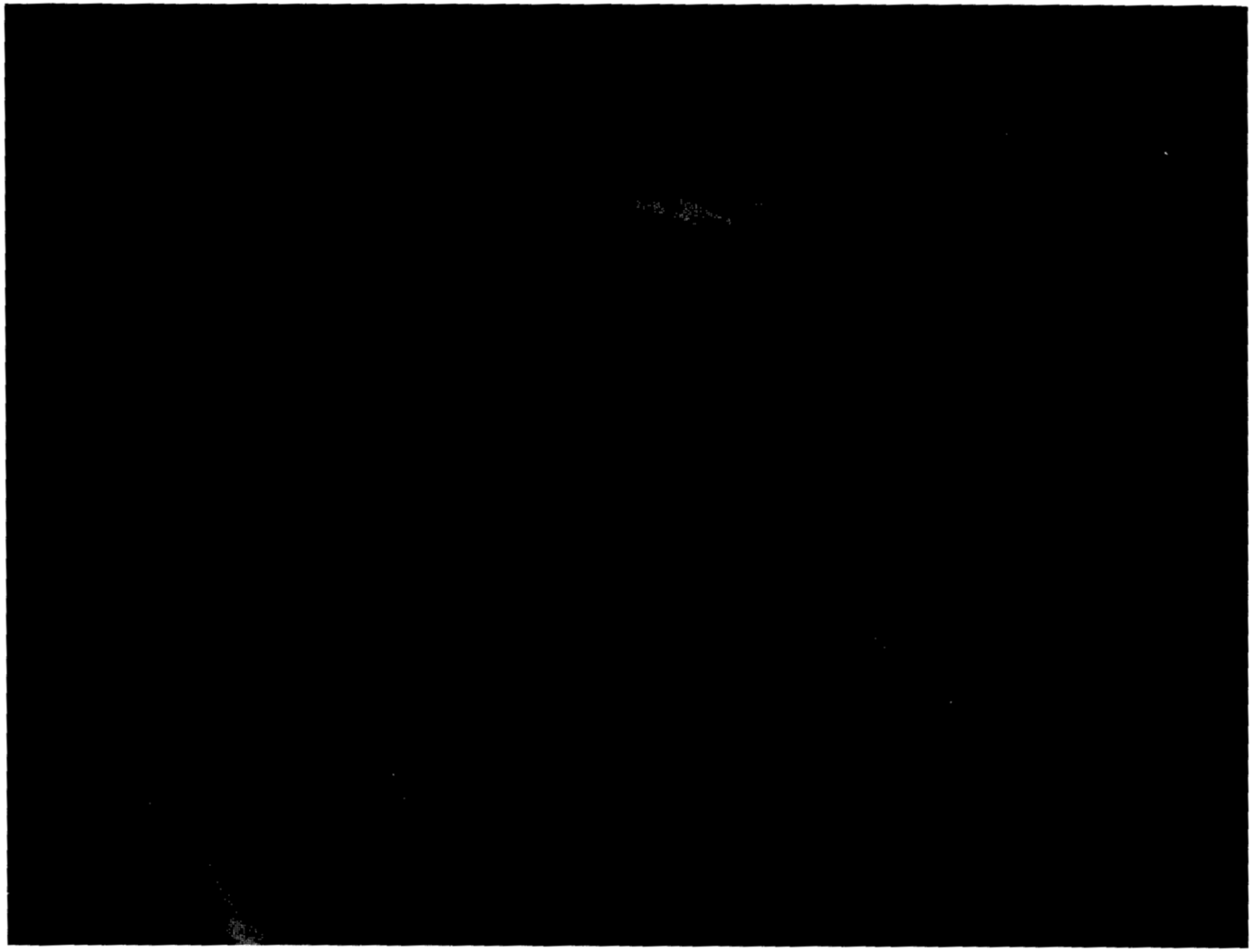

Figure F3.5-11.- Dense smoke after propagation of burning into insulator.

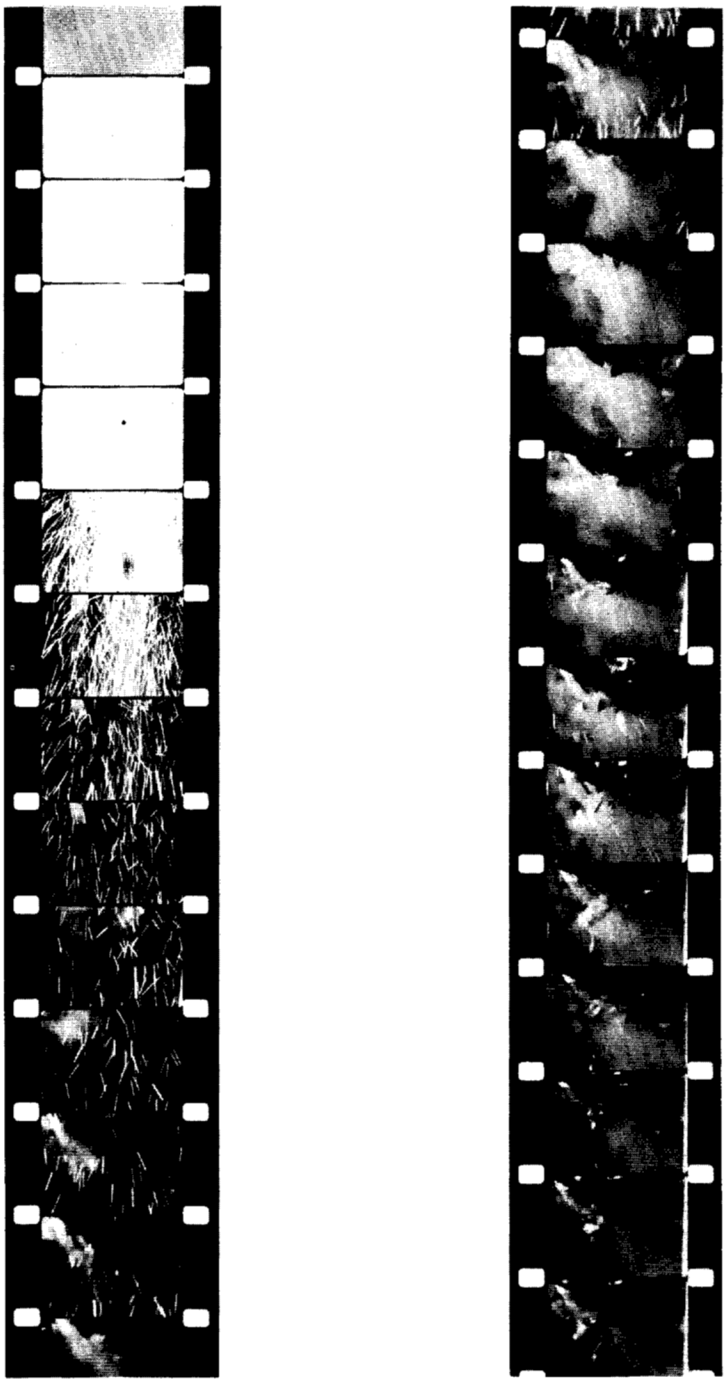

Figure F3.5-12.- External views of chamber-conduit interface at time of failure.

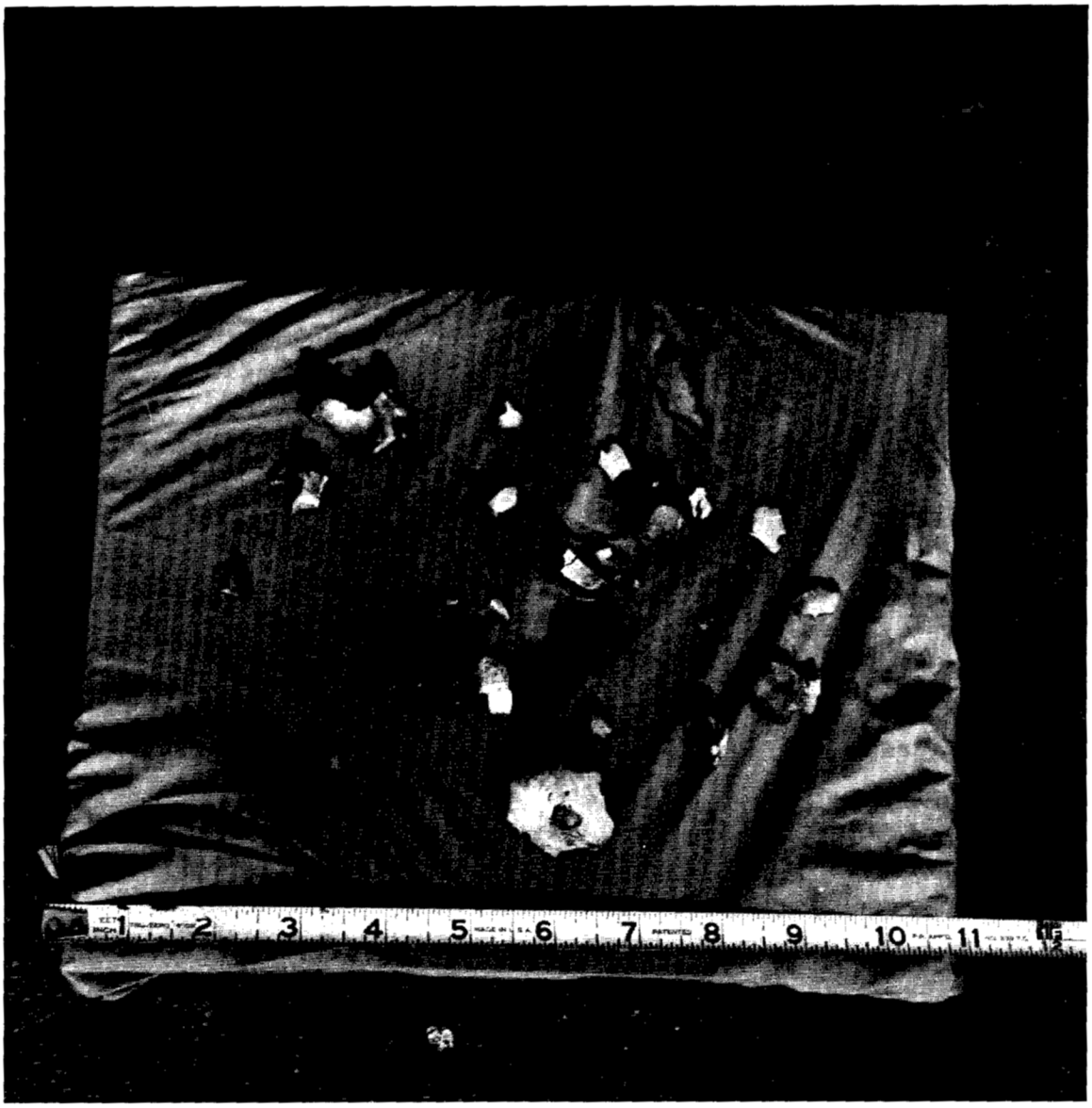

Figure F3.5-13.- Parts of probe insulator and tubing collected from area around test chamber.

Figure F3.5-14.- Portion of probe which remained in the test chamber.

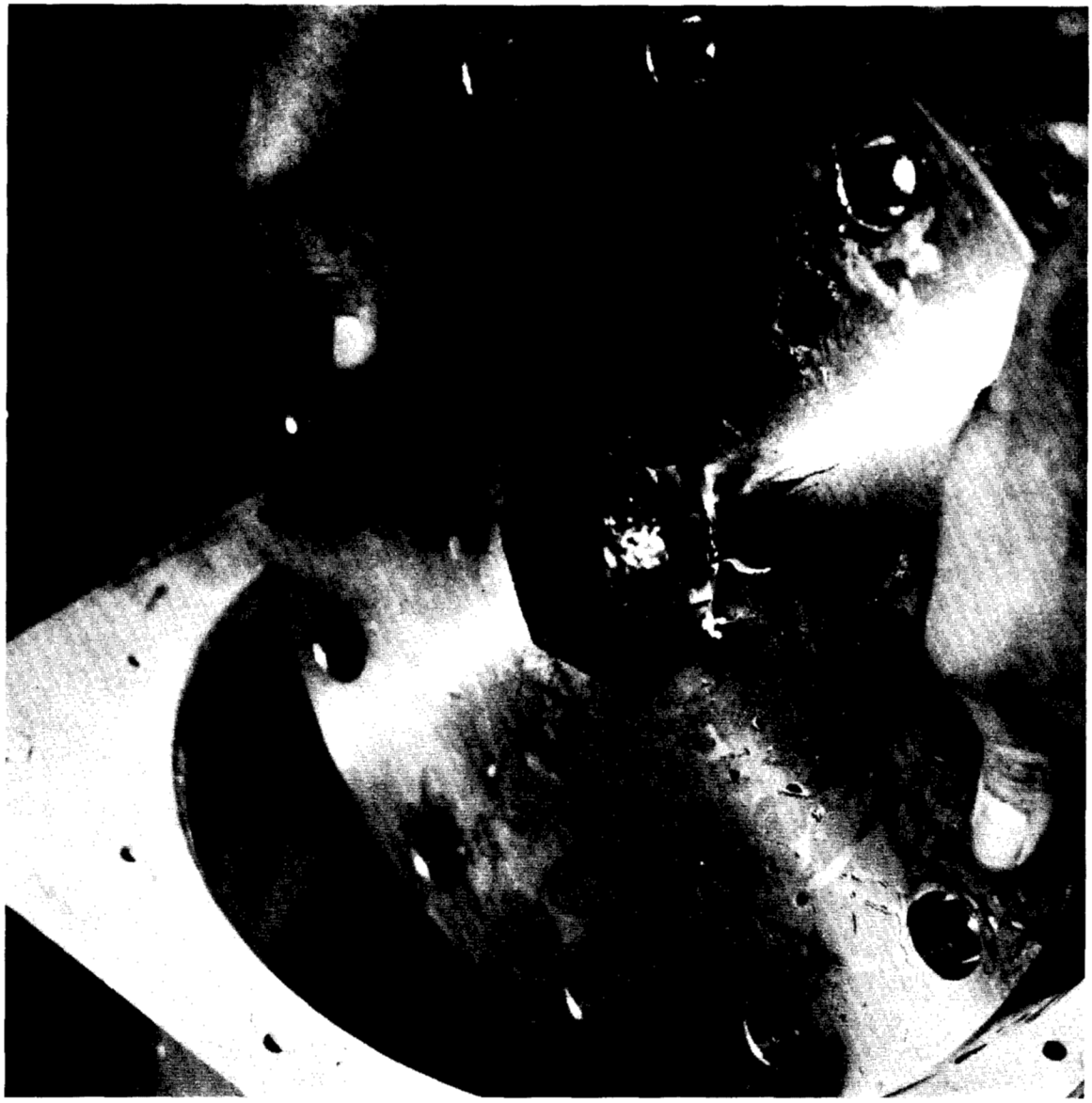

Figure F3.5-15.- External view of chamber flange on which conduit-quantity probe interface was mounted (after test).

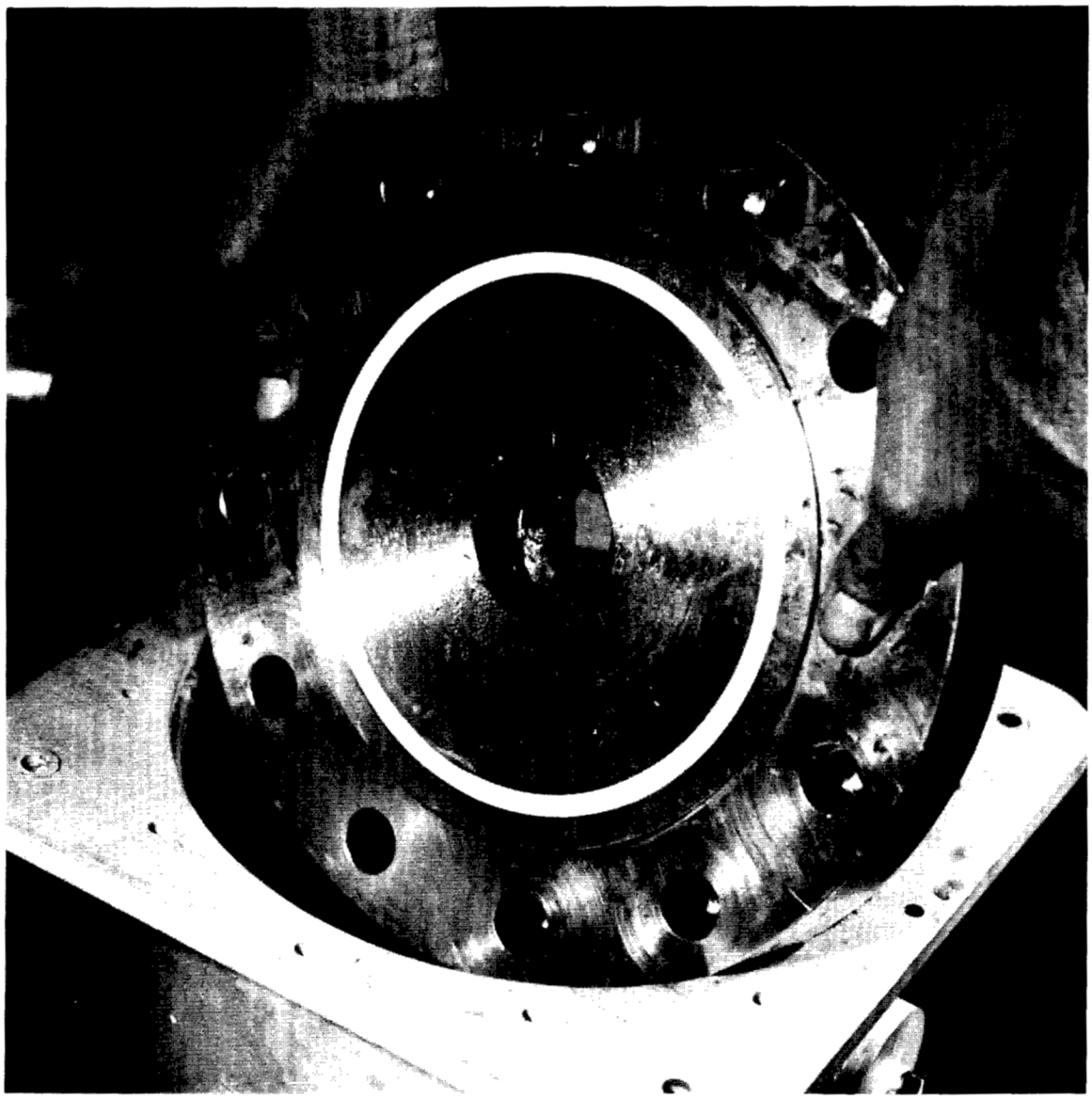

Figure F3.5-16.- View of chamber flange internal surface after test.

PART F3.6

ZERO-g TEFLON FLAME PROPAGATION TESTS

Objective

The objective of these tests was to measure the flame propagation rate along Teflon-insulated wire bundles in oxygen at 900 psia and -180° F in a zero-g environment. A second objective was to determine whether flames travelling along the fan motor lead wires would pass through the aperture in the motor case. Measurements are to be used to interpret the pressure and temperature history observed in the oxygen tank during the accident.

Apparatus

Tests were conducted at the Lewis Research Center's 5-Second Zero Gravity Facility. An experimental apparatus was designed and constructed which permitted the tests to be conducted in an oxygen environment of 920 psia ± 20 psi and -180° F ± 10°. The apparatus was installed on a standard drop test vehicle capable of providing the necessary supporting functions. An overall view of the drop vehicle is presented in figure F3.6-1 and a detailed photograph of the experimental apparatus is shown in figure F3.6-2. The basic components of the experimental apparatus are the combustion chamber with a sapphire window to permit high-speed photography, and an expansion tank as a safety feature in the event an excessive pressure rise were to occur. The apparatus was equipped with a fill and vent system, pressure relief system, and liquid nitrogen cooling coils. The test specimen was installed in the combustion chamber in a horizontal position as is shown in figure F3.6-3. This figure is typical of all installations. Ignition was caused by heating a 26-gage nichrome wire which was wrapped around the specimen. Chamber pressure and temperature were monitored throughout the test. High-speed photographic data (400 frames per second) were obtained using a register pin Milliken camera.

Approach

A total of eight tests were conducted on three test specimens. Each specimen was run in a one-g and a zero-g environment, and a one-g and zero-g test was repeated on two specimens to examine repeatability of the data. The three specimens were the following:

Type 1 - Fan motor conductor bundle - four wires and white sleeving

Type 2 - Fan motor conductor bundle - four wires and clear shrink sleeving

Type 3 - Aluminum Teflon feed-through assembly - four wires and no sleeving

The aluminum plate thickness for the Type 3 tests equaled that of the fan motor case. This specimen was used to determine whether a flame burning along the lead wires would continue through the aperture in a simulated motor case, and whether the aluminum would ignite.

Results

The zero-g linear propagation rate for fan motor wires in white pigmented Teflon sleeving (Type 1) was measured as 0.12 in/sec, and for the same wires in clear Teflon sleeving (Type 2), the rates in two separate tests were 0.16 and 0.32 in/sec. The corresponding flame propagation rate at one-g for both types of wire bundles was 0.55 in/sec measured in three tests. These results are listed in table F3.6-I. The flame in both zero-g and one-g tests pulsed as it spread along the wire bundles with the flame markedly more vigorous in the one-g cases. In all cases the Teflon was completely burned with little visible residue.

The flame propagation tests through an aluminum plate (Type 3) showed that the flame did not appear to have propagated through the Teflon grommeted aperture under zero-g conditions, but did pass through at one-g. Unfortunately, the pictures of the flames under zero-g were not clear enough to be certain that the flame failed to propagate through the aperture. Because the zero-g period lasts for less than 5 seconds following ignition, it is possible that flame propagation through the aperture would have been observed if more time at zero-g were available. These results are also listed in table F3.6-I.

Conclusions

The flame propagation rate along Teflon insulation in zero-g is reduced by about a factor of two from that observed in one-g. The propagation rate along the fan motor lead bundle in zero-g is in the range of 0.12 to 0.32 in/sec. These flame propagation rates are of a magnitude which is consistent with the time required to account for the duration of the pressure rise in the spacecraft oxygen tank.

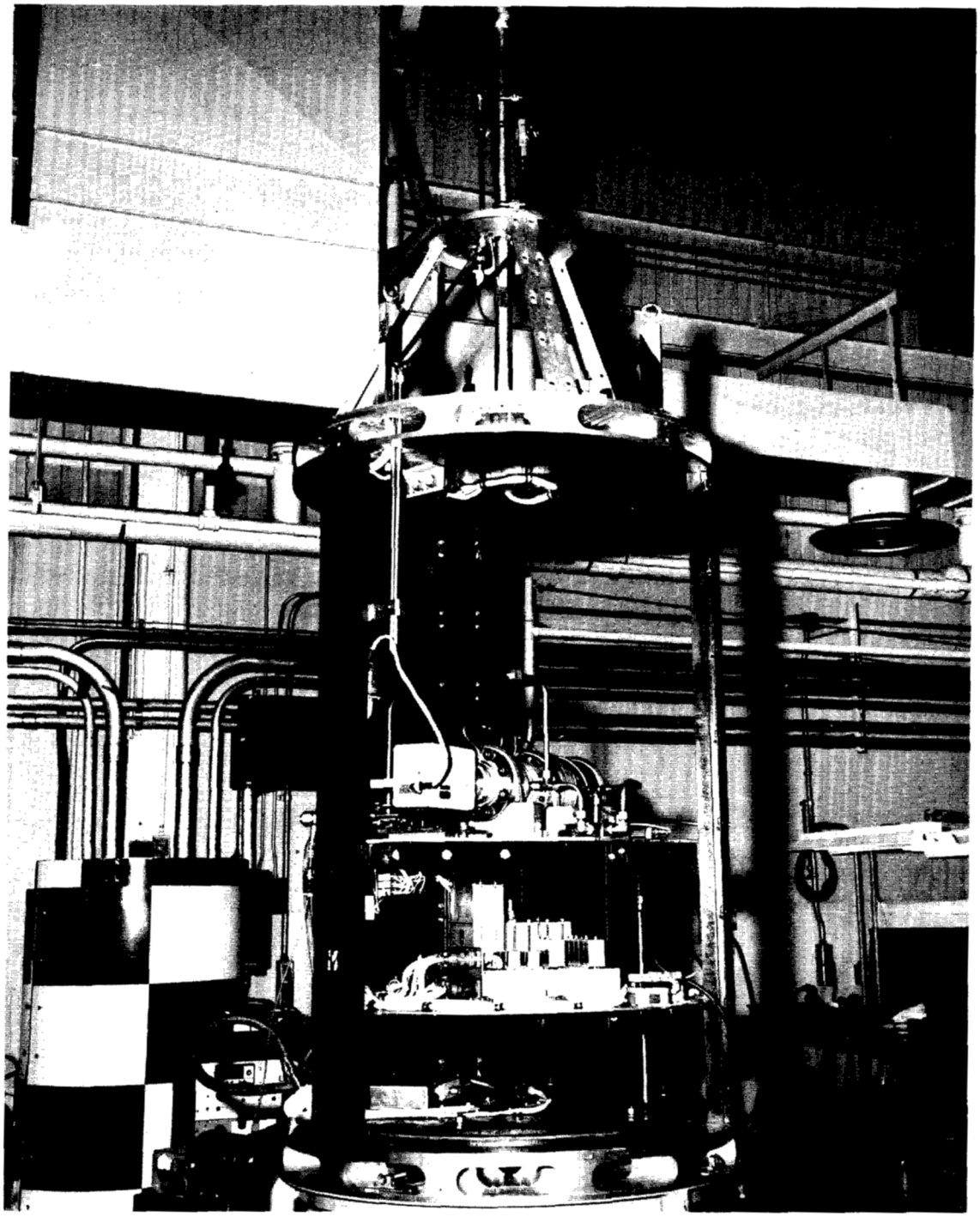

Figure F3.6-1.- 5-second drop vehicle.

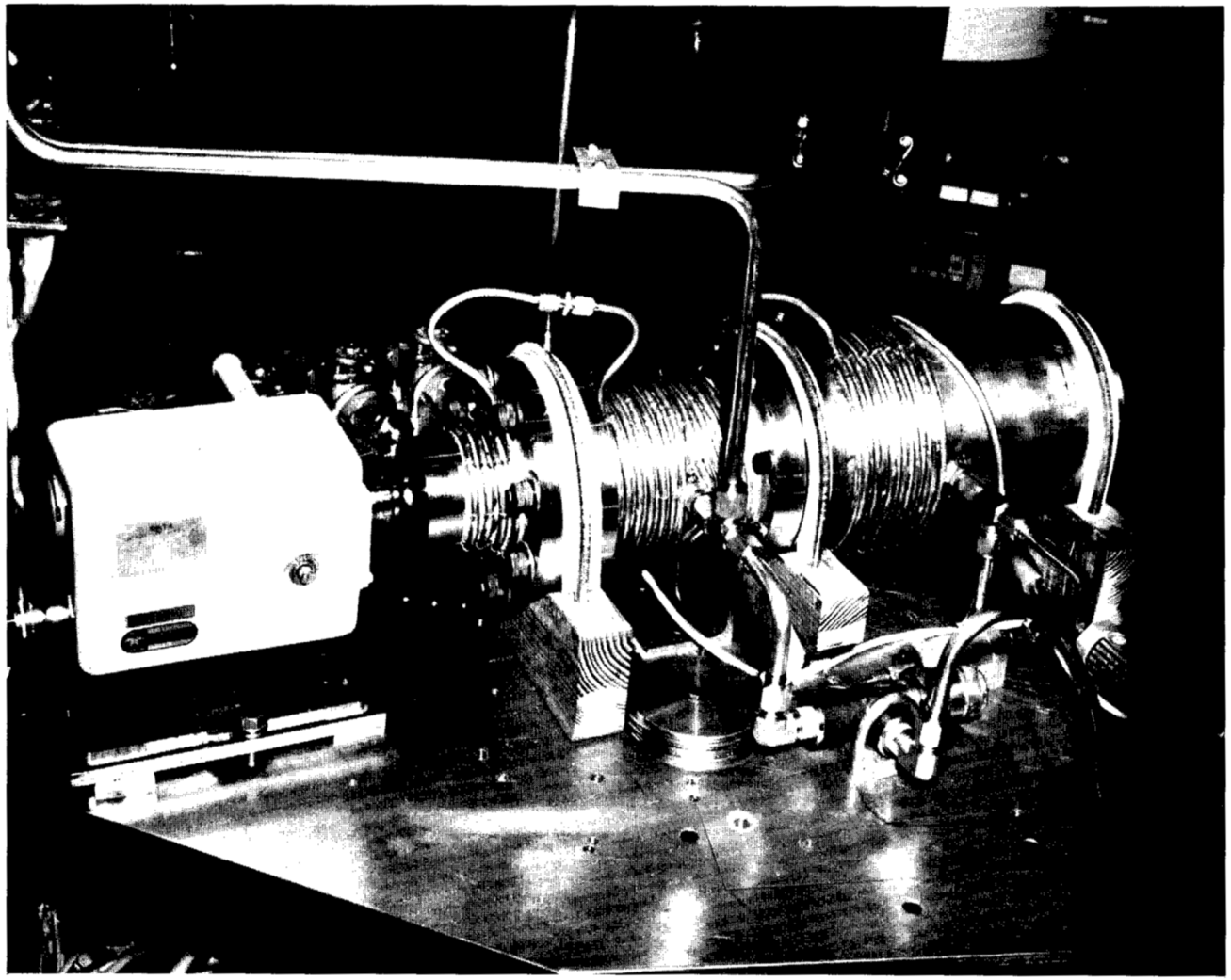

Figure F3.6-2.- Experimental combustion apparatus.

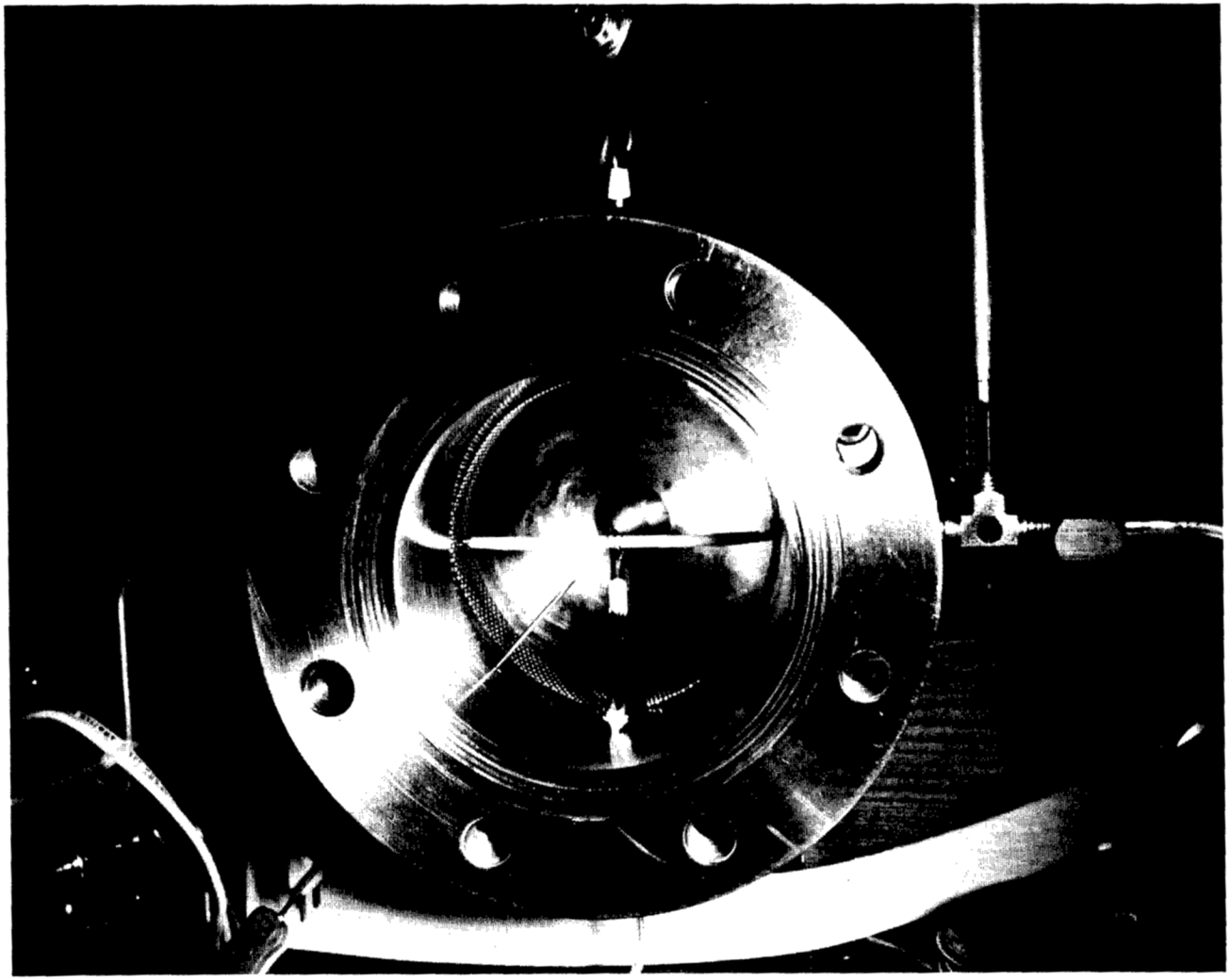

Figure F3.6-3.- Typical test specimen installation in combustion chamber.

TABLE F3.6-I.- SUMMARY OF RESULTS

Run no.	Test specimen	Gravity level	Average flame spread rate, in/sec	Comments
A-1-1 A-1-2 A-1-6	Type 1 Type 2 Type 1	One One One	0.55 0.55 0.55	The specimens burned vigorously. The flame progressed along the specimens in a pulsating fashion.
A-1-3 A-1-5 A-1-7	Type 2 Type 1 Type 2	Zero Zero Zero	0.16 0.12 0.32	The specimens burned in zero-g but not as vigorously as in normal gravity. The flame pulsated along the specimens in a similar way as in normal gravity but at a slower overall rate.
A-1-8	Type 3	One	-	The flame propagated through the aluminum holder but did not ignite it.
A-1-4	Type 3	Zero	-	The flame could not be clearly defined on the film. The aluminum holder did not ignite.

PART F3.7

FULL-SCALE SIMULATED OXYGEN TANK FIRE

Objectives

The purpose of this test was to simulate as closely as possible, in a one-g environment, the processes that occurred during the failure of oxygen tank no. 2 of Apollo 13. The data to be obtained include the pressure and temperature history which results from the combustion of Teflon wire insulation beginning at one of three likely ignition locations, as well as observing the manner in which the tank or conduit fails and vents its contents.

Apparatus

A Block I oxygen tank was modified to Block II configuration. The vacuum dome was removed and the tank was mounted in a vacuum sphere with the appropriate size and length of tubing connected. The heaters were disconnected and three hot-wire ignitors were installed. One ignitor was located on the bottom fan motor leads, one on the top fan motor leads, and another on the wire loop between the quantity probe and the heater-fan support. The connecting tubing, filter, pressure transducer and switch, relief valve, and regulator were flight-qualified hardware. The tank was mounted so that the long axis of the quantity probe was horizontal. Figure F3.7-1 shows the tank mounted in the chamber. Two television cameras and four motion picture cameras were mounted in the vacuum chamber. One camera operates at 64 frames/sec, two at 250 frames/sec, and another at 400 frames/sec. The two 250 frames/sec cameras were operated in sequence.

Results

The nichrome wire ignitor on the bottom fan motor leads was ignited. The tank pressure rose from an initial value of 915 psia to 990 psia in 48 seconds after ignition. The temperature measured by the flight-type resistance thermometer, mounted on quantity gage, rose 3° F from an initial value of -202° to -199° F in this 48-second period. The tank pressure reached approximately 1200 psia at 56 seconds after ignition and apparently the flight pressure relief valve which was set to open at 1005 psia could not vent rapidly enough to check the tank pressure rise. Two GSE pressure relief valves, set at higher pressures, apparently helped to limit the tank pressure to 1200 psia. The tank temperature rose abruptly after 48 seconds, following ignition, from -199° to -170° F in 3 seconds. After this time the temperature read off-scale above

2000° F. Failure of the temperature measuring wiring is indicated by the erratic readings that followed. These data are shown in figure F3.7-2. The pressure data shown beyond 56 seconds represent the venting of the tank contents. These pressure and temperature histories are qualitatively similar to the measured flight data but occur more rapidly than observed in flight.

The conduit failed close to where it attaches to the tank closure plate about 57 seconds after ignition (fig. F3.7-3). The two 250-frame/sec cameras and the 64-frame/sec camera failed to operate during this test. However, the 400-frame/sec camera suggests that the first material to issue from the ruptured conduit was accompanied by bright flame. The tank pressure declined from 1175 psia to 725 psia in 1 second following conduit rupture. High oxygen flow rates were observed from the conduit breach for about 15 seconds. A posttest examination of the ruptured conduit showed that the expulsion of the tank contents was limited by the 1/2-inch-diameter aperture in the tank closure plate. An examination of the internal components of the tank showed complete combustion of the Teflon insulation on the motor lead wires as well as almost complete combustion of the glass-filled Teflon sleeve. This is shown in figure F3.7-4.

Conclusions

The qualitative features of the pressure and temperature rises in oxygen tank no. 2 have been simulated by initiating Teflon wire insulation combustion on the lower fan motor lead wire bundle. The time from ignition of the total combustion process in the simulated tank fire is about three-fourths to one-half the time realized in the spacecraft accident. The conduit housing the electrical leads failed near the weld and resulted in a limiting exit area from the tank of about 1/2 inch diameter. The venting history is characteristic of the expulsion of liquid for the first 1-1/2 seconds. This was followed by a two-phase flow process.

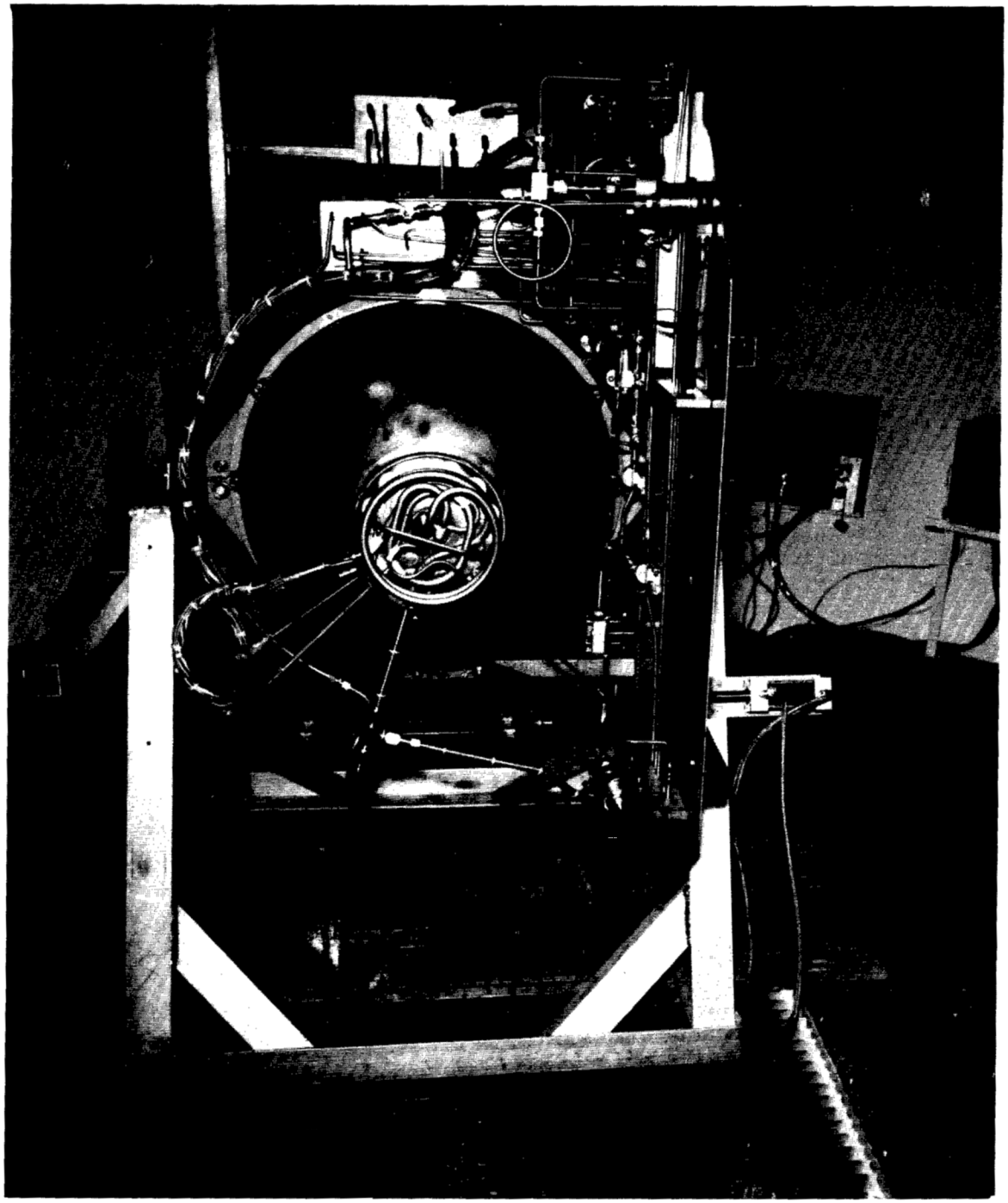

Figure F3.7-1.- Posttest oxygen tank setup.

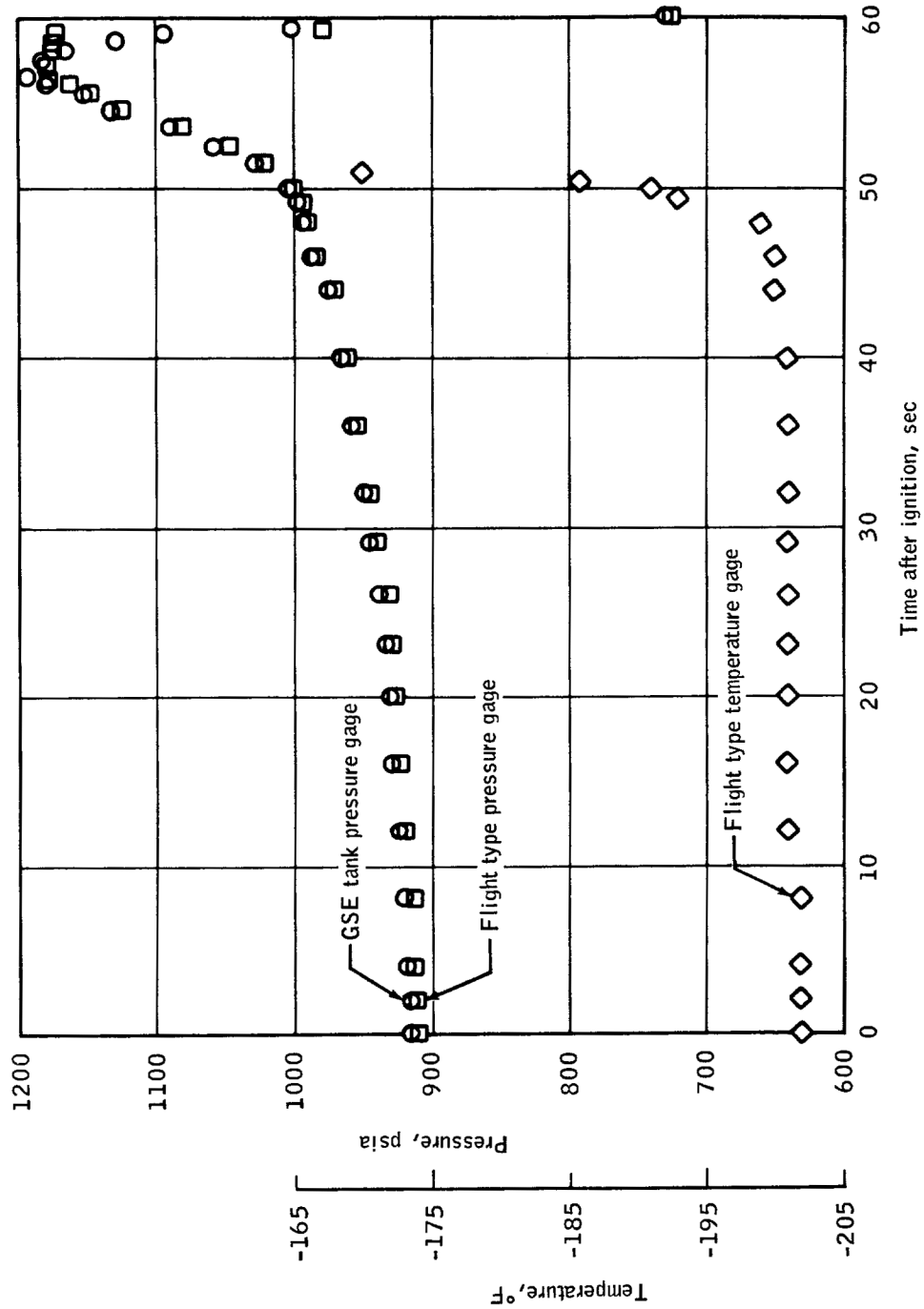

Figure F3.7-2.- Measured pressure and temperature time histories (preliminary data as of June 4, 1970).

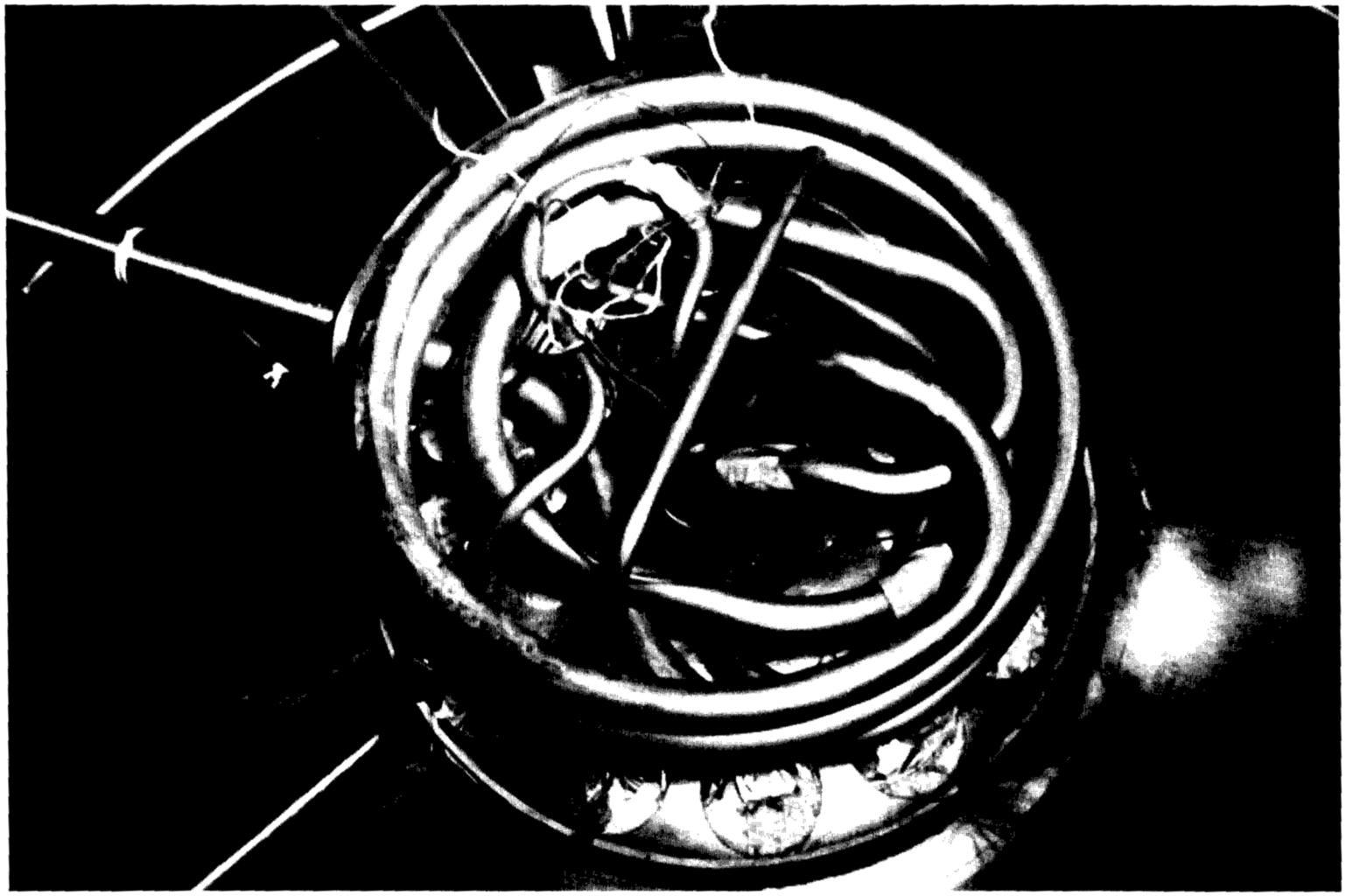

(a) Wide-angle view.
Figure F3.7-3.- View of failed conduit.

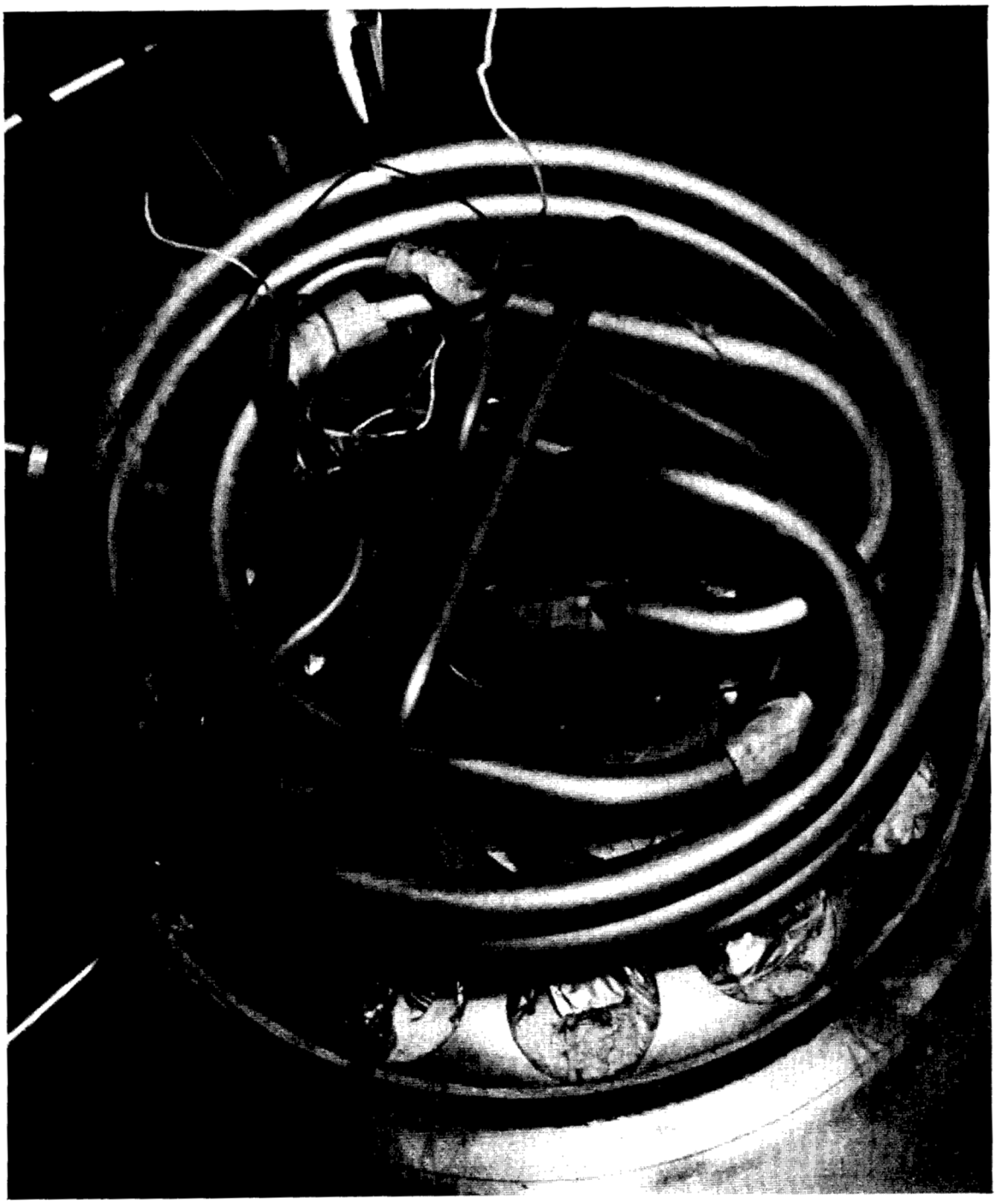

(b) Closeup view.

Figure F3.7-3.- Concluded.

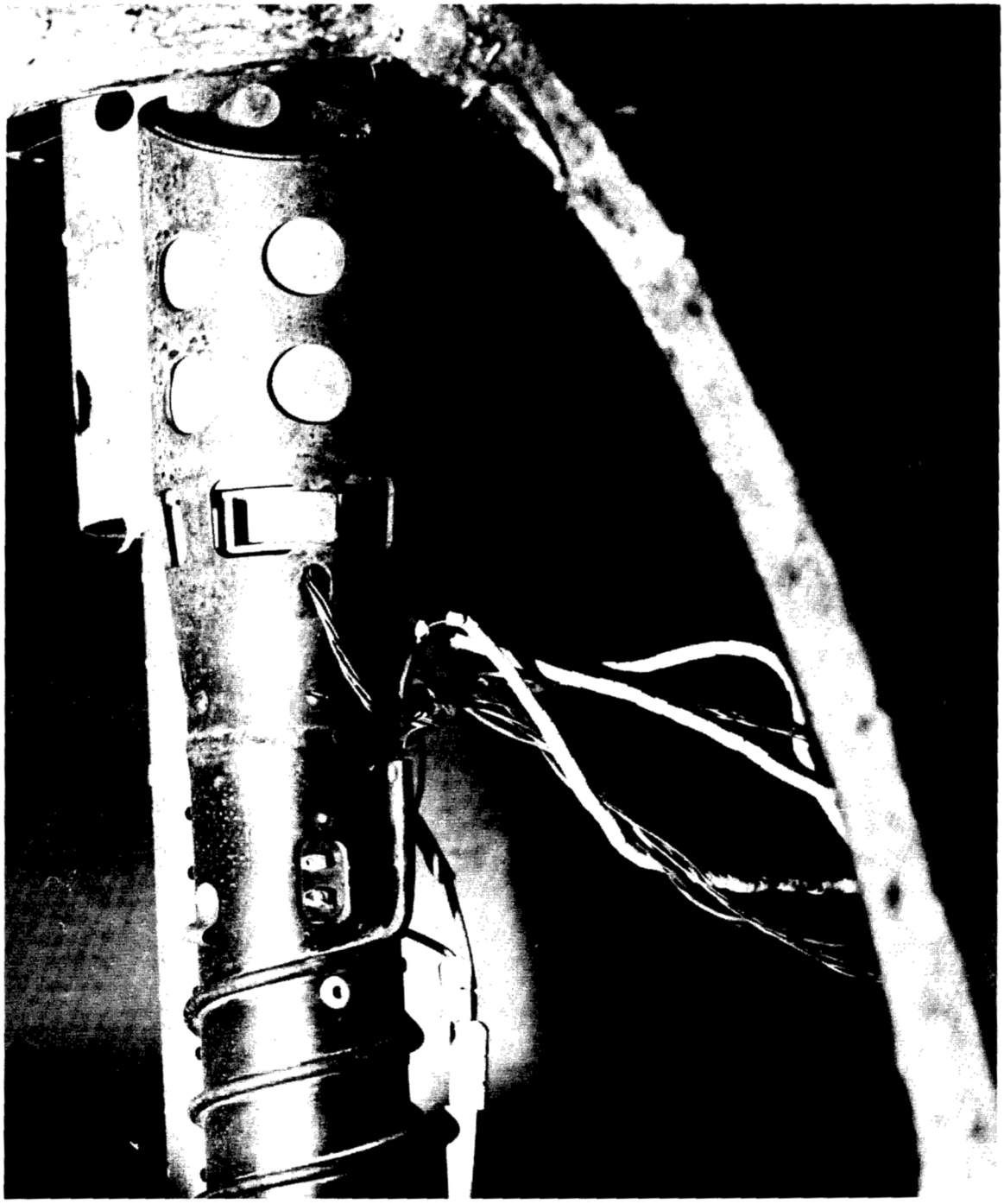

Figure F3.7-4.- Posttest internal view of tank components.

PART F3.8

ANALYSIS OF FLOW FROM RUPTURED OXYGEN TANK

Objective

The objective of this analysis was to compute the real gas discharge rate from the cryogenic oxygen tank no. 2 and provide the subsequent pressure history of various service module volumes.

Assumptions

1. Oxygen remains in equilibrium at all times. The oxygen properties were obtained from the tabulations and plots of references 2 and 3.

2. All orifice coefficients were taken to be unity and the orifices assumed to be choked.

3. All volumes and areas are invariant with time.

4. The effective volume of the oxygen tank is 4.7 ft^3 and is not changed by combustion processes.

5. All processes are isentropic both inside the oxygen tank and also between the oxygen tank and its discharge orifice.

6. Oxygen thermodynamic properties (ρ, p, h) are uniform throughout any given individual volume at any time.

7. The processes in volumes external to the oxygen tank are adiabatic. The total enthalpy in these volumes is equal to the average enthalpy of all prior discharged oxygen. Each volume acts as a plenum chamber for its respective vent orifice.

8. The initial tank conditions at t = 0 are p = 900 psi; ρ = 47.4 lb/ft^3; T = -190° F.

Method

Computations were based on several manually generated cross plots of the thermodynamic properties, correlations of intermediate computed results; and analytical and numerical integrations involving these

correlations. Choked orifice states were obtained by maximizing ρu for a given entropy.

Results

Figure F3.8-1 shows the mass flow rate per unit of effective orifice area plotted as a function of time. The two time scales shown are applicable to effective orifice diameters of 0.5 inch and 2.0 inches.

Figure F3.8-2 plots the total mass discharged from the oxygen tank against the same two time scales.

Figures F3.8-3 and F3.8-4 are plots of pressure time histories for various combinations of secondary volumes and orifices. The time scale in this case is only applicable to the 2-inch diameter exit orifice in the oxygen tank. The combinations of V and A* shown in figure F3.8-3 were chosen to roughly simulate the components of the SM as follows:

1. $V = 25\ ft^3$, $A^* = 2.08\ ft^2$ ($300\ in^2$). Simulates net volume of the oxygen shelf in bay 4 with effective venting of $300\ in^2$.

2. $V = 67\ ft^3$, $A^* = 2.08\ ft^2$ ($300\ in^2$). Simulates the bay 4 oxygen shelf and fuel cell shelf combined volume with venting of $300\ in^2$.

3. $V = 67\ ft^3$, $A^* = 1.39\ ft^2$ ($200\ in^2$). Same as case 2 but reduced venting area to rest of service module.

4. $V = 100\ ft^3$, $A^* = .43\ ft^2$ ($62\text{-}1/2\ in^2$). Simulates entire bay 4 with small venting.

5. $V = 200\ ft^3$, $A^* = .43\ ft^2$ ($62\text{-}1/2\ in^2$). Simulates combined bay 4 and tunnel volumes with venting past rocket nozzle only.

Also plotted are reference curves for each of the above volumes without any venting ($A^* = 0$).

Case 1 has a very rapid initial pressure rise with time due to the small volume ($25\ ft^3$) of the oxygen shelf. However, the mass efflux from this volume also increases rapidly with time so that it equals the influx at $t = 0.18$ second and the pressure peaks at approximately 8.8 psia.

---

*If the tank were initially at $p \approx 1000$ psi and the same entropy, then with a 2-inch diameter orifice the pressure would drop to 900 psi in 0.004 second with the discharge of 1 lb_m oxygen.

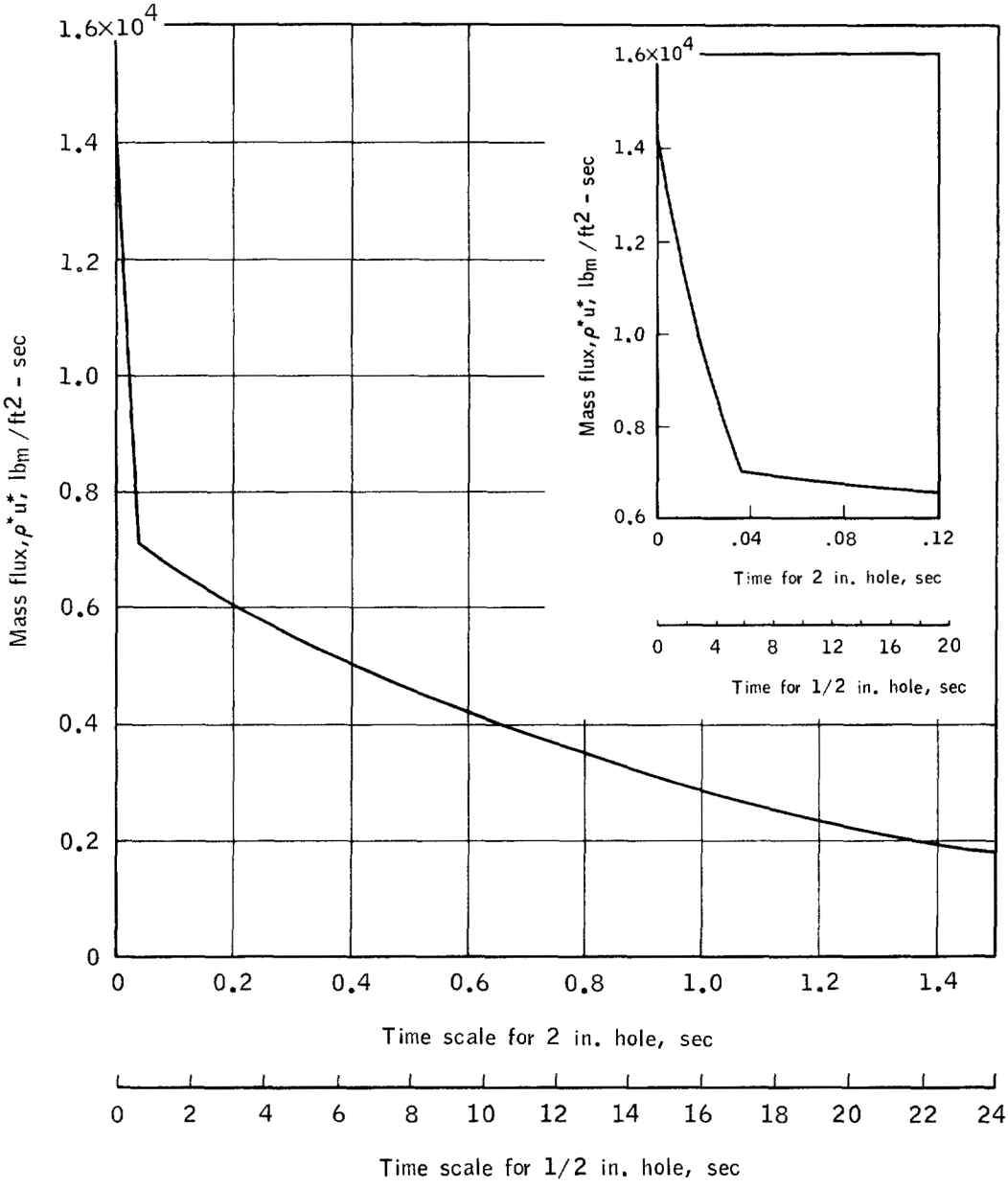

Figure F3.8-1.- Mass flow per unit area against time for 2 inch and 0.5 inch orifices.

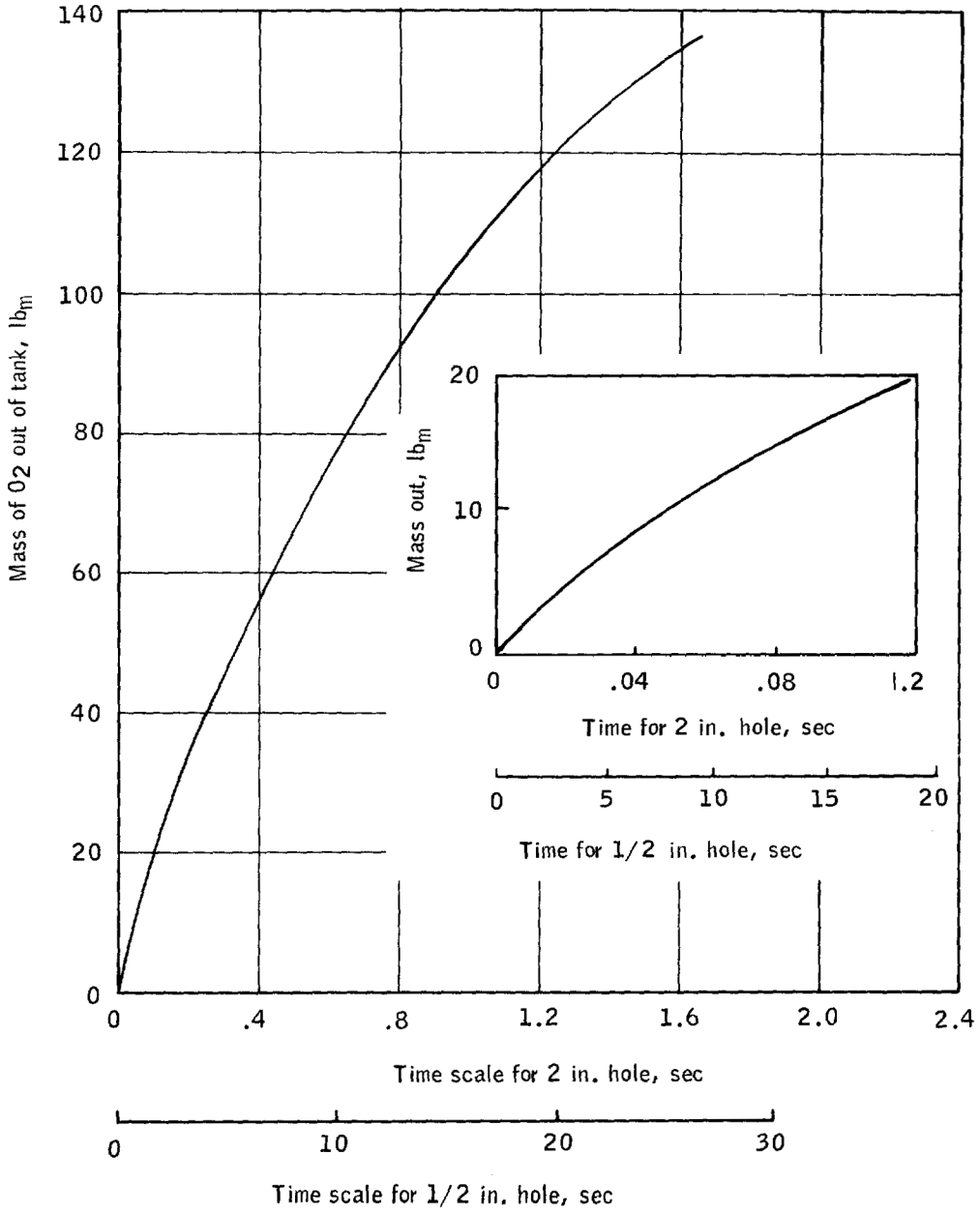

Figure F3.8-2.- Mass of oxygen expelled from tank against time.

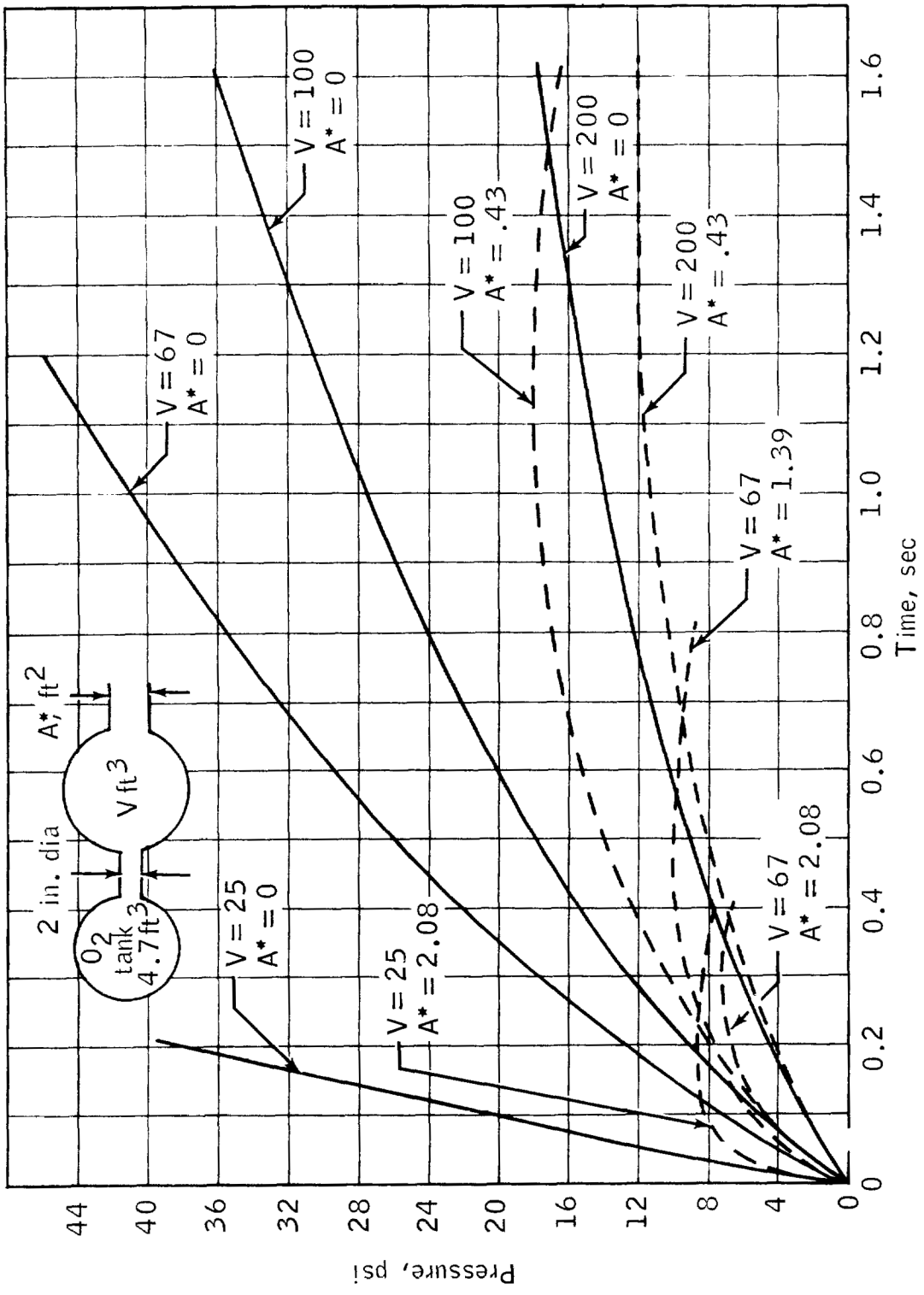

Figure F3.8-3.- Pressure rise against time.

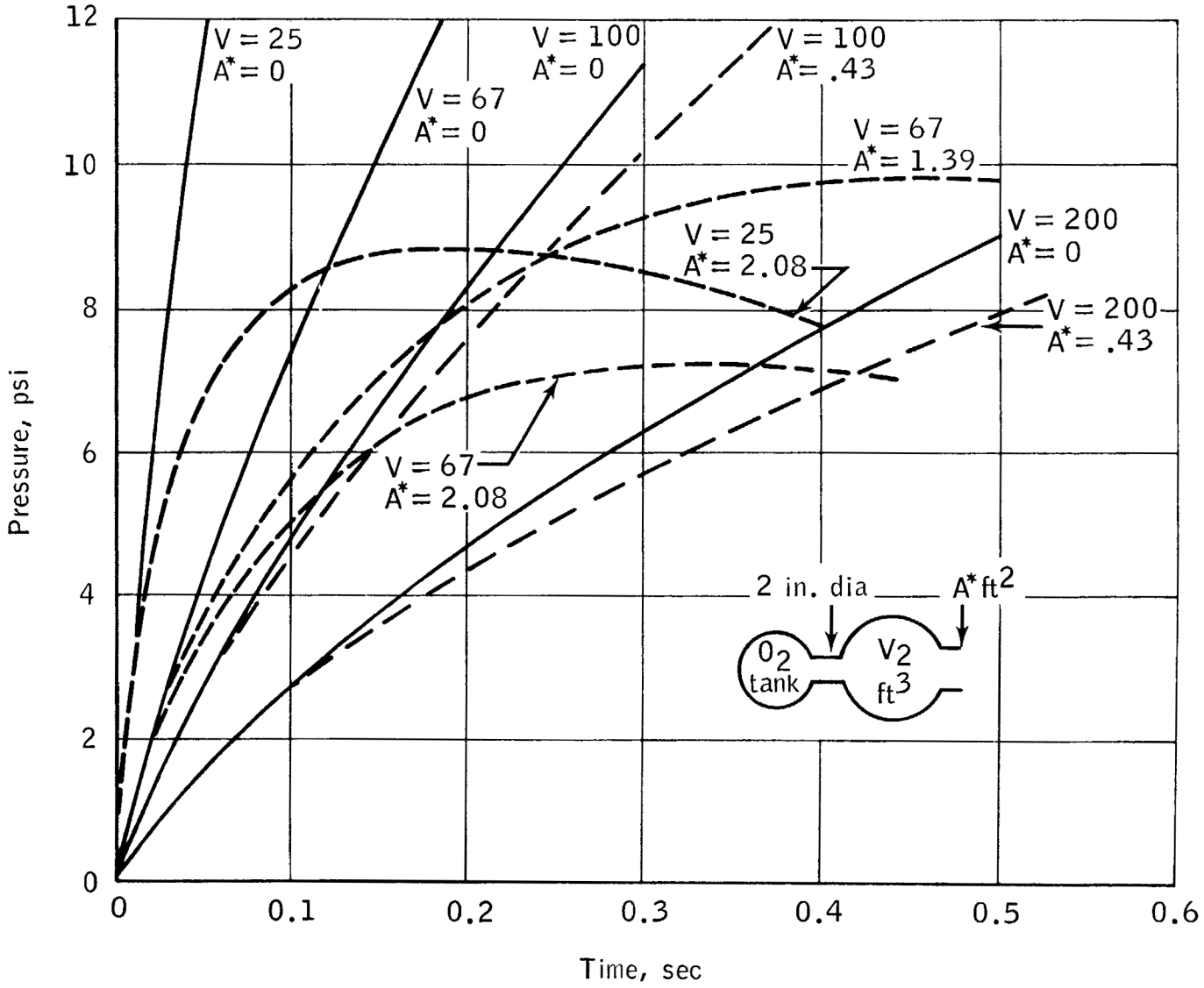

Figure F3.8-4.- Pressure rise against time (expanded scale).

The pressure of case 2, with V = 67 ft^3, rises less rapidly and consequently peaks at a later time (t = 0.32 sec) and a lower peak pressure (p $\approx$ 7.2 psi).

When the vent area for V = 67 ft^3 is decreased from 300 in^2 to 200 in^2 (case 3), the pressure rises more rapidly, peaks at a longer time (t $\approx$ 0.45 sec), and has a higher peak pressure (p $\approx$ 9.8 psia).

The large volume solutions with minimum vent areas (cases 4 and 5) have higher peak pressures (p $\approx$ 18 and 12 psia) occurring at much larger times (t = 1.1 and 1.5 sec).

Discussion and Conclusions

These "quasi-steady" two-volume, two-orifice, adiabatic calculations do not predict pressures in excess of 20 psia for a 2-inch diameter effective orifice in the oxygen tank. In fact, if the two larger volume simulations (cases 4 and 5) are excluded due to unrealistically low venting areas and/or the long time rise, then the maximum predicted pressure is below 10 psia. The smaller volumes representative of the oxygen shelf, or the oxygen shelf plus fuel cell shelf (which is fairly well intervented to the oxygen shelf) have shorter rise times which are more representative of the implied "time to panel failure" of Apollo 13. The effective venting area of these volumes is also more realistic.

On the basis of these approximate calculations, the following alternative possibilities might be considered:

1. The panel failure pressure is below 10 psi. Other experiments show this low failure pressure level to be unlikely.

2. The dynamic unsteady pressures exceed the computed quasi-steady pressures. A non-uniform pressure distribution with internal moving pressure waves is considered very probable with their importance being larger for the smaller times and volumes.

3. The oxygen tank orifice had an effective diameter greater than 2 inches. During the discharge of the first 9 pounds of oxygen, the orifice was choked with nearly saturated liquid oxygen and the coefficient was probably nearer 0.6 than 1. Thus an effective 2-inch diameter would require an even larger physical hole during this time.

4. The processes in the oxygen tank were not isentropic in a fixed volume. Either continued combustion inside the oxygen tank or the presence of a bubble of combustion products at the time of initial gas release could prevent the computed rapid decrease in mass flow with time (fig. F3.8-1) and therby increase the pressure rise rate and the peak pressure.

5. The processes in the external volume (V) are not adiabatic. Combustion of the Mylar insulation has been estimated to produce large pressures (several atmospheres) if the combustion process is rapid enough.

6. The oxygen processes are not in equilibrium. The possibility of super-satruation of the oxygen discharged into the bay and subsequent flashing to vapor might produce a strong pressure pulse.

PART F3.9

MYLAR-INSULATION COMBUSTION TEST

Objective

The purpose of this test was to determine the ignition properties and measure the rate of combustion of Mylar insulation in an initially evacuated simulated oxygen shelf space. The conditions of this test are achieved by ejection of oxygen from a 1000 psia/-190° F oxygen supply with ignition by pyrofuses placed on the Mylar blanket at several locations.

Apparatus

The basic dimensions and arrangement of the apparatus are shown in figure F3.9-1. An end view of the apparatus is shown in figure F3.9-2. Mylar blank material is placed on the bottom shelf. Oxygen is supplied through a regulator into a simulated tank dome volume. The dome contains a 2-inch diameter rupture disc which is designed to open at 80 psi. Pressures are measured during the course of combustion process. High-speed motion pictures are obtained through window ports in the chamber. The chamber volume and vent area simulate the oxygen tank shelf space.

Approach

Oxygen is supplied from a cryogenic source which is initially at 1000 psia/-190° F. Oxygen flows for a controlled time into the dome volume. The 2-inch disc ruptures at 80 psi. This exposes the initially evacuated chamber and its contents to a mixture of liquid and gaseous oxygen. A series of pyrofuses are then ignited in sequence. The data include high-speed motion pictures and pressure-time histories.

Results

A test in which oxygen was allowed to flow for 3 seconds from an initially 1000 psia/-190° F source resulted in complete combustion of a 14.5 ft^2 Mylar blanket sample. Five pyrofuses located at various locations on the Mylar blanket were sequentially activated at times ranging between 0.3 and 1.4 seconds after the disc ruptured. Examination of the chamber after this run showed that all of the Mylar blanket was consumed. The pressure rise rate with the addition of oxygen but before ignition was approximately 6 psi/sec. Ignition occurs when the pressure rises to

about 10 psi with subsequent combustion which causes a sharp increase in the pressure rise rate. The rate of pressure rise during the combustion process reaches approximately 42 psi/sec. The initial pressure rise rate of 6 psi/sec also corresponds to a measured rise rate obtained in an earlier test in which combustion did not occur. The pressure data are shown in figure F3.9-3. The conditions in the chamber before the test are shown in figure F3.9-4. Figure F3.9-5 shows the chamber just after the test.

Conclusion

The Mylar insulation blanket burns completely when ignited locally and exposed simultaneously to oxygen from a 1000 psi/-190° F source. The pressure rise rate increases from 6 psi/sec without combustion to about 42 psi/sec with the combustion of Mylar. A substantial increase in the pressure rise rate in the oxygen tank shelf space due to Mylar combustion might therefore be expected. From tests conducted elsewhere, it is further concluded that an ignition source is required to achieve Mylar/oxygen combustion.

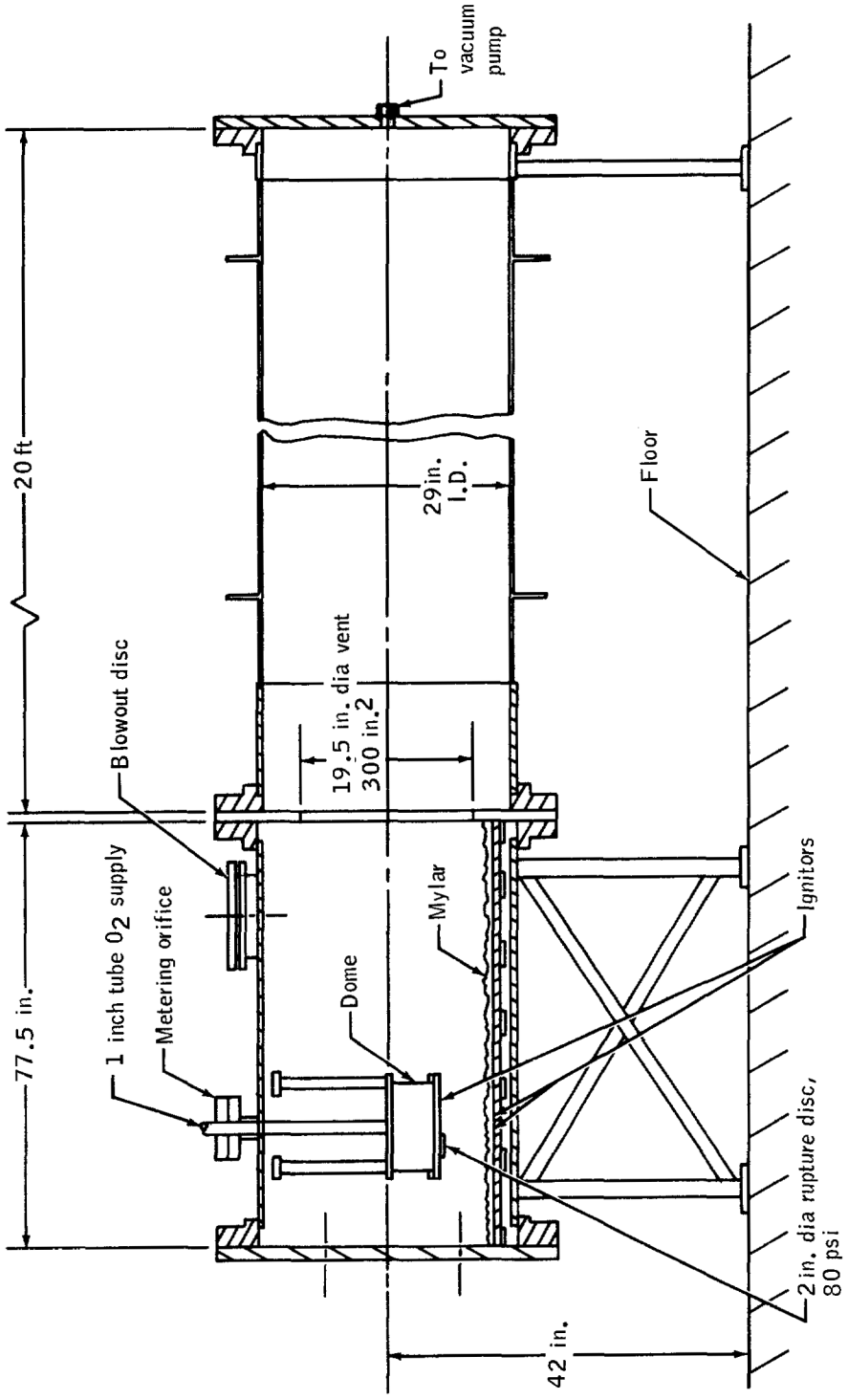

Figure F3.9-1.- Assembly of test fixture.

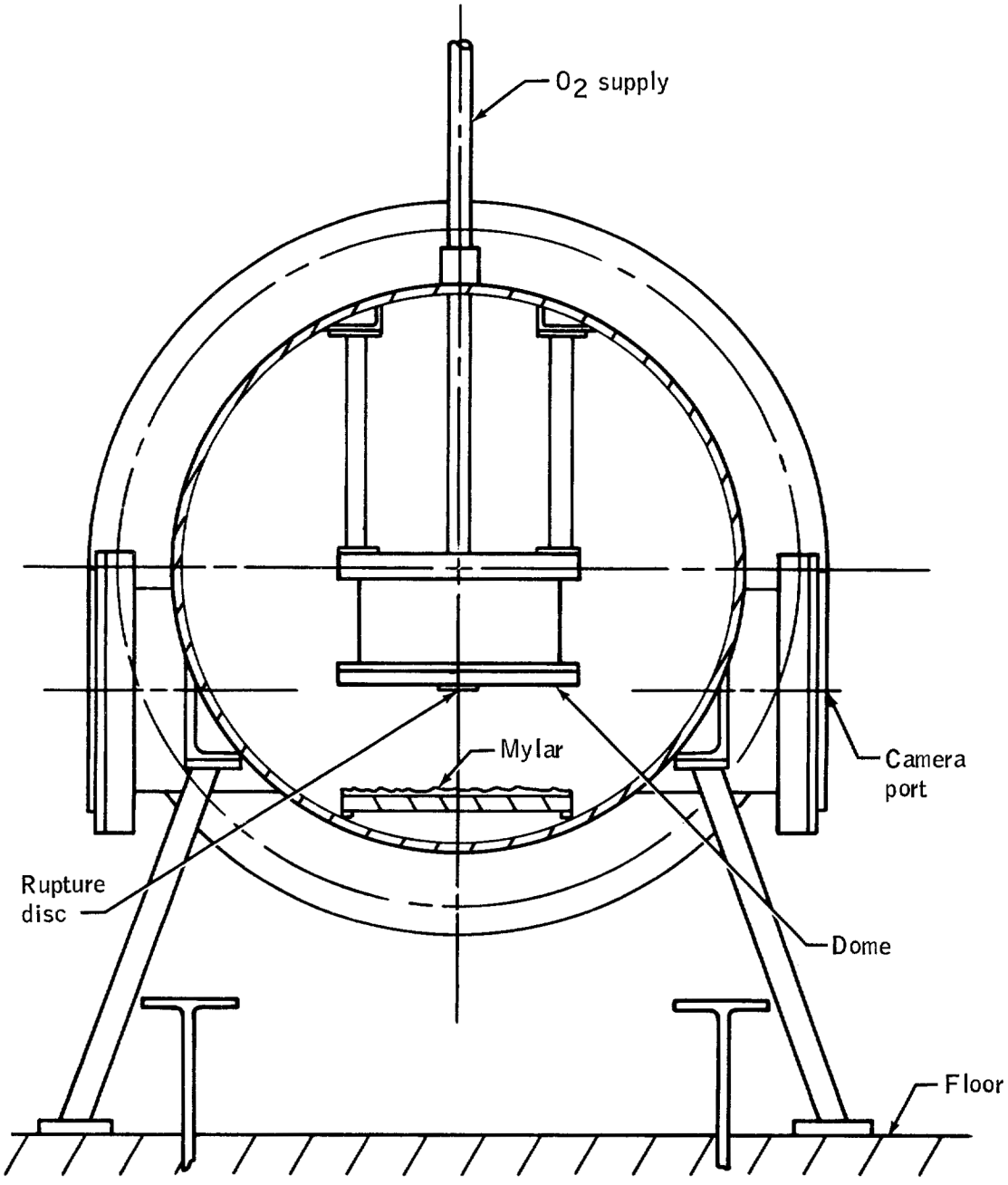

Figure F3.9-2.- Section through test fixture.

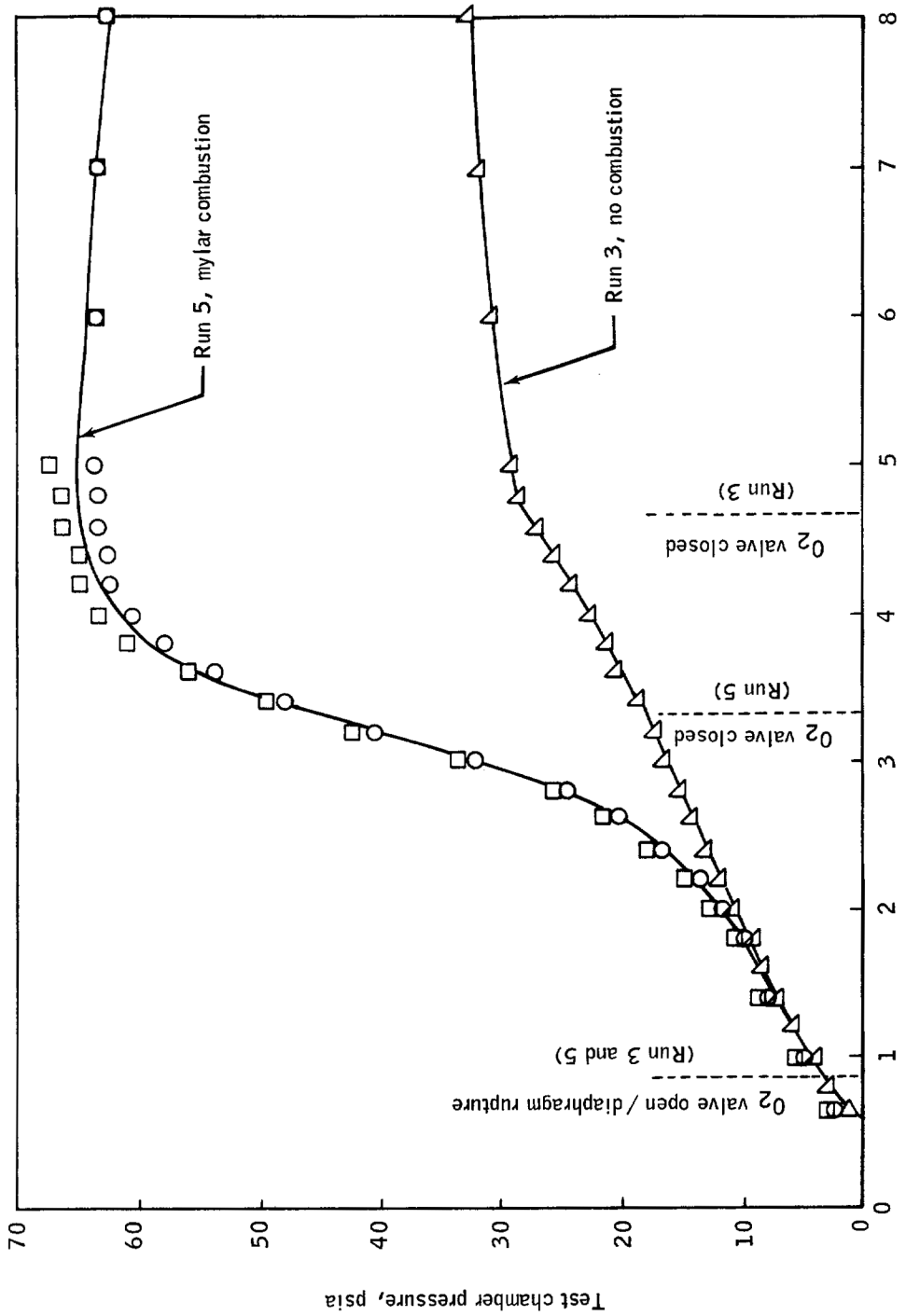

Figure F3.9-3.- Measured pressure histories for runs with and without Mylar combustion (initial oxygen tank temperature for Run 3 was -186° F and for Run 5 was -192° F).

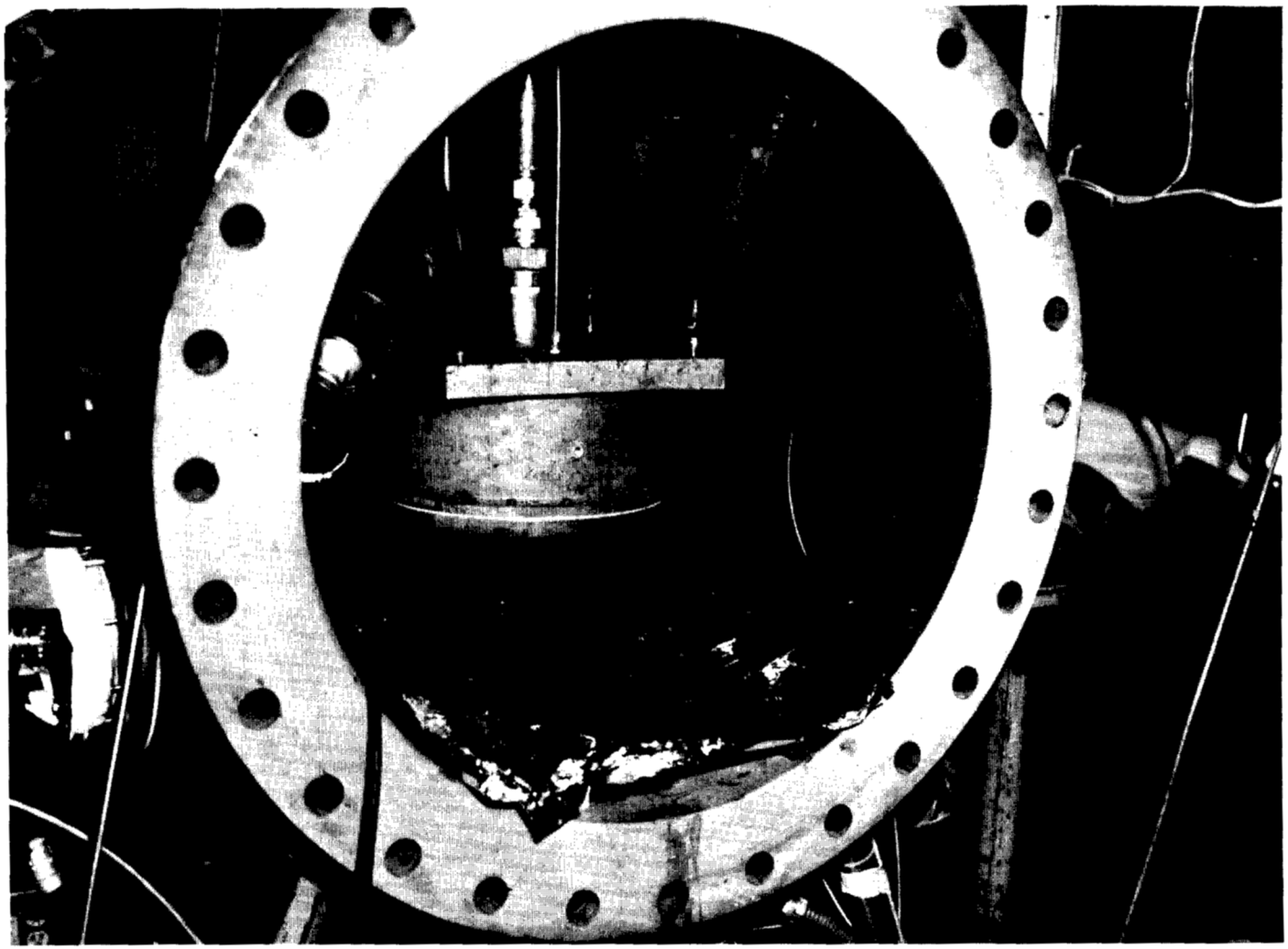

Figure F3.9-4.- View of chamber conditions before test.

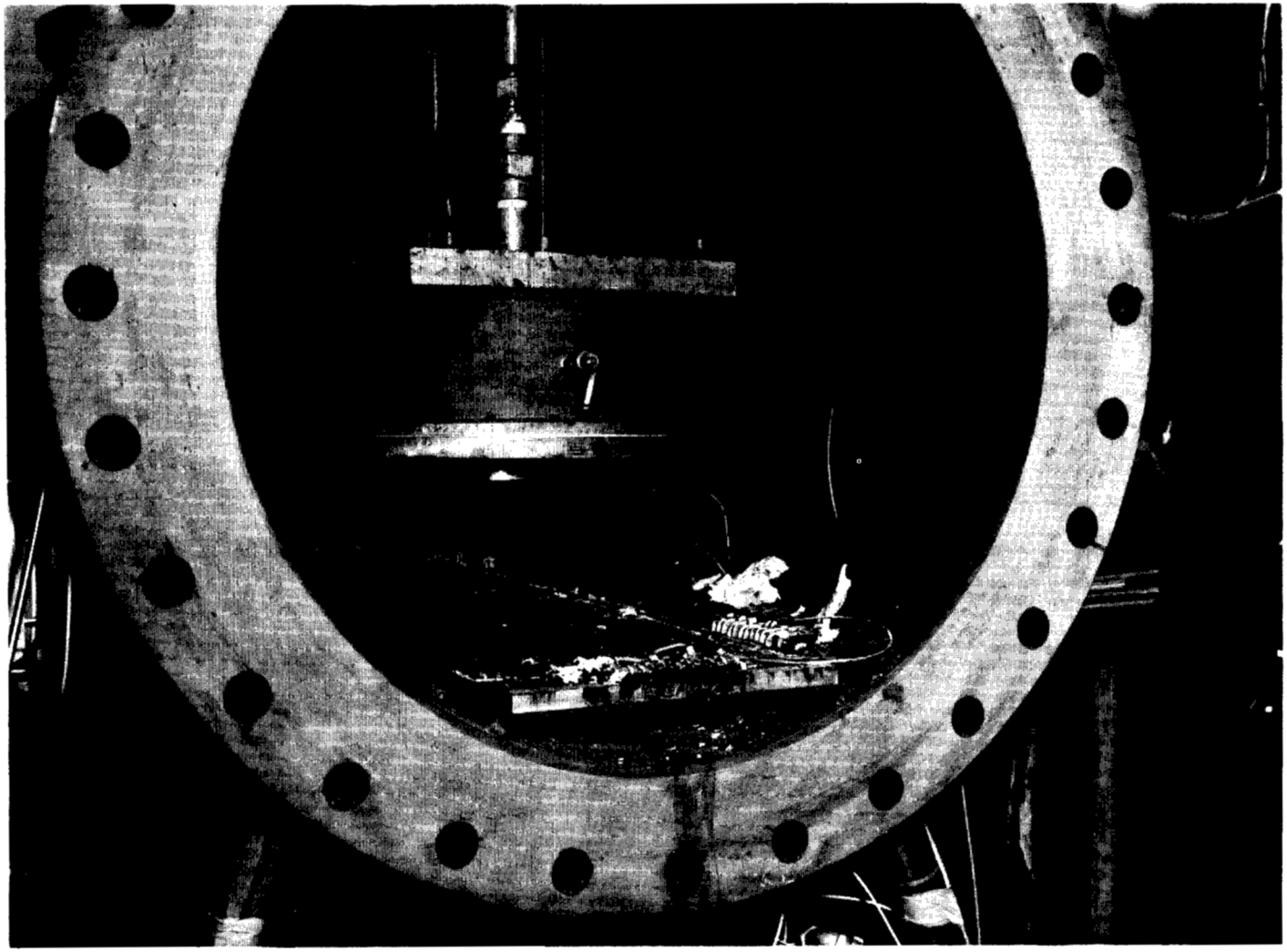

Figure F3.9-5.- View of chamber conditions after test.

PART F3.10

PANEL SEPARATION TESTS

Objectives

The objective of these tests was to demonstrate complete separation of the SM bay 4 cover panel in a manner that could be correlated with flight conditions. The panel failure mechanism and the pressure distribution that resulted in separation were also to be determined.

Approach

An experimental and analytical program utilizing one-half scale dynamic models of the SM bay 4 cover panel was conducted. Panels were attached through replica-scaled joints to a test fixture that simulated pertinent SM geometry and volume. Venting was provided between compartments and to space. A high-pressure gas system was used to rapidly build up pressure behind the cover panel as the input force leading to failure.

Size of the dynamic models (one-half scale) was determined primarily by material availability. The use of full-scale materials and fabrication techniques in the model was dictated by the need to duplicate a failure mechanism. Therefore, similarity laws for the response of structures led to scale factors of one-half for model time and one-eighth (one-half cubed) for model mass. From these scale factors for the fundamental units, some of the derived model to full-scale ratios are as follows:

Displacement	= 1/2	Force	= 1/4
Velocity	= 1	Pressure	= 1
Acceleration	= 2	Stress	= 1
Area	= 1/4	Energy	= 1/8
Volume	= 1/8	Momentum	= 1/8

A step-by-step approach to testing led to rapid learning as new factors were introduced. Initial tests were conducted on isotropic panels that scaled only membrane properties while more completely scaled sandwich panels were being fabricated. Testing started in atmosphere while preparations for vacuum testing were underway. In a similar manner, first tests concentrated on determining the pressure input required for separation and deferred the simulation of internal flow required to produce these distributions to later tests.

Analysis of the one-half scale bay 4 cover panel models used two computer programs. Initial dynamic response calculations using a nonlinear elastic finite difference program indicated that panel response was

essentially static for the class of pressure loadings expected in the tests. Subsequent calculations used static loadings with a nonlinear elastic finite element representation and the NASTRAN computer program.

Apparatus

Models.- Figure F3.10-1 shows the full-scale and model panel cross sections.

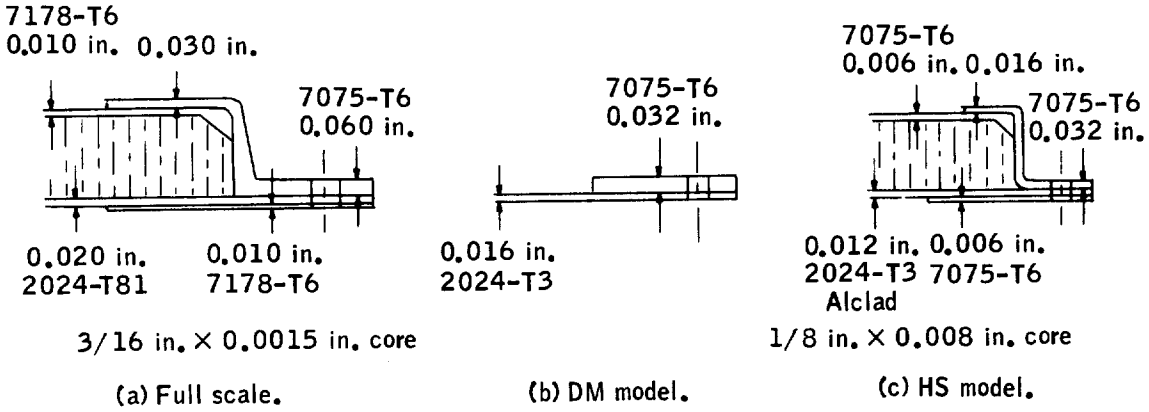

Figure F3.10-1.- Panel designs.

The full-scale panel is a honeycomb sandwich structure with a z-bar edge closeout attached to the SM by 1/4-inch bolts around the edges and to each of the bay 4 shelves. The first one-half scale panel models, designated DM and shown in figure F3.10-1(b), scaled membrane properties of the full-scale sandwich panel inner and outer face sheets with a single isotropic panel having the correct nominal ultimate tensile strength. The z-bar was simulated by a flat bar that represented the shear area of the outer z-bar flange. Fastener sizes, bolt patterns, and bonding material were duplicated from full scale.

One-half size honeycomb sandwich panels, designated HS and shown in figure F3.10-1(c), scaled both bending stiffness and membrane stiffness. Although core density of the sandwich models is slightly high, the dimensions, materials, bonding, and z-bar closeout are scaled. Some alloy substitutions were made but nominal strength requirements were met.

Test fixture.- The test fixture shown schematically in figure F3.10-2 and in the photographs of figure F3.10-3 is a one-half size boilerplate mockup of the SM bay 4 and central tunnel. Vent areas connect the bay 4 shelf spaces to the central tunnel and to each other. The tunnel also has

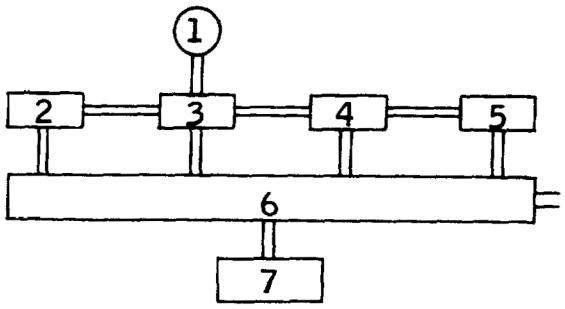

Volume	Description
1	Pressurization tank
2	Fuel cell space
3	O_2 Tank space
4	Upper H_2 tank space
5	Lower H_2 tank space
6	Tunnel
7	Other SM free volume

Figure F3.10-2.- Schematic of test fixture.

vents to space and to a large tank simulating the remaining free volume of the SM. Vent areas were adjusted in initial tests to obtain desired pressure distributions but were scaled from the best available data for final testing. The fixture also holds the pressurization system and instrumentation. True free volume was approached by adding several wooden mockups of equipment.

Pressurization system.- The pressurization system can also be seen in the photographs of figure F3.10-3. A 3000-psi accumulator is discharged on command through an orifice by mechanically rupturing a diaphragm. The gas expands into the oxygen shelf space of bay 4 through a perforated diffuser. In order to obtain uniform pressure over the entire panel for some tests, the diffuser was lowered so that it discharged into both the oxygen and hydrogen shelf spaces. For these particular tests, extra vent area was provided between all shelves to insure uniform pressure throughout bay 4. For most tests, a shield was placed between the diffuser and panel to minimize direct impingement.

Other.- Instrumentation consisted of strain gages, fast response pressure sensors, and high-speed motion picture cameras. Atmospheric tests were conducted in the Rocket Test Cell and vacuum tests at 1mm Hg pressure in the 60-Foot Vacuum Sphere at Langley Research Center.

(a) General view.

(b) Fixture with panel installed.

(c) Internal view.

Figure F3.10-3.- One-half size boilerplate mockup of the SM bay 4 and central tunnel.

Results and Discussion

Presentation of results.- The test program is summarized in table F3.10-I. Typical failures and pressure-time histories are illustrated in figure F3.10-4. Figure F3.10-5 is a sequence of prints from high-speed movie cameras that demonstrate separation of the sandwich panel models. Results of NASTRAN calculations on the one-half scale models are presented in figures F3.10-6 and F3.10-7.

Demonstration of panel separation.- Panel separation has been demonstrated with both membrane and sandwich panels. Two sandwich panels separated completely from the test fixture during vacuum tests. Two membrane panels, although less representative of flight conditions, also separated completely in vacuum tests. However, similar tests with membrane panels in atmosphere left portions of panels attached to the test fixture as illustrated in figures F3.10-4(b) and (c). Complete separation in atmosphere could not be achieved due to mass and drag of the air.

Pressure distributions.- Complete membrane panel separation was achieved only with nearly uniform pressure distribution over the entire bay 4 panel cover, shown in figure F3.10-4(d). When just the oxygen shelf space experienced high pressures, membrane panel separation was localized to the area of the panel over the oxygen shelf space as shown in figure F3.10-2(a). This type of local failure occurred in both atmosphere and vacuum. When scaled internal venting was introduced, model DM-10 lost a slightly larger portion of panel due to high pressure experienced by both the oxygen shelf and fuel cell shelf spaces while the rest of bay 4 was at low pressure.

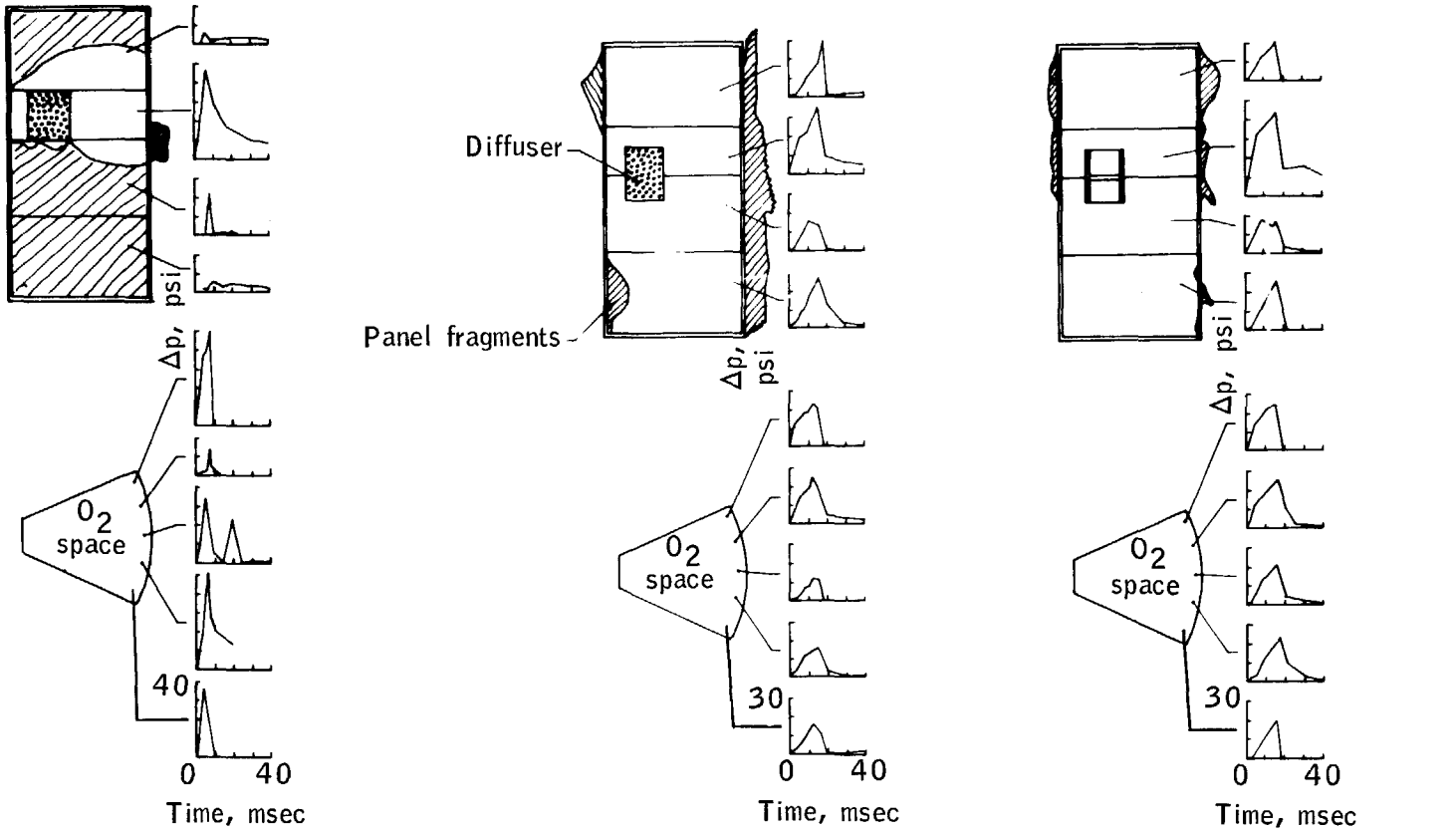

a. Membrane panel DM-2, atmosphere, band load

b. Membrane panel DM-3, atmosphere, uniform load

c. Membrane panel DM-4, atmosphere, uniform load, no direct impingement

Figure F3.10-4.- Failure modes and pressure-time histories.

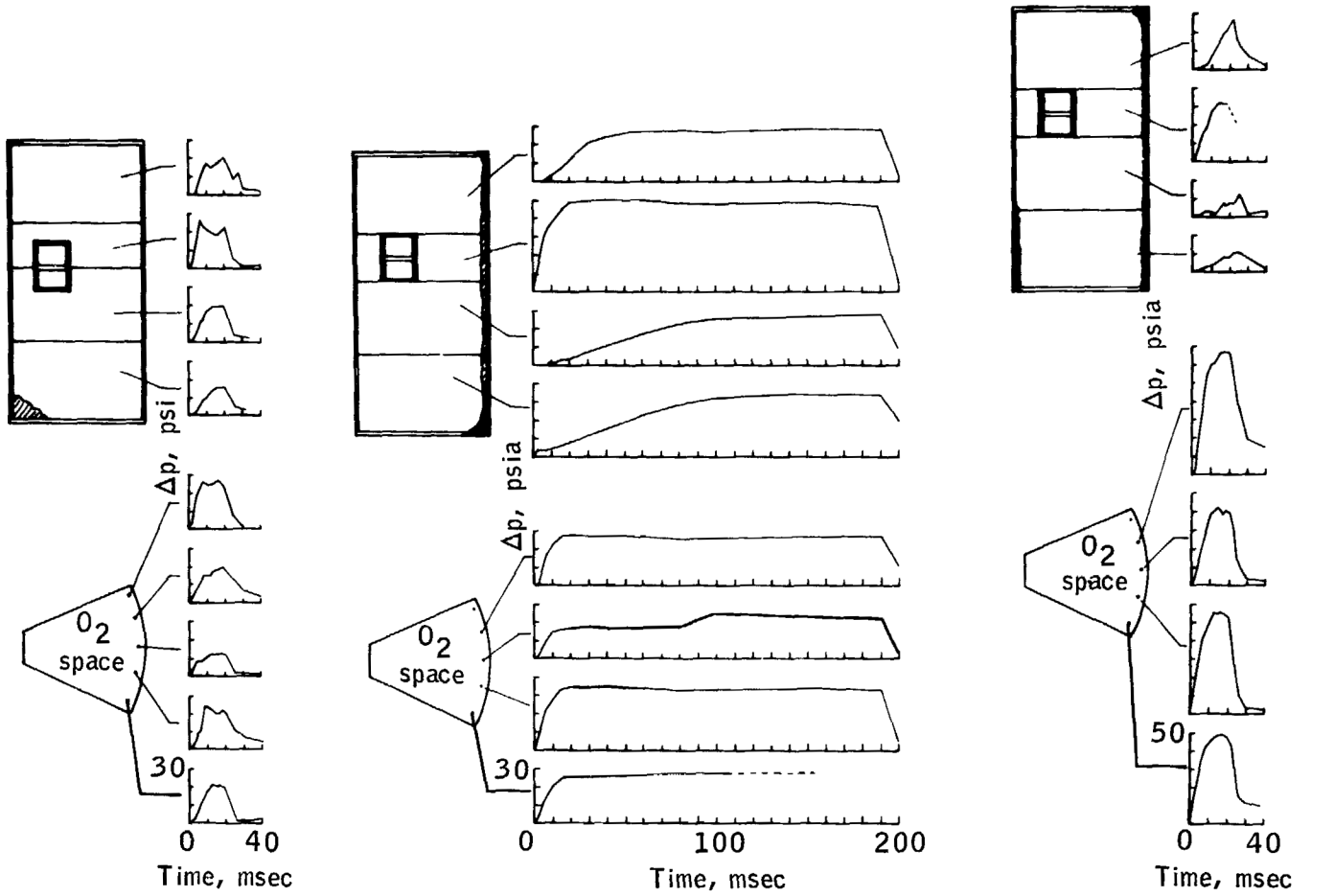

d. Membrane panel DM-6, vacuum, uniform load, no direct impingement

e. Sandwich panel HS-2, vacuum, no direct impingement

f. Sandwich panel HS-3, vacuum, no direct impingement

Figure F3.10-4.- Concluded.

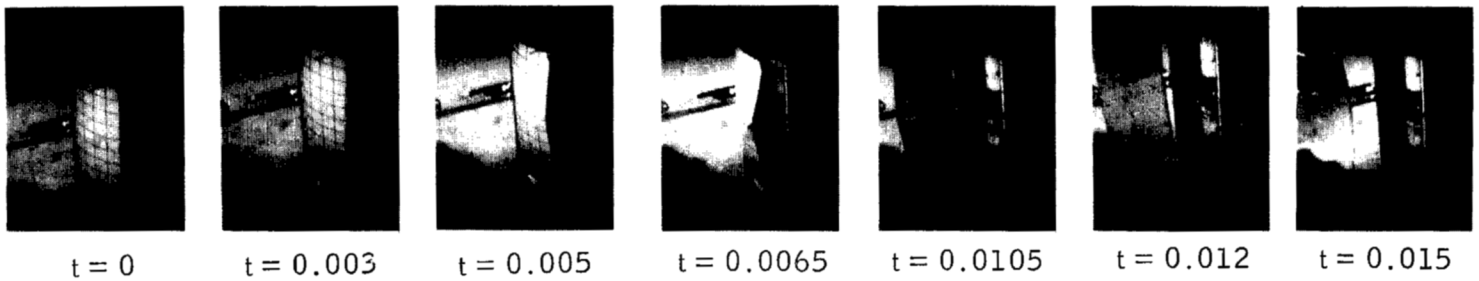

(c) Sandwich panel HS-2.

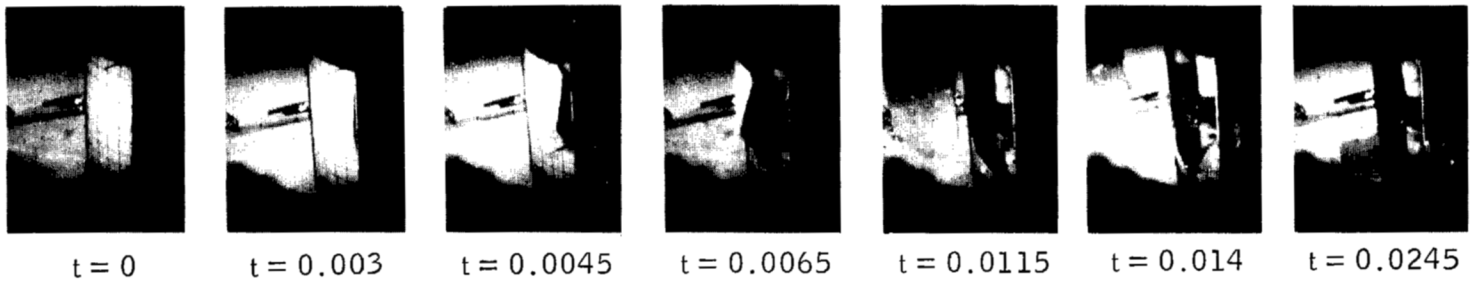

(b) Sandwich panel HS-3.

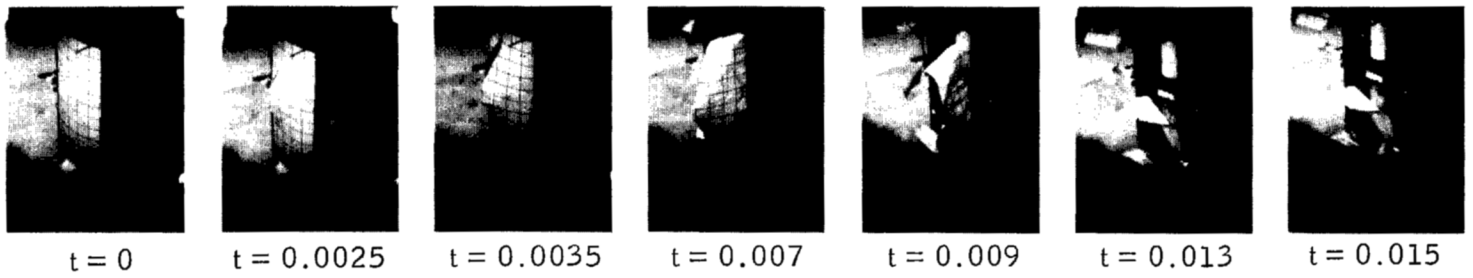

(a) Membrane panel DM-6.

Figure F3.10-5.- Sequential failure of two sandwich and one membrane panel (t = time from first observed failure).

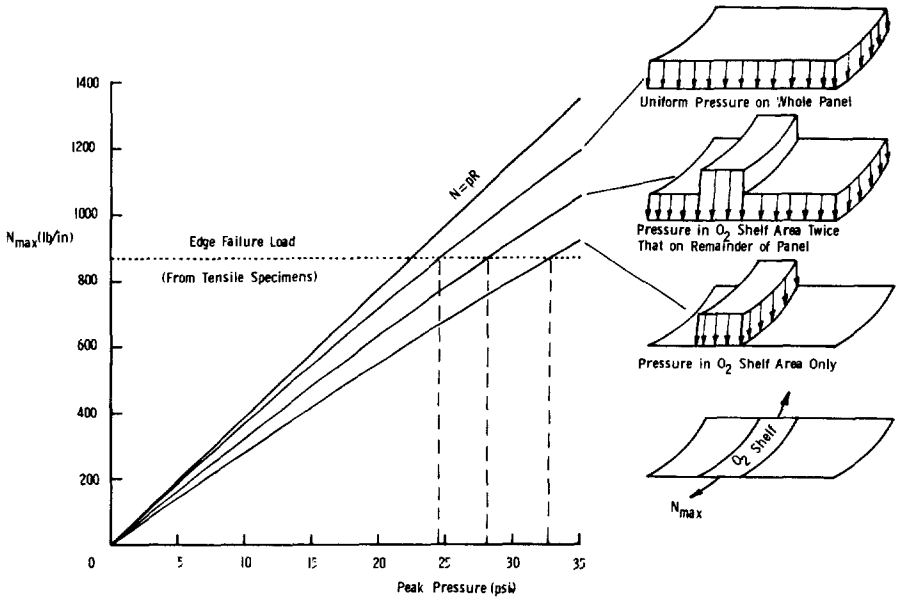

Figure F3.10-6.- Maximum edge load on half-scale honeycomb panel as predicted by NASTRAN.

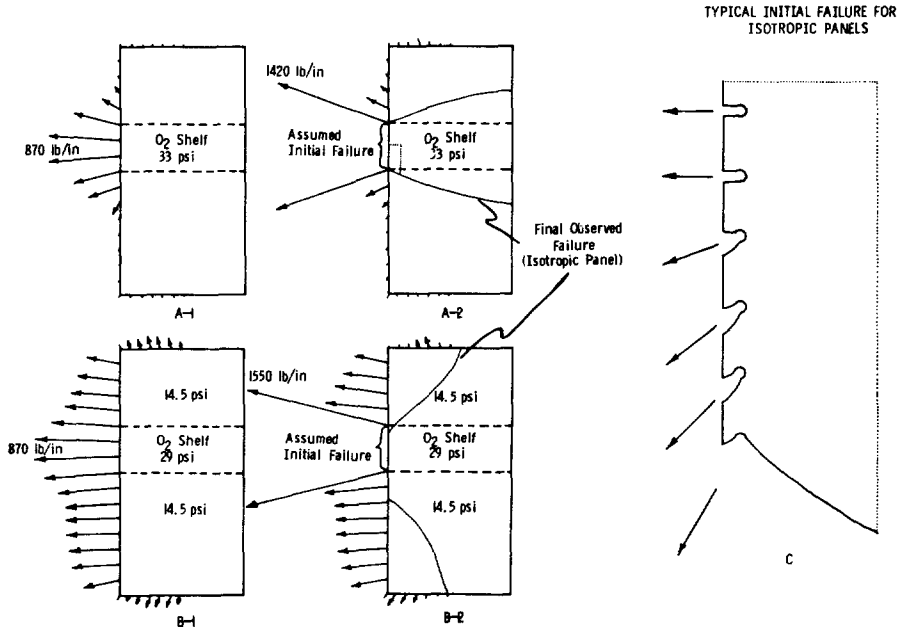

Figure F3.10-7.- Distribution of edge loads on half-scale Apollo 13 honeycomb panel as predicted by NASTRAN.

TABLE F3.10-I.- PANEL SEPARATION TEST SUMMARY

Model	Internal vents	Volume first pressurized	Diffuser	Load character	Pressure*		Failure
					Peak, psi	Rise time, sec	
Atmosphere tests							
DM-1-1	Not scaled	Oxygen shelf	Open	Band	24-30	0.020	None
DM-1-2	Not scaled	Oxygen shelf	Open	Band	30-58	0.005	Oxygen shelf area
DM-2	Not scaled	Oxygen shelf	Open	Band	34-52	0.006	Oxygen shelf area
DM-3	Not scaled	Bay 4	Open	Uniform	15-35	0.015	Nearly total (folded back)
DM-4	Not scaled	Bay 4	Shielded	Uniform	20-26	0.016	Nearly total (left edges)
Vacuum tests							
DM-5-1	Not scaled	Bay 4	Shielded	Uniform	14-20	-	None
DM-5-2	Not scaled	Bay 4	Shielded	Uniform	20-28	0.016	Total
DM-6	Not scaled	Bay 4	Shielded	Uniform	19-27	0.018	Total
DM-7	Not scaled	Oxygen shelf	Open	Band	25-40	0.005	Oxygen shelf area
DM-8	Not scaled	Oxygen shelf	Shielded	Band	20-37	0.012	Oxygen shelf area
DM-9	Not scaled	Oxygen shelf	Shielded	Band	18-23	0.040	None
DM-10	Scaled	Oxygen shelf	Shielded	-	21-39	0.070	Upper 2/3 of panel
HS-1	Scaled	Oxygen shelf	Shielded	-	-	-	None
HS-2	Scaled	Oxygen shelf	Shielded	-	23-32	0.190	Total
HS-3	Scaled	Oxygen shelf	Shielded	-	30-67	0.020	Total
HS-4	Scaled	Oxygen shelf	Shielded	-	30-44	0.020	None

*Range of peak pressures in the oxygen shelf space is indicated. Time from pressure release to peak pressure is rise time.

Complete separation of sandwich panels has been obtained with both uniform and nonuniform pressure distributions. Figure F3.10-8 shows the type of pressure time histories experienced by various sections of the panels. The pressure predictions are based on the internal flow model

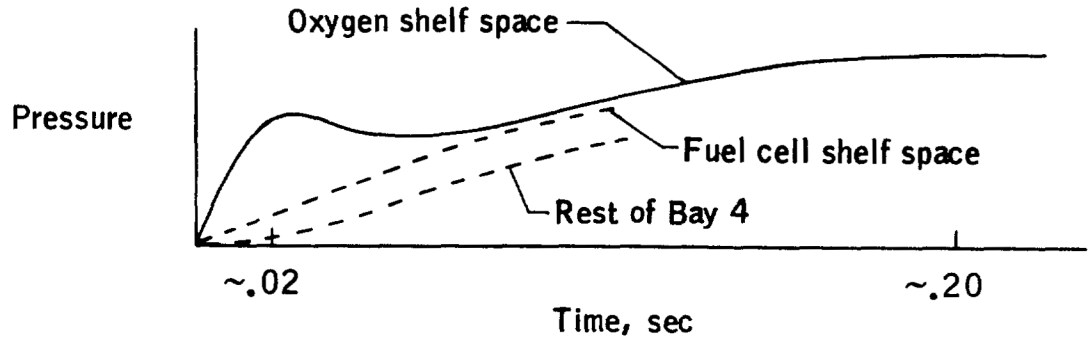

Figure F3.10-8.- Pressure build-up in bay 4.

of the Apollo 13 SM shown in figure F3.10-2 and have been verified in these experiments. Peak pressure levels were varied from test to test but the curve shape was always similar. One sandwich panel separated after about 0.02 second during the initial pressure rise in the oxygen shelf space, while overall panel loading was highly nonuniform as shown in figure F3.10-4(b). The other sandwich panel did not separate until about 0.19 second after all bay 4 compartments had time to fill with gas and arrive at a much more uniform loading, as shown in figure F3.10-4(e).

The effect of pressure distribution on peak pressures required for failure is shown by the NASTRAN calculation in figure F3.10-6. Included for reference is the linear membrane result, $N = pR$. The load required for edge failure was determined from tensile tests on specimens of the DM model joints. The peak uniform pressure at failure initiation is only 75 percent of peak pressure at the failure load with just the oxygen shelf space pressurized.

Failure mechanism.- The failure mechanism for complete separation of a membrane panel is demonstrated by the photographic sequence in figure F3.10-5(a). Failure is probably initiated by a localized high pressure near the edge of the oxygen shelf space. A crack formed where a shelf bolt head pulled through and rapidly propagated through the panel. Expansion of the pressurizing gas through the openings accelerated

panel fragments to very high velocities. Inertia loads from the high acceleration completed the separation. Membrane panels were observed to separate in three pieces--one large and two small fragments.

The failure of a sandwich panel under uniform loading in vacuum is shown in the picture sequence of figure F3.10-5(c). Failure started at the edge of the oxygen shelf space by pull-through of the edge bolts through the upper sandwich face sheet. Very rapid tearout along three edges followed, primarily by tension in the face sheets and tearing of the core material from the z-bar at the edge. The panel then rotated like a door and separated from the test fixture in one piece.

Nonuniform loading of a sandwich panel led to the failure shown in figure F3.10-5(b). Initial failure was at the panel edge near the fuel cell shelf. Tearout along one edge and the top rapidly followed, similar to the previous failure. However, the edge tear stopped before reaching the bottom and became a diagonal rip that left the lower third of the panel attached to the fixture. The upper two-thirds of the panel then rotated door-like and separated. Finally, a vertical tear propagated through the center of the remaining fragment, the bottom tore out, and rapid rotation separated the remnants in two pieces.

Figure F3.10-7 relates NASTRAN calculations to the observed failures. Predicted edge load direction and magnitude are illustrated for two pressure distributions. In figure F3.10-7, parts A-1 and B-1, panel edges are assumed fixed, while in figure F3.10-7, parts A-2 and B-2, the panel edge joint along the oxygen shelf space is assumed to have failed. Also shown in figure F3.10-7, parts A-2 and B-2, are typical observed failure patterns for these types of loadings on membrane panels. An enlargement of the dotted section of figure F3.10-7, part A-2, is shown in part C of the figure to indicate the type of edge failure observed. Arrows indicate the direction of force required to cause the pullout failures. The NASTRAN edge force patterns are consistent with these failures. In addition, figure F3.10-7, parts A-2 and B-2, indicates that tears into the membrane panels tend to remain normal to the direction of the edge forces.

Correlation with flight.- Tests with sandwich panels more closely similate flight conditions than tests with membrane panels due to initial failure characteristics and post-failure separation behavior. The separation behavior of sandwich model HS-3, figures F3.10-4(f) and F3.10-5(b), is also believed to be more representative of flight than the separation behavior of model HS-2, figures F3.10-4(e) and F3.10-5(c), for two reasons. First, although model HS-2 was tested with scaled internal venting between the compartments of bay 4 and the SM tunnel, the rest of the SM free volume had been closed. In the HS-3 model test, this vent area had been opened to a realistic value of 60 square inches. Second, the slow pressure buildup before separation of model HS-2 allowed SM tunnel pressure to rise well above the 10-psi limitation required to

prevent CM-SM separation. Pressurization leading to model HS-3 separation was so rapid (20 milliseconds) that SM tunnel pressure remained below the 10-psi limit. The time to failure would scale up to 40 milliseconds for the flight configuration.

Tests with models HS-3 and HS-4 have bracketed the most likely separation conditions. For both tests, internal venting was scaled and diffuser configuration and accumulator pressure were identical. Model HS-3 separated due to an initial air flow of 190 lb/sec through an orifice of 2.85 square inches. Separation was not achieved on model HS-4 when initial air flow was 135 lb/sec through a 2.0-square inch orifice, even though peak pressures of over 35 psi occurred in the oxygen shelf space after 20 milliseconds.

As a part of this study, an analysis has also been carried out at the Langley Research Center to estimate the distribution and time history of pressures within the Apollo 13 service module. Based on these calculations and the experimental results on panel separation, it appears that additional combustion outside the oxygen tank or rapid flashing of ejected liquid oxygen may have occurred to produce panel separation. A report of this analysis can be found in the official file of the Review Board.

Conclusions

Complete separation of one-half scale honeycomb sandwich models of the bay 4 cover panel in vacuum has been demonstrated. Separation was achieved by rapid air pressurization of the oxygen shelf space. Internal volumes and vent areas of the SM were scaled. Separations were obtained with both uniform and nonuniform pressure distributions. The separation resulting from a nonuniform loading that peaks 20 milliseconds after start of pressurization (40 milliseconds full scale) correlates best with hypotheses and data from flight. This particular panel separated in three pieces after an initial tear along the sides that allowed it to open like a door. Inertial loads are a major factor in obtaining complete separation after initial failure.

PART F4

MASTER LIST OF TESTS AND ANALYSES

This part presents a listing of tests and analyses grouped according to the following event categories:

Shelf Drop

Detanking

Quantity Gage Dropout

Short Generation

Ignition

Propagation of Combustion

Pressure Rise

Temperature Rise

Pressure Drop

Final Instrument Loss

Telemetry Loss

Tank Failure

Oxygen Tank No. 1 Pressure Loss

Panel Loss

Side Effects

Miscellaneous

MASTER LIST OF TESTS AND ANALYSES

[By Event]

Number (T/A) Location Monitors	Title	Objective - Description	Status - Results - Remarks
		"SHELF DROP"	
13-T-55(T) MSC P. Glynn R. Lindley	Tank Impact Test	Determine energy required to produce a dent in tank dome and determine the approximate input g level to tank.	C - May 26, 1970. A load of 7g was required to produce a dent in the tank shelf.
13-T-60 MSC P. Glynn S. Himmel	Quantity Gage Rivet Test	Apply incrementally increasing force to the load rivet supporting the quantity probe concentric tubes until the rivet fails. X-ray the rivet during significant failure stages to show the failure mechanism.	C - April 27, 1970. Shortly after a load of 105 lb was applied, a decrease to 90 lb was noted, indicating a failure. When the load was increased to 120 lb, the rivet failed by bending and subsequently pulling through the probe tubing.
A-92(T) LRC R. Herr R. Lindley	Shock Load Failure Test of Fan Motor Mounting Screws	Determine by test the shock load at which the four 4-40 x 1/4-inch steel fan mounting screws fail.	C - May 8, 1970. The four machine screws started yielding between 2000g and 2500g with complete failure in tension between 4000g and 4200g with an attached 0.875-lb mass.
		DETANKING	
13-T-07R3(T) Beech A/C S. Owens K. Heimburg	Apollo 13 Oxygen Detanking Simulation	Determine the effects on the tank wiring and components of the detanking sequence with the Inconel sleeve and Teflon block displaced in the top probe assembly.	ECD - June 18, 1970. Test in progress.

LEGEND: (T) - Test (A) - Analyses C - Completed ECD - Estimated Completion Date TBD - To Be Determined

MSC Form 343 (OT)

NASA — MSC

MASTER LIST OF TESTS AND ANALYSES

[By Event]

Number (T/A) Location Monitors	Title	Objective - Description	Status - Results - Remarks
		DETANKING	
13-T-08R1(T) MSC C. Propp K. Heimburg	Bench Test of Oxygen Tank Conduit	Determine whether the electrical loads and pressure cycling during KSC detanking raised the wire temperature in the conduit to damaging levels.	C - May 15, 1970. Maximum temperature of the conduit (at the midpoint) reached 325° F. Pressure cycling of the tank did not raise the temperature significantly. Inspection showed no degradation. Test results will be confirmed by TPS 13-T-07R3(T).
13-T-19(T) NR J. Jones K. Heimburg	Ground Support Equipment Filter Analysis	Identify contaminants (oil and glass beads) found in GSE filter pads during Apollo 13 oxygen tanking at KSC and determine if the filter material could be responsible for the failure to detank.	C - April 20, 1970. This test showed that the filter assembly did not contribute to the system malfunction. Oxygen-compatible lubricant was found on filter.
13-T-20(T) KSC H. Lamberth K. Heimburg	Heater Cycle Test at KSC	Determine if the oxygen tank heater cycled during the 7-hour period of prelaunch detanking at KSC.	C - May 1, 1970. Test results indicate that heater cycling would cause voltage drop on other channels. The prelaunch records during detanking show that the heaters did not cycle but remained continuously "on."
13-T-53(T) MSC C. Propp K. Heimburg	Heater Assembly Temperature Profile	Determine if the heater temperatures could have been high enough during the KSC detanking to degrade the fan motor lead wire insulation. Tests are to be carried out using nitrogen.	C - May 26, 1970. Tests indicate heater surface could reach 1000° F. Wire conduit could reach 750° F. Teflon insulation was damaged. A second detanking test resulted in thermal switch failure in the closed position with 65 V dc applied.

LEGEND: (T) - Test (A) - Analyses C - Completed ECD - Estimated Completion Date TBD - To Be Determined

MASTER LIST OF TESTS AND ANALYSES

[By Event]

Number (T/A) Location Monitors	Title	Objective - Description	Status - Results - Remarks
		DETANKING	
13-T-80 MSC C. Propp H. Mark	Thermostatic Switch Failure Tests	Determine the voltage and current levels at which the thermostatic switches weld shut in the closed position when they attempt to open in response to temperatures exceeding 80° F.	C - June 5, 1970. The thermostatic switches fail to open where currents exceeding 1.5 amps at 65 V dc are passed through them. The heater current used in the special detanking procedure at KSC was 7 amps at 65 V dc, well in excess of the measured failure current.
A-15(T) KSC T. Sasseen E. Baehr	Blowdown Characteristics of Oxygen Tanks	Determine the bleeddown time from 250 psig using GSE at KSC with the proper configuration for one tank and the fill tube completely disconnected for the other tank.	C - May 15, 1970. The test proved that both tanks did depressurize in practically identical times considering the difference in vent lines and back pressure. The test refuted the earlier assumption of a time difference between the different tank configurations. The significance is that blowdown data are not sensitive enough to determine the fill tube configuration.
		QUANTITY GAGE DROPOUT	
13-T-30(T) MSC R. Robinson R. Wells	Quantity Gage and Signal Conditioner Test	Determine the signal conditioner response under extreme transient conditions of ambient temperature, determine quantity gage failure indications, and define transient and steady-state energy levels supplied to every possible fault condition.	C - May 22, 1970. The quantity gage signal conditioner deviated less than 0.85 percent under extreme temperature excursions, the response of the gage to various electrical faults was catalogued, and an analysis of the energy level of faults was made. The significance of this test is that it permits interpretation of abnormal quantity gage readings at the time of the accident and eliminates the gage as a probable source of ignition.

LEGEND: (T) - Test (A) - Analyses C - Completed ECD - Estimated Completion Date TBD - To Be Determined

MSC Form 343 (OT)

NASA — MSC

MASTER LIST OF TESTS AND ANALYSES

[By Event]

Number (T/A) Location Monitors	Title	Objective - Description	Status - Results - Remarks
SHORT GENERATION			
13-T-11(T) MSC R. Robinson R. Wells	Fan Motor Inductive Voltage Discharge and Electrical Energy Release	Determine the amount of stored energy released from the fan motor when one power lead is opened.	C - May 7, 1970. The test showed a power release of 0.02 joule. Transient peak voltage of 1800 volts and current of 0.7 amp were measured. These data establish the energy potential from an open circuit failure of a fan motor.
13-T-22(T) MSC G. Johnson R. Wells	Inverter Operational Characteristics	Determine the operating characteristics of the spacecraft ac inverter when operated with three-phase, phase-to-phase, and phase-to-neutral step loads and short circuits.	C - April 20, 1970. Generally, faults introduced on a particular phase gave a voltage reduction on that phase and a voltage rise on the other phases. Clearing the faults gave the opposite response. This information assists in interpretation of flight data.
13-T-23(T) MSC J. Hanaway R. Wells	AC Transient Voltage Signal Duplication	To determine whether bus 2 transients are capable of producing the type of response seen in the SCS auto TVC gimbal command servo signals just prior to the oxygen tank failure.	C - April 22, 1970. This series of tests applied transients to the ac bus that dipped the bus voltage to 105, 95, 85, and 80 volts for durations of 50, 100, and 150 milliseconds. The transient that dipped the voltage to 85 volts for 150 milliseconds, caused a transient of 0.16 degree per second in the SCS signals, which matched the largest transient observed in the flight data. The significance of this is that it allows more precise timing of the duration, and estimation of the magnitude, of possible causes of ignition.

LEGEND: (T) - Test (A) - Analyses C - Completed ECD - Estimated Completion Date TBD - To Be Determined

NASA — MSC

MSC Form 343 (OT)

MASTER LIST OF TESTS AND ANALYSES

[By Event]

Number (T/A) Location Monitors	Title	Objective - Description	Status - Results - Remarks
		IGNITION	
13-T-01(T) MSC L. Leger I. Pinkel	Ignition of Fan Motor Winding by Electrical Overload	Determine if overloaded fan motor winding will cause ignition and combustion of the insulation in supercritical oxygen. Initial conditions were 115 volts, 1-amp fuse, current initially 1 amp and increased in 0.5-amp increments.	C - April 24, 1970. Windings were not fused by 400 Hz-5 amps; 8 amps dc fused winding wire. Ignition did not occur. Results were the same in nitrogen and oxygen at 900 psia, -180° F. NR test shows same result.
13-T-13(T) MSC C. Propp I. Pinkel	Spark Ignition Energy Threshold for Various Tank Materials	Determine if an electrical spark generated by tank wiring can ignite selected nonmetallic tank materials.	C - May 30, 1970. A single Teflon insulated wire may be ignited with energies as low as 0.45 joule with a spark/arc.
13-T-15(T) ARC L. Stollar H. Mark	Spark Source Ignition in Supercritical Oxygen	Determine if Teflon can be ignited with 115 V ac spark under various conditions in oxygen atmospheres.	C - April 30, 1970. Three tests in oxygen of 50 psig, 500 psig, and 940 psig at ambient temperature showed insulation ignited and burned in all cases. In oxygen at 940 psig and -190° F the Teflon insulation ignited and burned with a 138-psig pressure rise and no noticeable temperature rise.
13-T-21(T) MSC G. Johnson I. Pinkel	One-Amp Fuse Test	Determine the time/current characteristics to blow the 1-amp fuses in the tank fan circuit.	C - April 20, 1970. The fuses blow at the following currents and times: 4 amp - 0.05 second, 8 amps - 0.025 second. These values give approximately 16 joules.
13-T-24(T) MSC C. Propp I. Pinkel	Tank Materials Ignition Test	Exploratory test with electrical overloads and nichrome heaters to determine the ignition and combustion possibilities of tank materials in low and high pressure gaseous oxygen and ambient pressure liquid oxygen.	C - May 30, 1970. Drilube 822 and all of the different types of tank wiring ignited. Nickel wire was only partially consumed in LOX and solder could not be ignited. The power levels required to get ignition were far in excess of the amount available in the tank.

LEGEND: (T) - Test (A) - Analyses C - Completed ECD - Estimated Completion Date TBD - To Be Determined

NASA — MSC

MSC Form 343 (OT)

MASTER LIST OF TESTS AND ANALYSES

[By Event]

Number (T/A) Location Monitors	Title	Objective - Description	Status - Results - Remarks
		IGNITION	
13-T-25(T) MSC P. McLaughlin	Locked-Rotor Motor Fan Test	Determine motor behavior in a locked condition and check possibility of ignition and propagation.	C - April 19, 1970. Two motors were tested in LOX and powered for 2.3 and 1.0 hours, respectively. There was no indication of malfunction such as heating, arcing, or sparking. Posttest measurements showed no degradation of motor wire insulation.
13-T-28(T) MSFC R. Johnson I. Pinkel	Liquid Oxygen Impact Test of Tank Components	Obtain the impact sensitivity data on Ag-plated Cu wire (two sizes), nickel wire, 822 Drilube, and Pb-Sn solder.	C - May 22, 1970. Teflon insulated wire showed no reaction, Drilube 822 had one reaction of 20 tests, 60-40 solder ignited in 7 out of 20 tests. These results indicate that in one-g, Teflon and Drilube are acceptable in LOX from an impact sensitivity standpoint and that 60-40 solder is not acceptable.
13-T-33(T) NR B. Williams I. Pinkel	Spark/Electric Arc Ignition Test	Determine the spark/electric arc ignition characteristics of Teflon and other nonmetallic materials in a LOX/GOX environment by simulating specific component failures which could serve as possible ignition sources.	C - April 19, 1970. There was no ignition of the Teflon in the LOX at 1 atmosphere. This test was superceded by later tests.
13-T-34(T) NR B. Williams I. Pinkel	Closed Chamber Spark Ignition Test	Determine the possibility of igniting Teflon on a motor lead wire when the Teflon is penetrated by a grounded knife edge in pressurized LOX while the motor is running.	C - April 20, 1970. This was an early test designed for a quick appraisal and the desired test conditions were not realized.

LEGEND: (T) - Test (A) - Analyses C - Completed ECD - Estimated Completion Date TBD - To Be Determined

NASA — MSC

MSC Form 343 (OT)

MASTER LIST OF TESTS AND ANALYSES

[By Event]

Number (T/A) Location Monitors	Title	Objective - Description	Status - Results - Remarks
		IGNITION	
13-T-35(T) NR G. Johnson I. Pinkel	One-Amp Fuse Test	Determine the time/current characteristics of the 1-amp fuses in the tank fan circuit using a spacecraft regulator and inverter.	C - April 19, 1970. Fuses blow at the following times and currents: 0.010 second -7.3 amps, 0.012 second - 5.0 amps, 0.100 second - 3.1 amps, and 1.00 second - 2.0 amps.
13-T-36(T) NR R. Johnson I. Pinkel	Hot Wire Test of Nonmetallic Tank Materials	Determine if Teflon materials in the tank will ignite with ohmic heating at simulated tank environment.	C - April 20, 1970. This test shows that Teflon sleeving in supercritical oxygen can be ignited by the burn-through of a nichrome wire with 7 to 18 joules.
13-T-41(T) MSC R. Bricker I. Pinkel	Failed Wire Overload Ignition	Determine if a failure or defect in a wire could produce an overload condition with eventual ignition of wire insulation.	C - June 1, 1970. No ignition was obtained where fan motor wire was reduced to one strand with electric current ranging up to 5 amperes. Current-time duration was fixed by quick-blow 1-amp fuse used in fan motor circuit. In a separate test, a 3-amp current was held for 1 minute without ignition.
13-T-42(T) MSC C. Propp I. Pinkel	Ignition Capability of Quantity Gage Signal Conditioners	Determine if the quantity gage signal conditioners can supply sufficient energy to cause ignition in supercritical oxygen.	C - May 18, 1970. Test with signal conditioner showed that it is incapable of generating enough electrical energy to cause ignition of Teflon.
13-T-44(T) WSTF A. Bond I. Pinkel	High Pressure LOX Sensitivity of Metallics with Surface Oxide Penetrations	Determine if a freshly scored or abraded surface of tank metal would provide an environment suitable for initiation of fire under typical LOX tank operating conditions.	ECD - TBD. Tests to start June 5, 1970. Metallic materials will be 1100Al, 2024T-3Al, and 3003Al. Tests will be extended to include Alcoa AMS-3412 brazing flux.

LEGEND: (T) - Test (A) - Analyses C - Completed ECD - Estimated Completion Date TBD - To Be Determined

NASA — MSC

MSC Form 343 (OT)

MASTER LIST OF TESTS AND ANALYSES

[By Event]

Number (T/A) Location Monitors	Title	Objective - Description	Status - Results - Remarks
		IGNITION	
13-T-62(T) ARC T. Canning H. Mark	Ignition Test of Teflon Submerged in LOX	Determine the ignition potentiality of Teflon submerged in LOX from an electrical short.	C - May 4, 1970. This test shows that Teflon can be ignited by a low energy electrical spark (5 ± 3 joules) and gives sustained temperatures great enough to melt through the test fixture, ceramic feedthroughs and cause pressure increases.
13-T-68(T) ARC J. Parker H. Mark	Flow Reactor Test	Determine the effect of flowing oxygen over a heated polymer.	C - May 4, 1970. The initial stage of degradation follows a first-order process. The temperature at which spontaneous ignition occurs is 500° C.
13-T-69(T) ARC J. Parker H. Mark	Arc Test of Tank Materials Submerged in LOX at One Atmosphere	Determine ignition energy required from a short circuit to cause ignition in atmospheric oxygen.	C - May 4. 1970. All materials could be ignited but burning was very marginal. Ignition energy under these conditions was not determined.
13-T-70(T) ARC J. Parker H. Mark	Ignition Test on Tank Materials in High-Pressure LOX	Determine the ignition energy required from a short circuit to cause ignition in high-pressure LOX.	C - May 4, 1970. The test indicated that spark energies of 2.5 joules would ignite Teflon and initiate a metal-Teflon reaction.
		PROPAGATION OF COMBUSTION	
13-T-04R2(T) NR/MSC/KSC E. Tucker I. Pinkel	Sample Analysis of Residual Oxygen in S/C 109 Surge Tank	Determine the contaminates present in the residual oxygen in the surge tank as an aid in identifying the possible source of combustion.	C - May 30, 1970. Tests showed trace contaminate level had not changed from that or original tank fill.

LEGEND: (T) - Test (A) - Analyses C - Completed ECD - Estimated Completion Date TBD - To Be Determined

MASTER LIST OF TESTS AND ANALYSES

[By Event]

Number (T/A) Location Monitors	Title	Objective - Description	Status - Results - Remarks
PROPAGATION OF COMBUSTION			
13-T-06(T) MSC R. Bricker I. Pinkel	Ignition of Oxygen Tank Metals by Burning Teflon	Determine if burning Teflon can ignite metals at cryogenic conditions and attempt to ignite quantity probe aluminum tube by igniting the probe wires.	C - May 27, 1970. Iron, Inconel, and aluminum were ignited by burning Teflon in a series of tests. A separate test showed that a flame propagating along Teflon insulation will enter the quantity probe insulator. Posttest examination showed that about a 2-inch diameter hole had burned through the 3/8-inch thick stainless steel tank closure plate.
13-T-12(T) MSC R. Bricker I. Pinkel	Propagation Rates of Ignited Teflon Wire Insulation and Glass-Filled Teflon	Determine the flame propagation rate of various forms of Teflon used in the oxygen tank.	C - May 15, 1970. Flame propagation rate for Teflon insulation in 900 psia/-180° F oxygen was 0.2 to 0.4 in/sec downward. In 900 psia/75° F oxygen, Teflon gives 0.4 to 0.9 in/sec downward and 2 to 10 in/sec upward, and glass-filled Teflon gives 0.09 to 0.17 in/sec downward.
13-T-18(T) NR E. Tucker I. Pinkel	Inspection and Contamination Analysis of CM Oxygen System Components - S/C 109	Determine the contaminates present and damage incurred in components of the oxygen system as an aid in identifying the source and extent of the anomaly.	ECD - TBD. Work in progress. Laboratory analysis of contaminants in oxygen system components is to begin June 18, 1970.
13-T-48(T) MSC A. Bond I. Pinkel	Comparison of Uncolored and Color-Filled Teflon Flame Propagation Rates	Determine the electrical conductivity and the flame propagation of colored, uncolored, and fingerprint-contaminated Teflon.	C - May 15, 1970. This test was done under TPS 13-T-12. The fingerprint portion will be done at a later date.

LEGEND: (T) - Test (A) - Analyses C - Completed ECD - Estimated Completion Date TBD - To Be Determined

MASTER LIST OF TESTS AND ANALYSES

[By Event]

Number (T/A) Location Monitors	Title	Objective - Description	Status - Results - Remarks
		PROPAGATION OF COMBUSTION	
13-T-49(T) LeRC A. Bond I. Pinkel	Teflon Flame Propagation in Zero-g	Determine the propagation rates for fan motor and temperature sensor wire bundle at zero-g for comparison with data from tests performed at one-g.	ECD - June 17, 1970. Zero-g flame propagation rate over fan motor wire bundles in clear Teflon sleeving is 0.12 in/sec and in white pigmented sleeving 0.15 to 0.32 in/sec. Measurement of zero-g flame propagation rate along wire in oxygen tank conduit to start June 10.
13-T-56(T) MSC R. Bricker I. Pinkel	Teflon Spark Ignition	Determine the ignition energy of a variety of Teflon materials not associated with Apollo 13.	ECD - August 1, 1970.
13-T-57(T) MSC R. Bricker I. Pinkel	Teflon Propagation Rates	Determine the bounds of Teflon propagation rates in supercritical oxygen.	ECD - August 30, 1970. Tests to start end of June. Tests will establish flame propagation rates for Teflon insulation formulations which differ from present Apollo insulations; to provide possible candidate insulations of reduced fire hazard.
13-T-58(T) MSC C. Propp I. Pinkel	Ignition and Flame Propagation Tests of Fan Motor Lead-Wire System	To determine whether lead wire flame will propagate into fan motor and ignite the interior when immersed in oxygen at 900 psi and -180° F.	C - May 22, 1970. Flame propagates into fan motor house without ignition of any metals or stator windings.
13-T-59(T) MSC C. Propp B. Brown	Oxygen Tank Combustion Propagation Test	Determine the pressure time history curve of an oxygen tank if the lower motor lead wires are ignited between the entrance to the motor and the exit from the heater assembly.	C - June 4, 1970. Ignition point was located at lower fan motor. Flame propagated along wire insulation to tank conduit approximately 1-1/2 as fast as observed in Apollo 13 flight oxygen tank. Tank failure occurred in conduit close to tank closure plate.

LEGEND: (T) - Test (A) - Analyses C - Completed ECD - Estimated Completion Date TBD - To Be Determined

MASTER LIST OF TESTS AND ANALYSES

[By Event]

Number (T/A) Location Monitors	Title	Objective - Description	Status - Results - Remarks
PROPAGATION OF COMBUSTION			
13-T-63(T) ARC J. Parker H. Mark	Products of Combustion of Teflon in LOX	Determine the principal products of combustion of Teflon in oxygen.	C - May 4, 1970. The principal product of combustion was COF_2 with an energy release of 121 kcal/mole.
13-T-64(T) LRC J. Hallisay W. Erickson	Propagation Rate of Teflon Combustion in Supercritical Oxygen	Determine the propagation rate of combustion along a wire in supercritical oxygen.	C - June 2, 1970. Test gives downward propagation rate of 0.25 in/sec for a single black wire.
13-T-67(T) ARC J. Parker H. Mark	DTA on Motor Components	Perform a differential thermal analysis on aluminum and Teflon in air.	C - May 4, 1970. This test shows that approximately 793 kcal/mole of heat are released when Teflon, aluminum, and oxygen react.
A-86(A) LRC G. Walberg W. Erickson	Computer Prediction of Products from Oxygen/Teflon Combustion	Compute the flame temperature and major combustion products for a range of oxygen/Teflon ratios and assumed heat losses.	C - May 19, 1970. The maximum flame temperature is 4360° F and the major products of combustion are COF_2, CF_4, and CO_2. F_2 mole fraction is 0.10 at highest temperature.
13-T-17R1(T)			See Pressure Rise.
13-T-25(T)			See Ignition.

LEGEND: (T) - Test (A) - Analyses C - Completed ECD - Estimated Completion Date TBD - To Be Determined

MASTER LIST OF TESTS AND ANALYSES

[By Event]

Number (T/A) Location Monitors	Title	Objective - Description	Status - Results - Remarks
PRESSURE RISE			
13-T-17R1(T) MSC C. Propp W. Erickson	Oxygen Tank Wiring Conduit Propagation Rate and Pressure Buildup	Determine the propagation rate of combustion and the pressure increase in the tank conduit filled with supercritical oxygen when the wiring is ignited at the electrical connector end of the conduit.	C - May 17, 1970. Ignition started in conduit behind electrical connector. Conduit ruptured approximately 2 to 3 seconds after ignition.
13-T-26(T) MSC P. McLaughlan F. Smith	Flowmeter Test	Determine the effects of oxygen pressure and temperature variations on flowmeter output to analyze why the flowmeter behavior led the remaining instrumentation in the timeline prior to failure.	C - April 27, 1970. During the ambient temperature test a step pressure increase would result in a spike in the flowmeter output but the flowrate indication would not show any other change. At low temperatures an increase or decrease in pressure would give an indicated corresponding change in flow. At constant pressure a temperature change would give an indicated flow change. All of these effects were known and the data do not have to be corrected for any unexpected behavior of the flowmeter.
13-T-46(T) ARC A. Bond F. Smith	Filter Clogging by COF_2	Determine if the oxygen tank filter can be clogged by COF_2 snow.	ECD - TBD. This test has not yet been conducted.
B-62(T) MSC C. Propp E. Cortright	Simulated Tank Fire	Investigate pressure-temperature profiles and propagation patterns within a closely simulated oxygen tank with various ignition points.	This test was conducted under TPS 13-T-59.

LEGEND: (T) - Test (A) - Analyses C - Completed ECD - Estimated Completion Date TBD - To Be Determined

NASA — MSC

MSC Form 343 (OT)

MASTER LIST OF TESTS AND ANALYSES

[By Event]

Number (T/A) Location Monitors	Title	Objective - Description	Status - Results - Remarks
		PRESSURE RISE	
A-87(A) MSC/LRC R. Ried/ G. Walberg W. Erickson 13-T-37(T)	Energy Required to Account for Observed Pressure Rise	Determine the energy required to explain the observed pressure rise in oxygen tank no. 2. An isentropic compression of the oxygen is considered as well as a constant density process with heat addition.	C - May 19, 1970. The minimum energy required (isentropic) is about 10 Btu and the maximum (constant density) is about 130 Btu. See Final Instrument Loss.
		TEMPERATURE RISE	
13-T-38(T) B-62(T)			See Final Instrument Loss. See Pressure Rise.
		PRESSURE DROP	
13-T-02(T) MSC C. Propp V. Johnson	Relief Valve Blowdown Investigation	Determine the differential pressure between a simulated oxygen tank and the flight pressure transducer as a function of a mass flow through the relief valve. Also determine the response of the flight transducer to a step pressure stimulus.	C - April 27, 1970. The maximum pressure difference between the tank and the flight transducer was 9 psig at a flow rate of 182 lb/hr. The pressure stimulus of 75 psi was transmitted to the flight transducer in 24 milliseconds and reached 100 percent of the step pressure in 57 milliseconds. This test shows that the flight transducer will follow the system pressure under high flow rates and step pressure increases and will not introduce significant errors in the TM data.

LEGEND: (T) - Test (A) - Analyses C - Completed ECD - Estimated Completion Date TBD - To Be Determined

MASTER LIST OF TESTS AND ANALYSES

[By Event]

Number (T/A) Location Monitors	Title	Objective - Description	Status - Results - Remarks
PRESSURE DROP			
13-T-16(T) Parker A/C W. Chandler V. Johnson	Relief Valve Flow Tests	Determine the flow rate of the relief valve at temperatures from 360° R to 1060° R.	C - May 15, 1970. The flow rate at these temperatures ranged from approximately 0.016 to 0.034 lb-m/sec. This is greater than is required to produce the observed pressure drop.
13-T-27(T) MSC P. Crabb N. Armstrong	Oxygen Relief Valve System Simulation at 80° F	Determine the pressure drop between the filter and the relief valve, and the flight pressure transducer response to a step pressure increase.	C - April 21, 1970. The maximum recorded pressure drop between the simulated tank and pressure transducer was 18 psi. A 500-psi step increase in the "tank" was measured by the pressure transducer with a delay of about 100 milliseconds. This test indicates that under conditions of warm gas and an open filter, the pressure transducer will follow actual tank pressure with reasonable accuracies in magnitude and time.
13-T-31(T) Parker A/C L. Johnson S. Himmel	Relief Valve Flow Rate	Determine flow rate through a fully open relief valve.	C - April 21, 1970. The crack pressure of the valve was 1005 psig and it was fully open at 1010 psig. The maximum flow rate of GOX was 34.5 lb/hr and 108 lb/hr for LOX.
A-24(A) MSC W. Chandler F. Smith	Oxygen Tank Filter	Determine flow rates and pressure drops through lines and filter to account for those pressure measurements noted during the flight. Consider the case of a completely clogged filter.	C - May 14, 1970. The analysis showed that if the filter had been clogged, the rate of pressure drop would have been much greater than that observed in the data. Analysis shows that the pressure relief valve can reduce the oxygen tank pressure at the rate shown in the telemetry data.

LEGEND: (T) - Test (A) - Analyses C - Completed ECD - Estimated Completion Date TBD - To Be Determined

NASA — MSC

MSC Form 343 (OT)

MASTER LIST OF TESTS AND ANALYSES

[By Event]

Number (T/A) Location Monitors	Title	Objective - Description	Status - Results - Remarks
		PRESSURE DROP	
A-55(A) MSC W. Rice N. Armstrong	Premature Relief Valve Opening	To determine if a premature relief valve opening would account for the 15 seconds of constant tank pressure after the initial pressure rise, assuming several gas temperatures.	C - May 14, 1970. This analysis showed that the relief valve flow would have caused a pressure drop, not a plateau.
13-T-71(T)			See Tank Failure.
		FINAL INSTRUMENT LOSS	
13-T-37 Beech A/C R. Urbach R. Wells	Pressure Transducer Test	Determine the pressure transducer output characteristics at extremely low temperatures.	C - April 21, 1970. The pressure transducer gives erratic readings below -250° F. Temperatures in the oxygen tank were always above -190° F.
13-T-38(T) Beech A/C W. Rice	Temperature Sensor Response	Determine the temperature sensor response time in a rapidly changing temperature environment.	C - April 18, 1970. This test gave sensor response rates of 3° to 12° F per second over a range of +60° to -317° F.
A-3(A) MSC G. Johnson J. Williams	Time Tabulation of Alarms	To determine times and causes for caution and warning alarms during the mission.	C - May 14, 1970. These data were used by Panel 1 in their analyses of mission events.

LEGEND: (T) - Test (A) - Analyses C - Completed ECD - Estimated Completion Date TBD - To Be Determined

MASTER LIST OF TESTS AND ANALYSES

[By Event]

Number (T/A) Location Monitors	Title	Objective - Description	Status - Results - Remarks
		TELEMETRY LOSS	
A-2(A) MSC M. Kingsley J. Williams	High Gain Antenna Signal Loss	To explain the difficulties associated with acquiring high-gain antenna operation at 55 hours 5 minutes into the mission.	C - May 14, 1970. This was not a specific antenna problem which could be isolated to this mission. Previous missions have encountered similar problems. This difficulty is not considered significant to the Apollo 13 incident.
		TANK FAILURE	
13-T-29(T) Boeing S. Glorioso B. Brown	Fracture Mechanics Data for EB Welded Inconel 718 in LOX	Determine the fracture toughness and LOX threshold of electron beam welded Inconel 718 tank materials.	C - June 3, 1970. Test results show that a through fracture greater than 3 inches long would be required to cause rupture of the pressure vessel.
13-T-40(T) MSC S. Glorioso B. Brown	Torch Test of Inconel 718	Determine the burn-through tolerance of Inconel 718, by prestressing the specimen to tank operating pressure and burning through the specimen with an oxyacetylene torch.	C - May 18, 1970. The significant result of this test is that fairly large holes must be burned through Inconel 718 to cause catastrophic failure.
13-T-61(T) MSC S. Glorioso B. Brown	Crack Growth of Cracked Inconel EB Welds	Weld specimens (0.125 inch thick) containing cracks will be tested in liquid nitrogen and subjected to a mean stress corresponding to a relief valve pressure in the supercritical oxygen tank with a superimposed cyclic stress equal to that caused by heater operation.	ECD - July 15, 1970.
13-T-71(T) LeRC W. Chandler S. Himmel	Supercritical Oxygen Blowdown Test	Determine the transient thermodynamic process involved in sudden venting of supercritical oxygen to a hard vacuum.	ECD - June 16, 1970. Apparatus being assembled for this test.

LEGEND: (T) - Test (A) - Analyses C - Completed ECD - Estimated Completion Date TBD - To Be Determined

MASTER LIST OF TESTS AND ANALYSES

[By Event]

Number (T/A) Location Monitors	Title	Objective - Description	Status - Results - Remarks
		TANK FAILURE	
A-38(A) MSC P. Glynn B. Brown	Stress Analysis of Oxygen Tank Neck Areas	To determine whether failures of the oxygen tank neck area might be initiated by the combined effects of pressure and thermal stresses.	C - May 19, 1970. The analysis was performed using three assumptions on thermal inputs. In all cases analysis showed that the conduit would fail rather than the vessel.
A-39(A) MSC P. Glynn B. Brown	Complete Tank Stress Analysis	To provide information on the complete design stress analysis and on the assumption of membrane stress made in the fracture mechanics analysis with particular emphasis on low discontinuity areas.	C - May 13, 1970. Received two cursory stress analysis reports. Factors of safety acceptable for all conditions analyzed.
A-40(T) Boeing Co. P. Glynn B. Brown	Fracture Test on Oxygen Tank	Carry out fracture mechanics tests and analysis of the oxygen tank.	C - June 3, 1970. Test shows that the failure mode of the tank would have probably been leaking and not a rupture.
A-57(T) MSC/Boeing P. Glynn B. Brown	Tensile Test at Low and Elevated Temperatures	Determine the tensile strength of Inconel 718 and EB weld in the temperature range from -320° to +1800° F.	C - May 20, 1970. All information furnished on typical ultimate and yield strength data showed adequate safety margins for pressures reached in tank.
A-59(A) MSC/Boeing J. Kotanchik B. Brown	Fracture Mechanics Review of All Apollo Pressure Vessels	To assess the adequacy of previous fracture analyses and to identify areas where additional data are needed.	ECD - June 19, 1970. Analysis is underway.

LEGEND: (T) - Test (A) - Analyses C - Completed ECD - Estimated Completion Date TBD - To Be Determined

MASTER LIST OF TESTS AND ANALYSES

[By Event]

Number (T/A) Location Monitors	Title	Objective - Description	Status - Results - Remarks
		OXYGEN TANK NO. 1 PRESSURE LOSS	
13-T-39(T) Beech A/C W. Rice H. Mark	Oxygen Tank Blowdown	Determine the rate of pressure decay from oxygen tank XTA 00041 through simulated delivery and vent line fracture starting at 78 percent density level, and 900 psig and ending at ambient pressure.	C - April 20, 1970. Vent through delivery line (0.1870D x 0.015W) reached 350 psia in 25 seconds and 160 psia in 600 seconds. Vent through vent line (0.3750D x 0.015W) reached 415 psia in 3 seconds and ambient in 360 seconds.
A-36(A) MSC W. Chandler E. Baehr	Hardware Damage - Tank 1	Determine what hardware damage would be required to explain the loss of pressure from oxygen tank no. 1.	C - May 18, 1970. The analysis shows that a hole from 0.076 inch to 0.108 inch in diameter would be required to explain the pressure loss in tank no. 1.
		PANEL LOSS	
13-T-50(T) MSC R. Bricker W. Erickson	Oxygen Impingement Test on Mylar Insulation	Determine if Mylar insulation can be ignited by a jet of hot oxygen.	C - June 5, 1970. The lowest pressure at which the Mylar will burn in a static oxygen atmosphere with flame ignition is 0.5 psia. Impingement of 1000° F and 1200° F oxygen at 80 psia did not ignite the Mylar blanket. (A test is being prepared to attempt to ignite Mylar in the configuration of the oxygen tank area.)
13-T-54(T) NR D. Arabian S. Himmel	Fuel Cell Radiator Inlet Temperature Response Test	Determine thermal response of temperature sensor installed on EPS water-glycol line.	C - May 20, 1970. Results indicate that under no-flow conditions the flight profiles could not be reproduced. Initial response of the temperature sensor occurred in 0.25 second after heat application.

LEGEND: (T) - Test (A) - Analyses C - Completed ECD - Estimated Completion Date TBD - To Be Determined

MSC Form 343 (OT)

NASA — MSC

MASTER LIST OF TESTS AND ANALYSES

[By Event]

Number (T/A) Location Monitors	Title	Objective - Description	Status - Results - Remarks
		PANEL LOSS	
13-T-65(T) LRC H. Morgan W. Erickson	One-Half Scale Panel Separation Test	Determine the pressure impulse necessary to cause complete panel separation and determine the mode of failure. A 1/2-scale model of SM bay 4 is used with structurally scaled test panels. Tests are to be run in vacuum with appropriate vent areas. Panel loading is simulated by a rapid pressure pulse.	C - June 2, 1970. Complete separation of 1/2-scale honeycomb panel models in vacuum was demonstrated for a rapid band loaded pressure pulse and for uniform pressure. Separation for nonuniform loading occurred within about 20 milliseconds. Peak pressures that occur in the oxygen shelf space are near 50 psia, 25 psia in fuel cell shelf, and somewhat less than 10 psia in tunnel volume.
13-T-66(T) LRC M. Ellis W. Erickson	Hot Oxygen Impingement on Mylar Ignition Test	Determine if the Mylar insulation blanket will be ignited by a jet of hot oxygen and estimate the rate of combustion.	C - May 18, 1970. Mylar blanket can be ignited by a hot oxygen (1500° F) jet at pressures above 10 psia. Combustion of a 1-foot square sample requires about 15 seconds. More rapid combustion occurs with 70° F at 10 psia oxygen when Mylar is ignited with Pyrofuse.
13-T-75(T) MSFC J. Nunelley W. Erickson	Heats of Combustion of Teflon, Mylar and Kapton	Determine the heats of combustion of Teflon, Mylar, aluminized Mylar, and aluminized Kapton.	C - May 27, 1970. Heats of combustion were: Teflon - 2200 Btu/lb, Mylar - 9850 Btu/lb, Kapton - 10,700 Btu/lb.
13-T-76(T) MSFC C. Key W. Erickson	Threshold Oxygen Pressure for Mylar & Kapton Flame Propagation	Determine the threshold oxygen pressure for flame propagation of Mylar and Kapton films.	C - May 27, 1970. Ignition threshold oxygen pressure ranged from 0.5 to 1.5 psi for both aluminized Mylar and Kapton under static conditions.

LEGEND: (T) - Test (A) - Analyses C - Completed ECD - Estimated Completion Date TBD - To Be Determined

NASA — MSC

MSC Form 343 (OT)

MASTER LIST OF TESTS AND ANALYSES

[By Event]

Number (T/A) Location Monitors	Title	Objective - Description	Status - Results - Remarks
PANEL LOSS			
A-65(A) MSC P. Glynn V. Johnson	CM-SM Heat Shield and Attach Fittings Analysis	Determine if there is any reasonable possibility of estimating the pressure loads applied to the bay 4 panel by reviewing the design of the CM heat shield structure and the CM-SM attach fittings.	C - May 22, 1970. Visual inspection of the bolt assembly between the CM-SM interface revealed no thread damage. It is improbable that the bulkhead experienced any structurally significant pressures during the event.
A-68(A) MSC M. Windler W. Hedrick	Panel Trajectory	To determine if the bay 4 panel is in lunar or earth orbit; if so, to investigate the possibility of getting photographs of the panel on some future manned space flight.	C - May 15, 1970. Analysis revealed that the most probable trajectory led to an impact of the panel on the Moon.
A-88(A) LRC G. Walberg W. Erickson	Prediction of Combustion Products from Oxygen/Mylar Oxidation	Compute the flame temperature and major combustion products for an oxygen/Mylar reaction over a range of oxygen/Mylar ratios.	C - May 25, 1970. Flame temperature is 4750° and 5400° F for stoichiometric combustion at 1.5 and 60 psia. For oxygen/Mylar molar ratios of 10, the flame temperature is 2350° and 2400° F at 1.5 and 60 psia. Combustion products are CO_2 and H_2O below 3500° F and include CO and O at the higher temperatures.
A-93(A) LRC R. Trimpi W. Erickson	Calculated Pressure Rise in Bay 4 Due to Combustion	Calculate the pressure rise in the oxygen tank shelf which could result from various modes of tank rupture. Consider cases with and without combustion.	C - June 8, 1970. A maximum pressure rise of about 9 psia is achieved in the oxygen shelf space for no combustion based on initial tank conditions of 900 psia/-190° F and a 2-inch diameter orifice. This pressure occurs at 180 milliseconds after rupture. An estimate with combustion of 0.2 lb_m of Mylar indicates a pressure rise of about 33 psia.

LEGEND: (T) - Test (A) - Analyses C - Completed ECD - Estimated Completion Date TBD - To Be Determined

NASA — MSC

MSC Form 343 (OT)

MASTER LIST OF TESTS AND ANALYSES

[By Event]

Number (T/A) Location Monitors	Title	Objective - Description	Status - Results - Remarks
		PANEL LOSS	
A-94(T) LRC M. Ellis W. Erickson	Mylar Combustion Tests with Supercritical Oxygen in Simulated Shelf Space	Observe the nature of the combustion of Mylar insulation blanket with supercritical oxygen in a simulated shelf space volume. Measure the resulting pressure rise for various modes of ignition and simulated tank rupture.	C - June 6, 1970. Mylar insulation blanket burns completely when ignited by pyrofuse and exposed to oxygen exhausting from a chamber at 900 psia/-190° F. Duration of combustion process is about 2 to 4 seconds. The pressure rise rate with combustion in these tests is about 7 times that measured with no combustion.
A-95(A) LRC R. Trimpi W. Erickson	Analysis of Temperature by Sensors Outside Shelf Space	Use the flight measured temperature-time histories for sensors outside shelf space to estimate the temperature of the gas which flows from shelf space.	C - June 9, 1970. Examination of the temperature-time histories suggests heat addition outside of oxygen tank.
		SIDE EFFECTS	
13-T-32(T) NR R. Johnson R. Wells	Fuel Cell Valve Module - Reactant Valve Shock Test	Determine the effect of a high g load on the fuel cell reactant shutoff valves.	C - April 20, 1970. This test showed that the reactant valves shut under lower shock loads than the RCS valves. Since a portion of the RCS valves closed at the time of the incident, the reactant valves probably closed due to the shock loading.
13-T-26(T)			See Pressure Rise.

LEGEND: (T) - Test (A) - Analyses C - Completed ECD - Estimated Completion Date TBD - To Be Determined

NASA — MSC

MSC Form 343 (OT)

MASTER LIST OF TESTS AND ANALYSES

[By Event]

Number (T/A) Location Monitors	Title	Objective - Description	Status - Results - Remarks
		MISCELLANEOUS	
13-T-43(T) MSC C. Propp S. Himmel	Development of Service Procedure for Apollo 14	Develop new operating procedures for ground operations to prevent stratification in the oxygen tanks.	ECD - TBD. Test has not yet been conducted.
13-T-51(T) NR J. Diaz F. Smith	LOX Tank Fan Motor Examination	Identify nonmetallic motor parts and provide information on their usage. Identify surfaces containing Drilube 822 and look for signs of corrosion.	C - May 12, 1970. The motor parts were identified for the use of Panel 1. Drilube 822 was used on threaded areas of the motor housing and mounting hardware. The motor showed evidence of corrosion at areas of contact of dissimilar metals.
13-T-52(T) WSTF M. Steinthal I. Pinkel	N_2O_4 and A-50 Reactivity with Teflon Insulated Wire	Determine the reactivity of Teflon in N_2O_4 and A-50 when arcing or short circuiting occurs.	ECD - June 12, 1970. The overload test has been completed and the arcing test is being prepared. The overload test shows a maximum temperature rise of 2° F and maximum pressure rise of 2 psi. There have been no reactions with either N_2O_4 or A-50.
13-T-72(T) MSC C. Propp H. Mark	Reactivity of Hydrogen Tank Materials	Hydrogen materials will be ignited in gaseous hydrogen at various temperatures. Ignition will be by a nichrome wire electrically heated until failure occurs.	ECD - June 30, 1970. The test has not yet been conducted.
13-T-73(T) MSC C. Propp H. Mark	Spark Ignition Threshold and Propagation Rates for Hydrogen Tank Material in Gaseous Hydrogen	Determine spark ignition threshold and combustion propagation rates for hydrogen tank material in gaseous and supercritical hydrogen at various temperatures.	ECD - June 19, 1970. The test has not yet been conducted.

LEGEND: (T) - Test (A) - Analyses C - Completed ECD - Estimated Completion Date TBD - To Be Determined

NASA — MSC

MSC Form 343 (OT)

MASTER LIST OF TESTS AND ANALYSES

[By Event]

Number (T/A) Location Monitors	Title	Objective - Description	Status - Results - Remarks
		MISCELLANEOUS	
13-T-74(T) MSC C. Propp H. Mark	Ignition of Specific Configurations in Hydrogen	Details depend on results of 13-T-72 and 73. Will mockup hydrogen tank configuration.	ECD - July 1, 1970. The test has not yet been conducted.
A-39(T) ARC E. Winkler H. Mark	Teflon/Aluminum Ignition in Inert Atmosphere	Determine whether it is possible to ignite Teflon and aluminum in an inert atmosphere.	C - May 15, 1970. A Teflon and powdered aluminum mixture could be made to burn. High ignition energies (greater than 10 joules) were necessary and it was found that the aluminum had to be finely divided before it would burn.

LEGEND: (T) - Test (A) - Analyses C - Completed ECD - Estimated Completion Date TBD - To Be Determined

PART F5

FAULT TREE ANALYSIS - APOLLO 13 ACCIDENT*

INTRODUCTION

This report contains a fault tree analysis of the applicable portions of the electrical power and cryogenic systems involved in the Apollo 13 incident. It was prepared by the Boeing Company under the direction of MSC and at the request of the Apollo 13 Review Board.

PURPOSE

The purpose of this analysis is to identify potential causes that could lead to the loss of the SM main bus power, to show their logical associations, and to categorize them as being true or false for the Apollo 13 incident based upon available data, analyses, and tests. The prime emphasis is to identify the initiating cause, and secondarily, the sequence of events leading to the loss of SM main bus power.

SCOPE

This fault tree identified the applicable ECS/cryogenic system hardware and potential causes, down to the component or groups of components level. The logical association of the potential causes is shown graphically and is developed tracing the system functions backwards. Each potential cause is categorized as being true or false where flight data, ground tests, technical analyses, and/or engineering judgment provide sufficient rationale. The main thread to determine the initiating cause is identified in the fault tree. The tree does not include unrelated or secondary effects of the failure (i.e., quantity gage malfunction, panel blow-off, fire in the service module).

Pages F-108 through F-114 provide information on symbology, terminology, abbreviations, references, and schematics for reference during review of the fault tree. Page F-111 identifies what pages of the fault tree are associated with the various segments of the system. Page F-115 pictorially depicts the required layout of the pages of the fault tree to provide an overview of the complete system.

---

*Extracted from "Fault Tree Analysis - Apollo 13 Incident," dated June 5, 1970, under Contract NAS 9-10364 - Task Item 9.0, for MSC Apollo 13 Review Board, Action Item 35.

DESCRIPTION OF FAULT TREE DEVELOPMENT PROCESS:

BEGINNING FROM THE DEFINED UNDESIRED EVENT, "FUEL CELL POWER NOT AVAILABLE ON SM BUSES", THE CAUSATIVE FACTORS HAVE BEEN SHOWN BY MEANS OF LOGIC DIAGRAMMING. GIVEN THAT A SPECIFIED EVENT CAN OCCUR, ALL POSSIBLE CAUSES FOR THAT EVENT ARE ARRAYED UNDER IT. IT IS IMPORTANT TO NOTE THAT THIS LISTING INCLUDES ALL POSSIBLE WAYS IN WHICH THE EVENT CAN OCCUR. NEXT, THE RELATIONSHIP OF THESE CAUSATIVE FACTORS TO ONE ANOTHER AND TO THE ULTIMATE EVENT IS EVALUATED AND A DETERMINATION AS TO WHETHER THE DEFINED CAUSES ARE MUTUALLY INDEPENDENT, OR ARE REQUIRED TO COEXIST, IS MADE. THE SYMBOLOGY EMPLOYED TO ILLUSTRATE THE THOUGHT PROCESS IS AS FOLLOWS:

FAILURE/CAUSE STATEMENT - FAILURES ARE SHOWN WITHIN THE LOGIC BLOCKS - TRUE AND FALSE STATEMENTS AND RATIONALE ARE ADJACENT TO THE APPLICABLE BLOCKS.

"OR" GATE - THOSE CAUSES WHICH ARE CAPABLE, INDEPENDENTLY, OF BRINGING ABOUT THE UNDESIRED EVENT ARE ARRAYED HORIZONTALLY BELOW THE "OR" SYMBOLS.

"AND" GATE - THOSE CAUSES WHICH MUST COEXIST ARE ARRAYED HORIZONTALLY BELOW THE "AND" SYMBOLS.

"INHIBIT" GATE - THOSE FACTORS WHICH INTRODUCE ELEMENTS OF CONDITIONAL PROBABILITY, AND WHICH ARE REQUIRED TO COEXIST WITH OTHER CAUSES, ARE DEFINED AS "INHIBIT" FUNCTIONS.

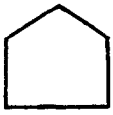

"HOUSE" - THOSE CAUSATIVE FACTORS WHICH ARE NORMALLY EXPECTED TO EXIST, OR TO OCCUR, ARE SHOWN AS "HOUSES".

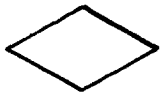

"DIAMOND" - TERMINATED FOR THIS SUB-BRANCH; FURTHER DEVELOPMENT NOT REQUIRED FOR THIS ANALYSIS.

"CUT CORNER" - INDICATES THIS IS A KEY OR NODAL BLOCK. ANALYSIS OF THESE BLOCKS WAS PERFORMED IN GREATER DEPTH SINCE THEY "CONTROL" SIGNIFICANT PORTIONS OF THE FAULT TREE.

TRUTH STATEMENT CATEGORIZATION:

EACH FAILURE STATEMENT IS REVIEWED TO DETERMINE WHETHER IT IS TRUE OR FALSE. THE TYPE DATA USED TO SUPPORT A STATEMENT BEING TRUE OR FALSE IS IDENTIFIED. IN ADDITION, THE SUPPORTING DATA SOURCES ARE REFERENCED.

CODE KEY

CATEGORY	DATA TYPE
F = FALSE	FD = PER FLIGHT DATA
T = TRUE	A = PER ANALYSIS
	GD = PER GROUND DATA
	EJ = PER ENGINEERING JUDGEMENT
	TE = PER TEST
	SL = SUBORDINATE LOGIC (SUPPORTED BY SUB-TIER LOGIC.)

EXAMPLE: F - FD = FALSE PER FLIGHT DATA

REFERENCES:

1. MSC APOLLO INVESTIGATION TEAM PANEL 1, PRELIMINARY REPORT, DATED APRIL 1970

2. APOLLO 13 UNPUBLISHED FLIGHT DATA, AVAILABLE AT NASA/MSC BUILDING 45, 3RD FLOOR, DATA ROOM

3. NASA/MSC TPS 13-T-58, IGNITION OF DESTRATIFICATION MOTOR TEST

4. MSC APOLLO INVESTIGATION TEAM PANEL 1, APOLLO 13 CRYOGENIC OXYGEN TANK 2 ANOMALY REPORT (INTERIM DRAFT), DATED MAY 22, 1970

5. NASA/MSC TPS 13-T-53, HEATER ASSEMBLY TEMPERATURE PROFILE

6. NASA/MSC TPS 13-T-59, OXYGEN TANK IGNITION SIMULATION

LIST OF ABBREVIATIONS

AL.	-	ALUMINUM
ASSY	-	ASSEMBLY
CAP	-	CAPABILITY
CRYO	-	CRYOGENIC
CU	-	COPPER
ECS	-	ENVIRONMENTAL CONTROL SYSTEM
ELEC	-	ELECTRICAL
EOI	-	EARTH ORBIT INSERTION
EPS	-	ELECTRICAL POWER SYSTEM
FAB	-	FABRICATION
FC	-	FUEL CELL
FIG.	-	FIGURE
GEN	-	GENERATE OR GENERATED
H_2	-	HYDROGEN
H_2O	-	WATER
MECH	-	MECHANICAL
MSC	-	MANNED SPACECRAFT CENTER
NASA	-	NATIONAL AERONAUTICS AND SPACE ADMINISTRATION
NEG.	-	NEGATIVE
NO.	-	NUMBER
O_2	-	OXYGEN
OS-X	-	OXYGEN SUPPLY CONNECTION 1, 2 OR 3
PARA.	-	PARAGRAPH
PRELIM.	-	PRELIMINARY
PRESS	-	PRESSURE OR PRESSURIZED
QTY	-	QUANTITY
REF.	-	REFERENCE
RF	-	RADIO FREQUENCY
S/C	-	SPACECRAFT
SM	-	SERVICE MODULE
STRUCT	-	STRUCTURE OR STRUCTURAL
SYS	-	SYSTEM
TEMP	-	TEMPERATURE

F-111

SIMPLIFIED SCHEMATIC OF EPS AND CRYOGENIC OXYGEN SYSTEM

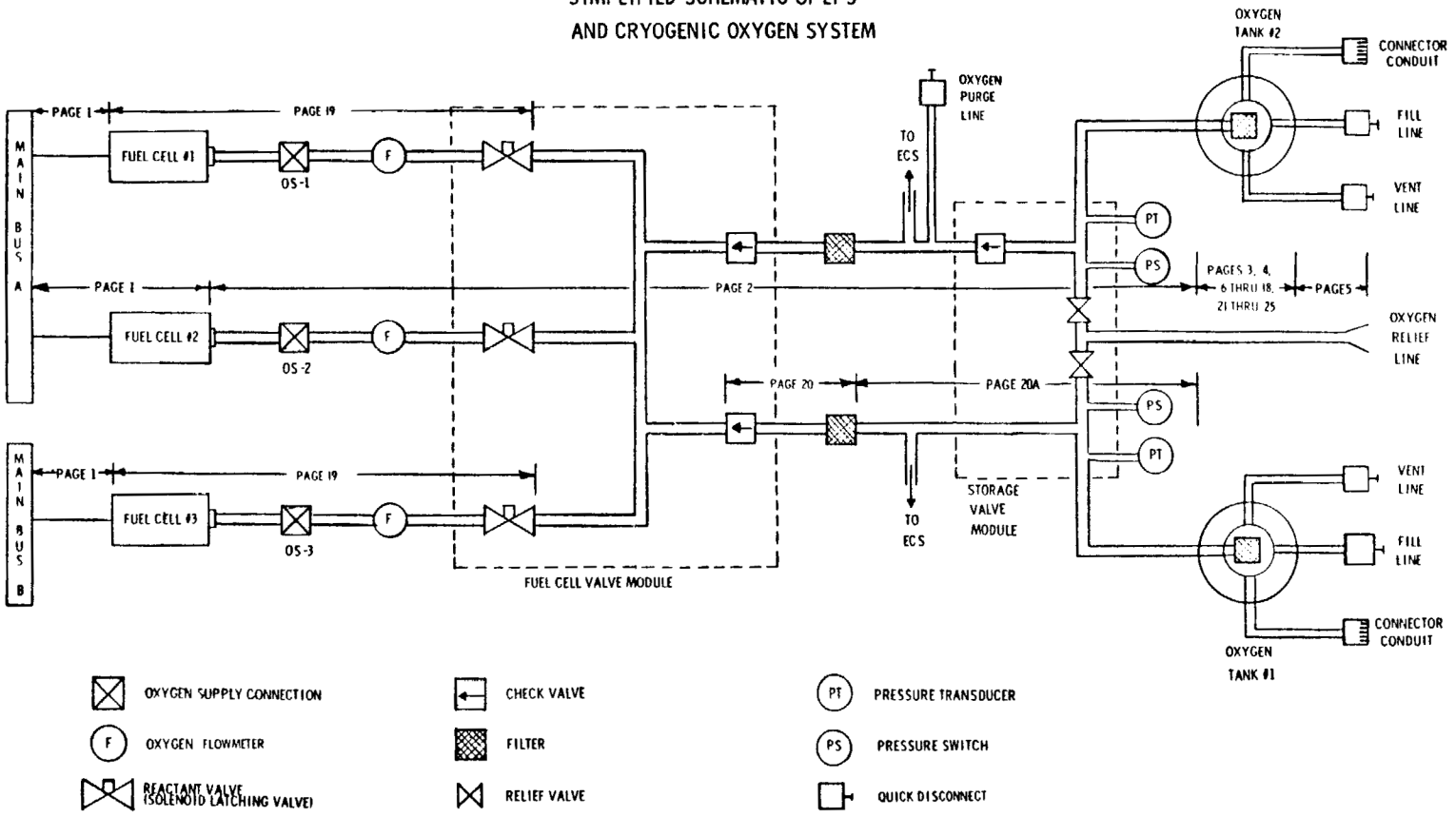

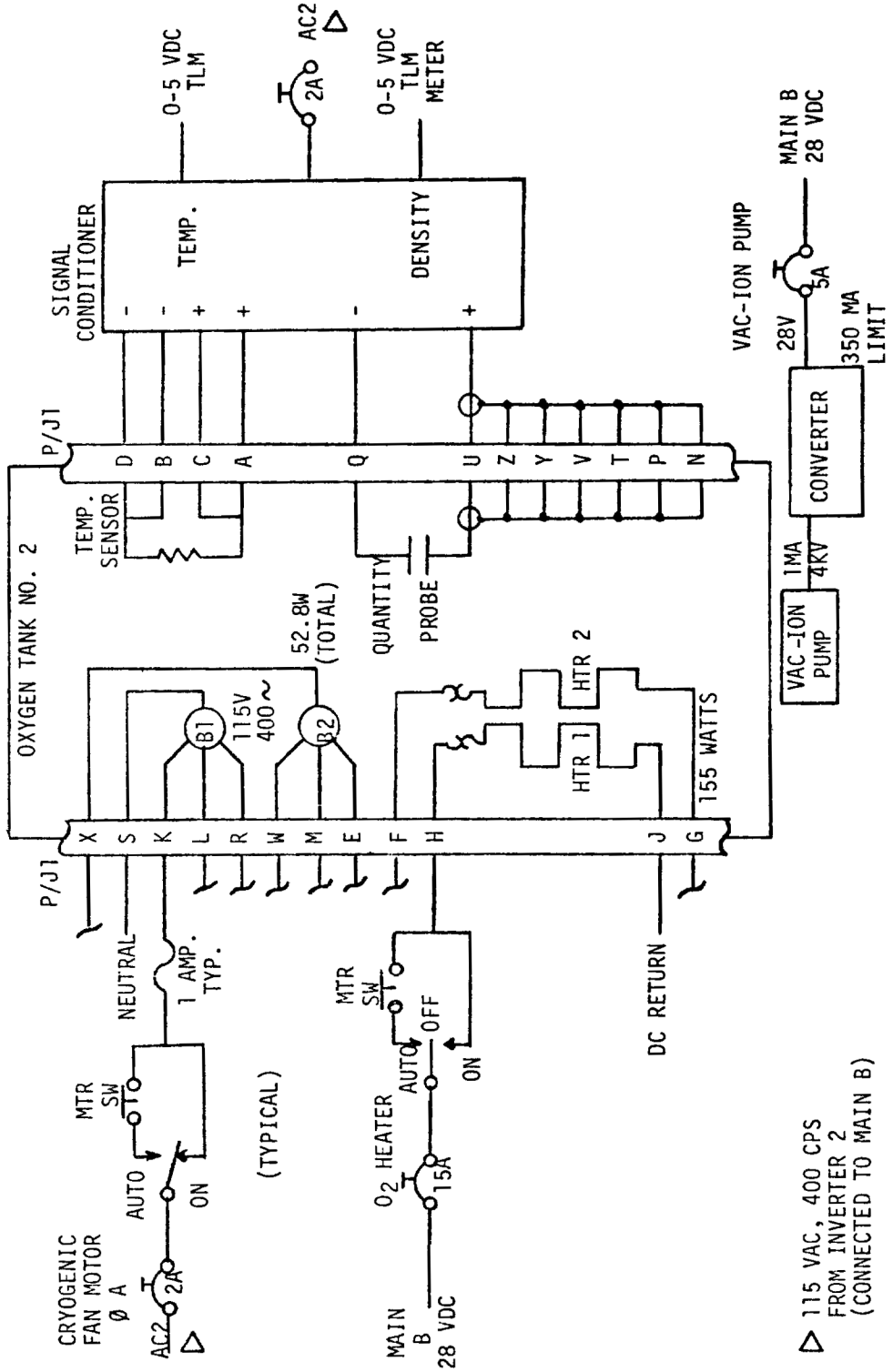

OXYGEN TANK NO. 2 ELECTRICAL SCHEMATIC

vi

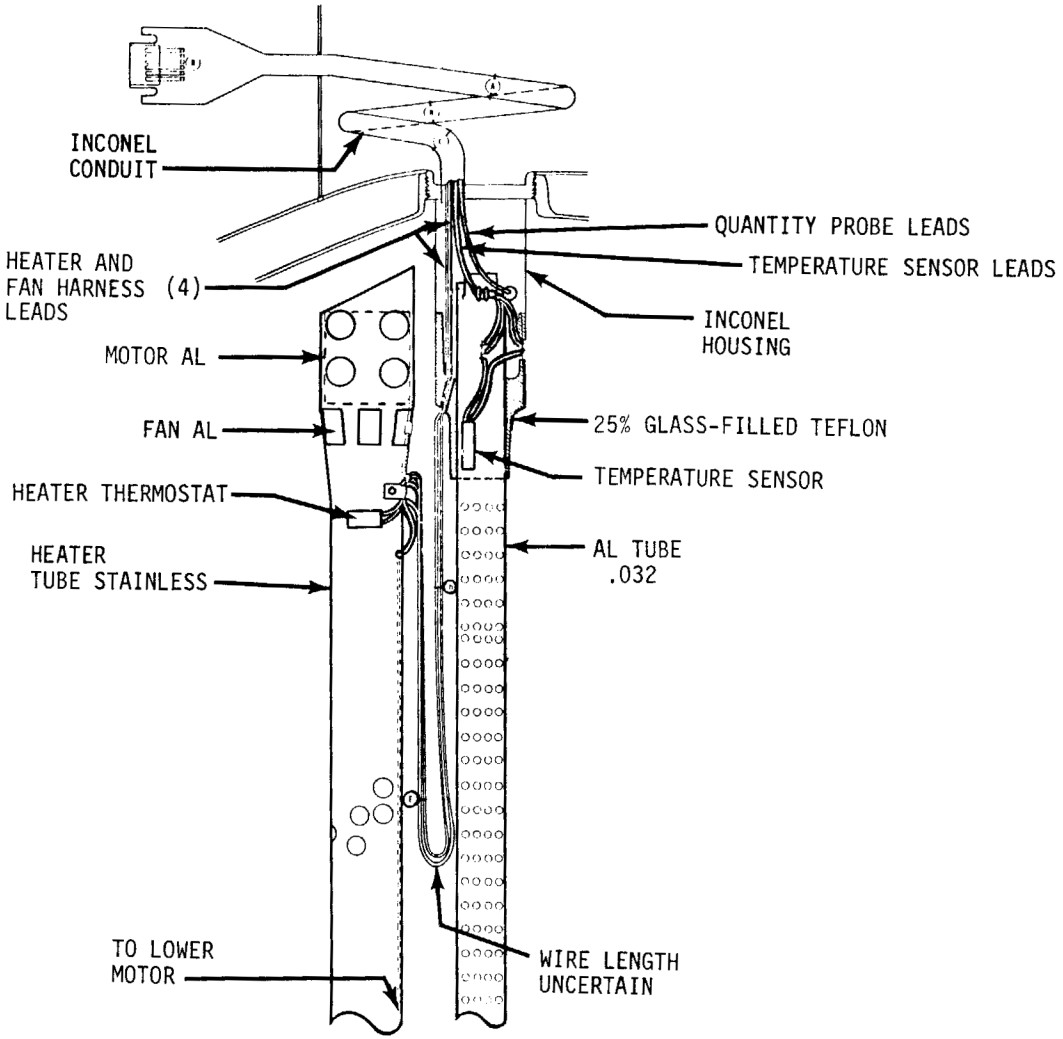

UPPER HEATER AND PROBE ASSEMBLY

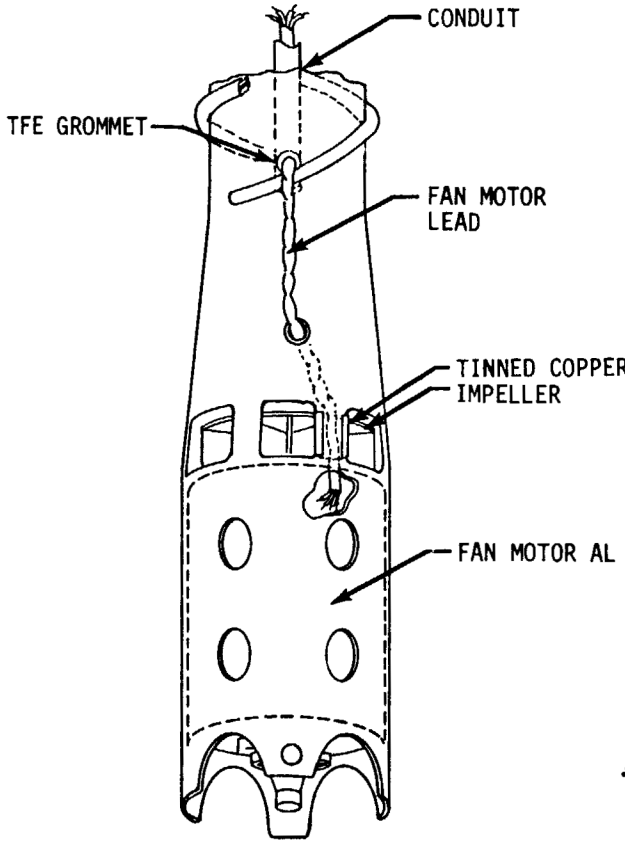

DETAIL OF HEATER ASSEMBLY

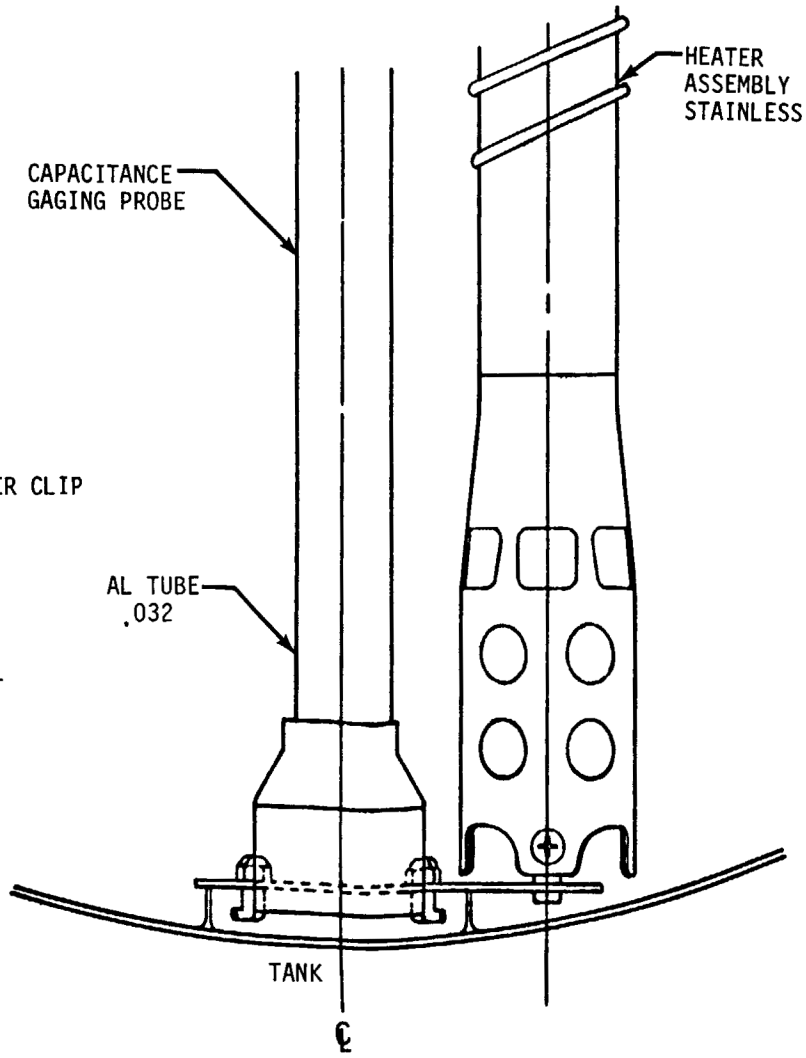

LOWER HEATER AND PROBE ASSEMBLY

FAULT TREE SHEET LAYOUT*

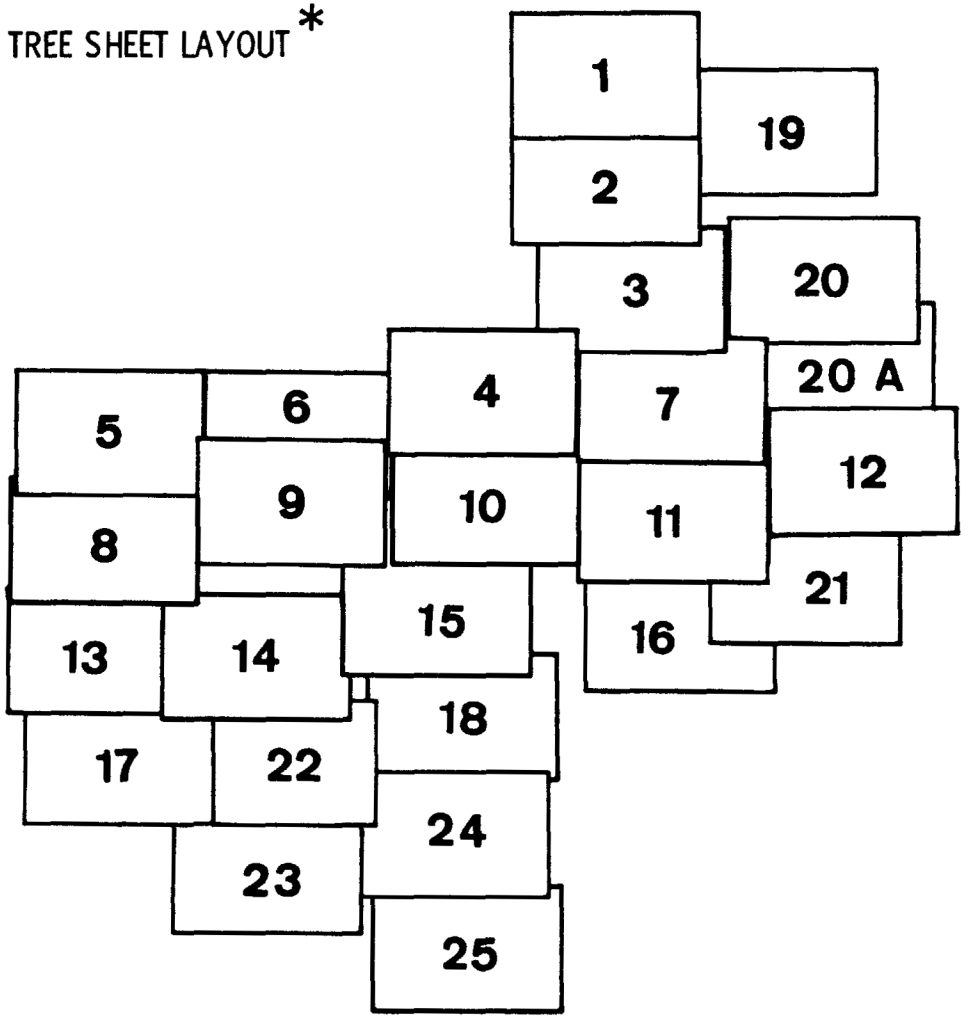

*TO ASSEMBLE FAULT TREE, LAYOUT PAGES IN THE POSITIONS SHOWN ABOVE

F-115

FAULT TREE ANALYSIS

June 5, 1970

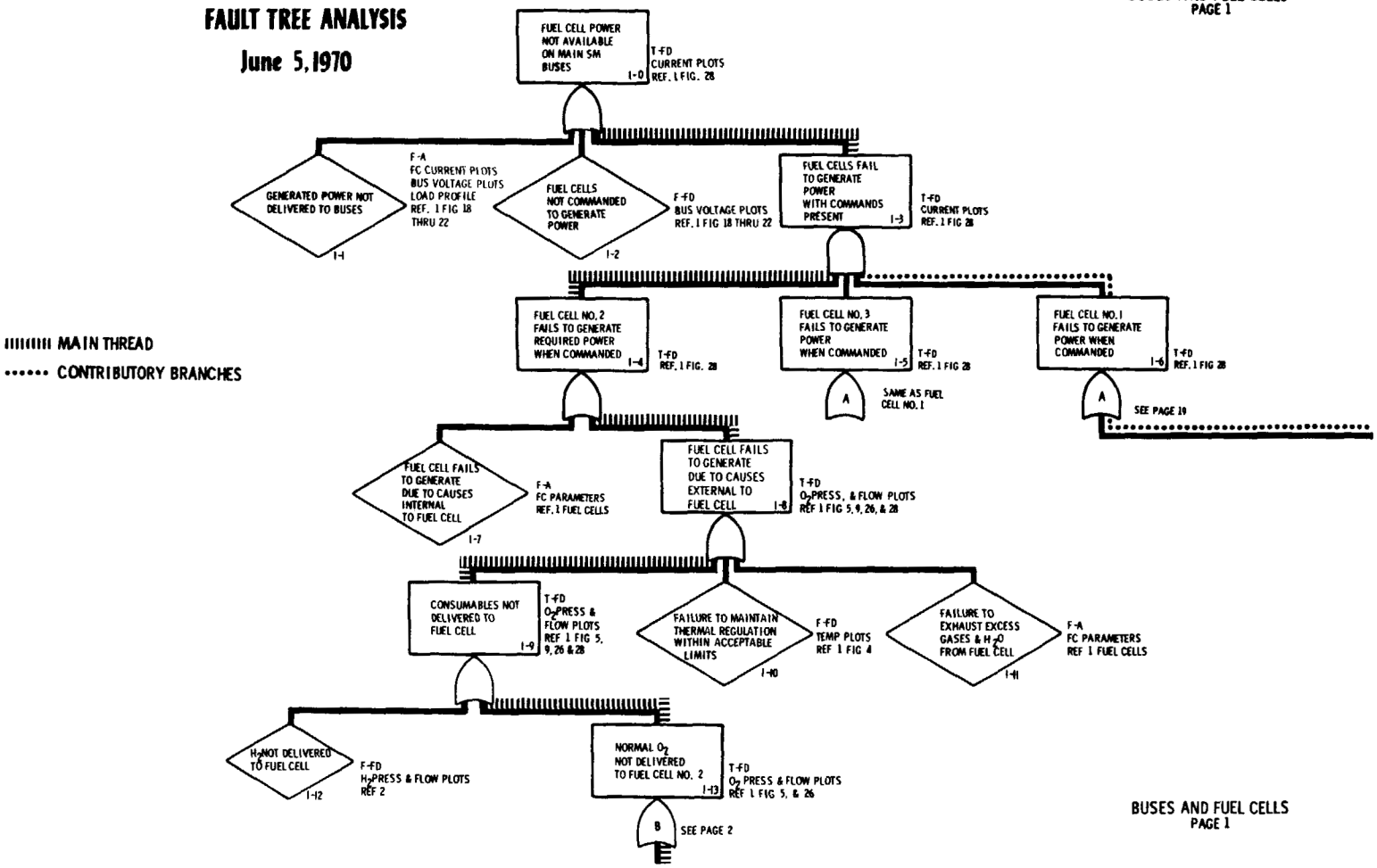

MAIN THREAD

CONTRIBUTORY BRANCHES

BUSES AND FUEL CELLS
PAGE 1

FUEL CELL NO. 2 INTERCONNECT SYSTEM
PAGE 2

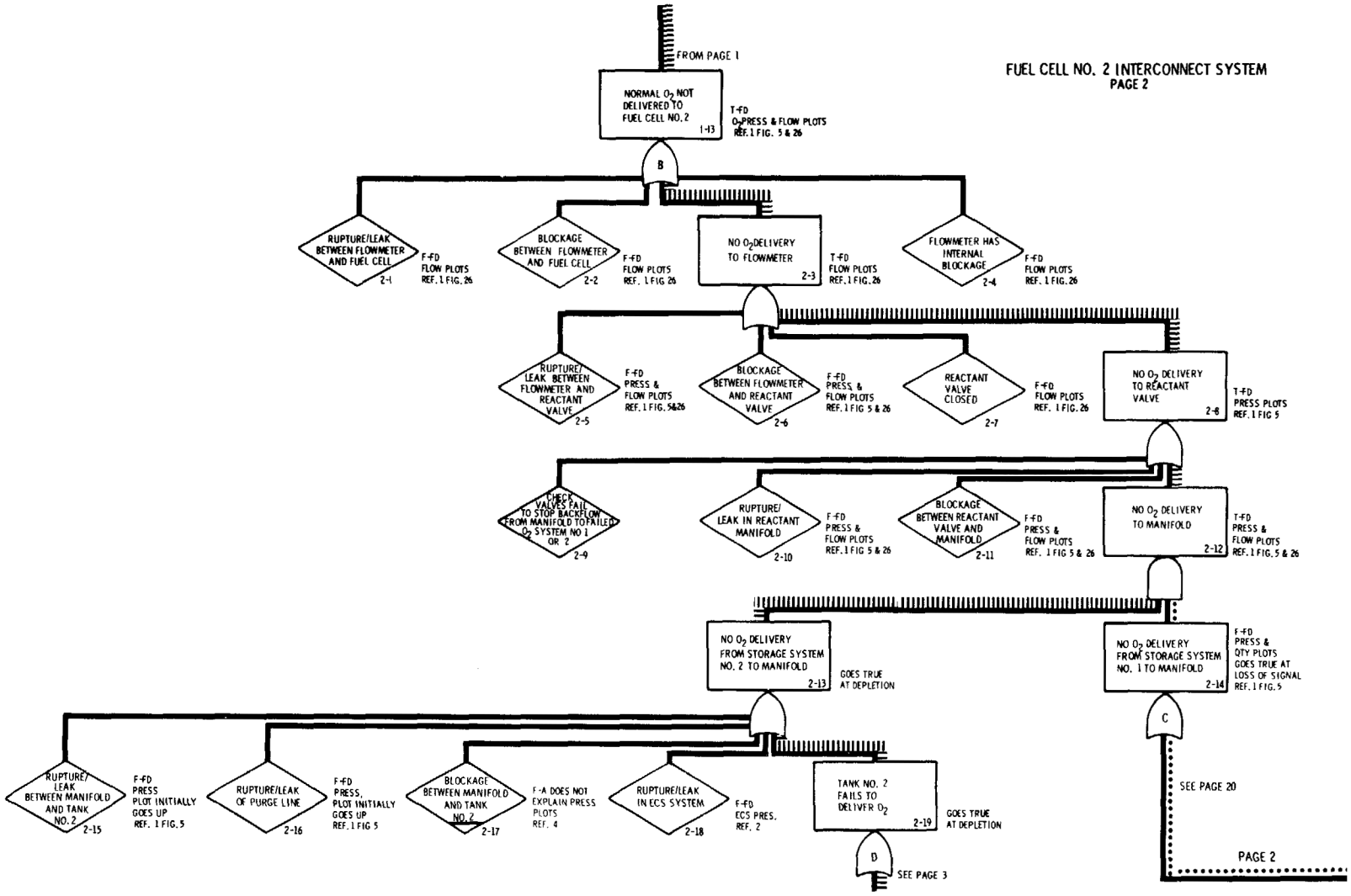

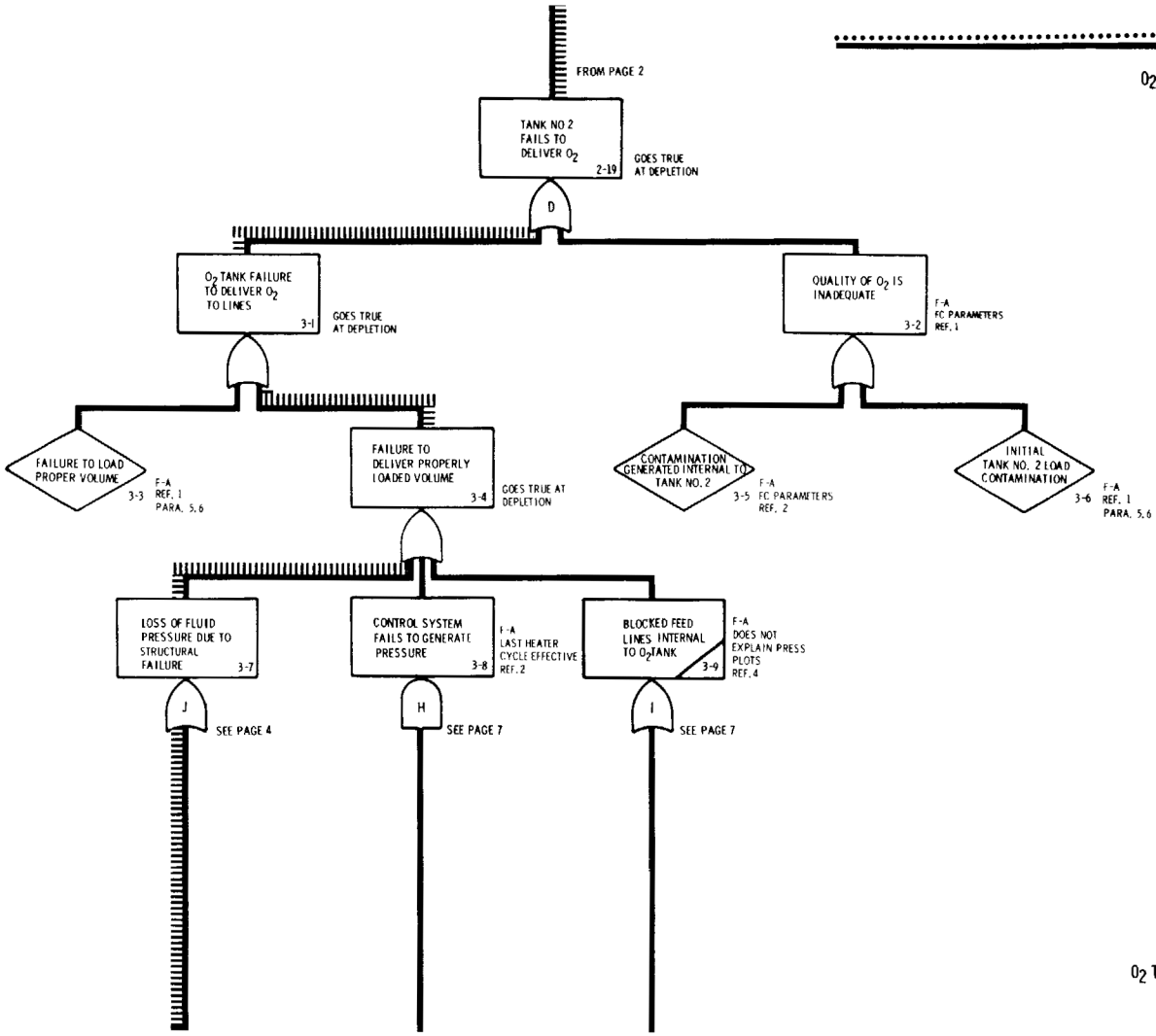

O_2 TANK NO. 2
PAGE 3

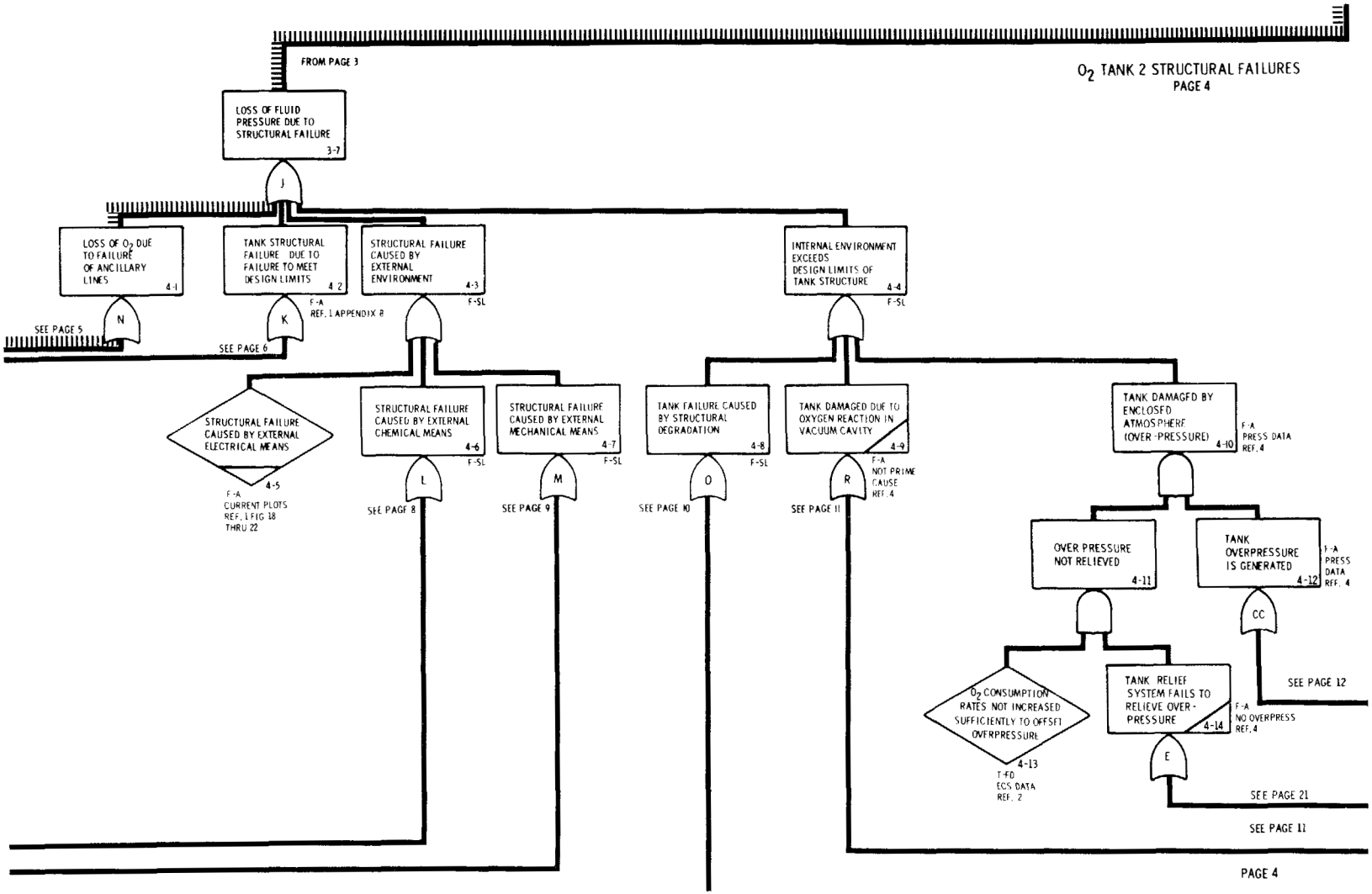
FROM PAGE 3
O_2 TANK 2 STRUCTURAL FAILURES
PAGE 4
LOSS OF FLUID PRESSURE DUE TO STRUCTURAL FAILURE 3-7
J
LOSS OF O_2 DUE TO FAILURE OF ANCILLARY LINES 4-1
TANK STRUCTURAL FAILURE DUE TO FAILURE TO MEET DESIGN LIMITS 4-2
F-A REF. 1 APPENDIX B
STRUCTURAL FAILURE CAUSED BY EXTERNAL ENVIRONMENT 4-3 F-SL
INTERNAL ENVIRONMENT EXCEEDS DESIGN LIMITS OF TANK STRUCTURE 4-4 F-SL
N
K
SEE PAGE 5
SEE PAGE 6
STRUCTURAL FAILURE CAUSED BY EXTERNAL ELECTRICAL MEANS 4-5
F-A CURRENT PLOTS REF. 1 FIG 18 THRU 22
STRUCTURAL FAILURE CAUSED BY EXTERNAL CHEMICAL MEANS 4-6 F-SL
STRUCTURAL FAILURE CAUSED BY EXTERNAL MECHANICAL MEANS 4-7 F-SL
TANK FAILURE CAUSED BY STRUCTURAL DEGRADATION 4-8 F-SL
TANK DAMAGED DUE TO OXYGEN REACTION IN VACUUM CAVITY 4-9
F-A NOT PRIME CAUSE REF. 4
TANK DAMAGED BY ENCLOSED ATMOSPHERE (OVER-PRESSURE) 4-10
F-A PRESS DATA REF. 4
L
M
O
R
SEE PAGE 8
SEE PAGE 9
SEE PAGE 10
SEE PAGE 11
OVER PRESSURE NOT RELIEVED 4-11
TANK OVERPRESSURE IS GENERATED 4-12
F-A PRESS DATA REF. 4
CC
SEE PAGE 12
O_2 CONSUMPTION RATES NOT INCREASED SUFFICIENTLY TO OFFSET OVERPRESSURE 4-13
T-FD ECS DATA REF. 2
TANK RELIEF SYSTEM FAILS TO RELIEVE OVER-PRESSURE 4-14
F-A NO OVERPRESS REF. 4
E
SEE PAGE 21
SEE PAGE 11
PAGE 4

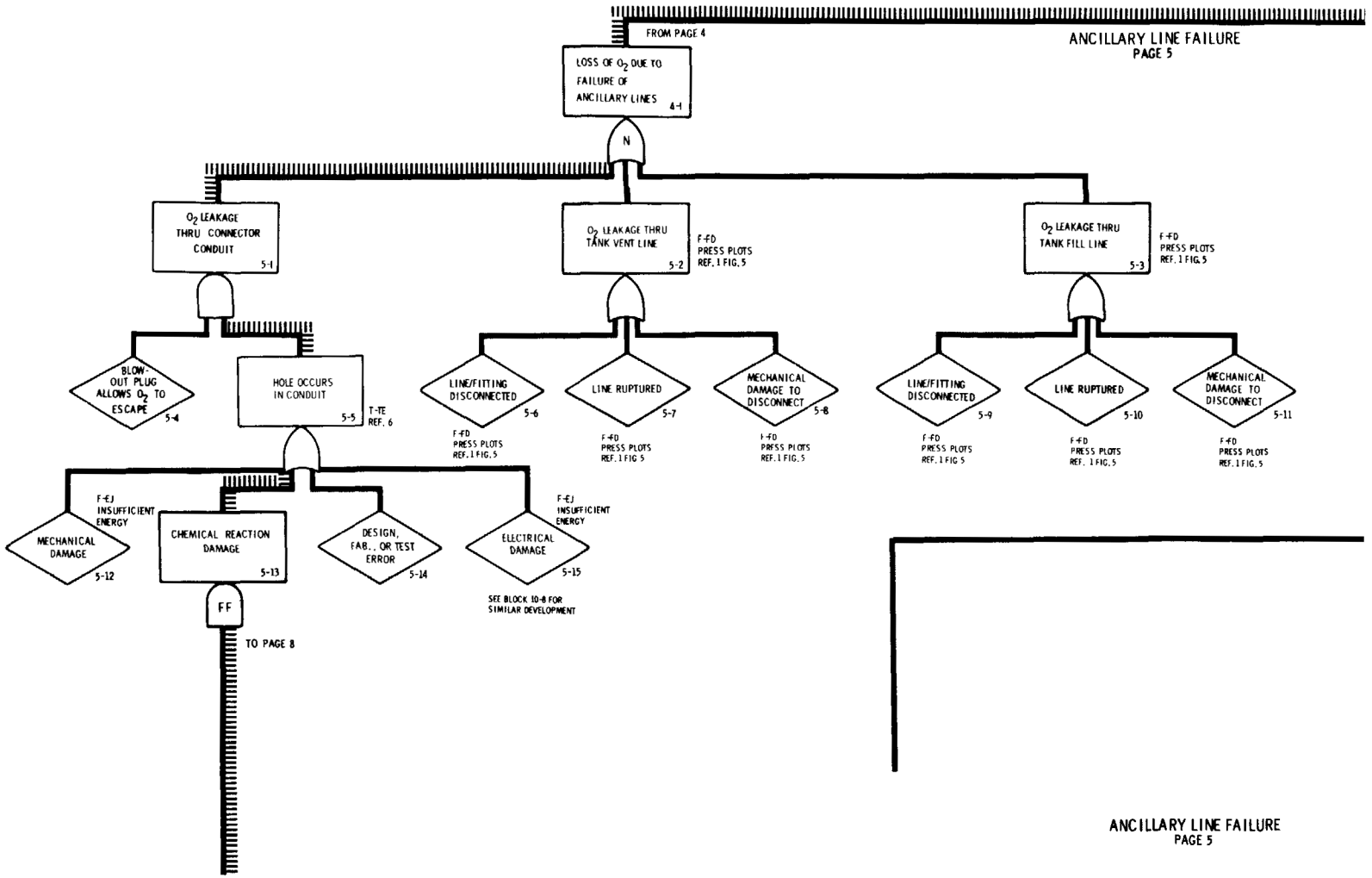
FROM PAGE 4
ANCILLARY LINE FAILURE
PAGE 5
LOSS OF O_2 DUE TO FAILURE OF ANCILLARY LINES 4-1
N
O_2 LEAKAGE THRU CONNECTOR CONDUIT 5-1
O_2 LEAKAGE THRU TANK VENT LINE 5-2
F-FD PRESS PLOTS REF. 1 FIG. 5
O_2 LEAKAGE THRU TANK FILL LINE 5-3
F-FD PRESS PLOTS REF. 1 FIG. 5
BLOW-OUT PLUG ALLOWS O_2 TO ESCAPE 5-4
HOLE OCCURS IN CONDUIT 5-5
T-TE REF. 6
LINE/FITTING DISCONNECTED 5-6
F-FD PRESS PLOTS REF. 1 FIG. 5
LINE RUPTURED 5-7
F-FD PRESS PLOTS REF. 1 FIG 5
MECHANICAL DAMAGE TO DISCONNECT 5-8
F-FD PRESS PLOTS REF. 1 FIG. 5
LINE/FITTING DISCONNECTED 5-9
F-FD PRESS PLOTS REF. 1 FIG 5
LINE RUPTURED 5-10
F-FD PRESS PLOTS REF. 1 FIG. 5
MECHANICAL DAMAGE TO DISCONNECT 5-11
F-FD PRESS PLOTS REF. 1 FIG. 5
F-EJ INSUFFICIENT ENERGY
MECHANICAL DAMAGE 5-12
CHEMICAL REACTION DAMAGE 5-13
DESIGN, FAB., OR TEST ERROR 5-14
F-EJ INSUFFICIENT ENERGY
ELECTRICAL DAMAGE 5-15
SEE BLOCK 10-8 FOR SIMILAR DEVELOPMENT
FF
TO PAGE 8
ANCILLARY LINE FAILURE
PAGE 5

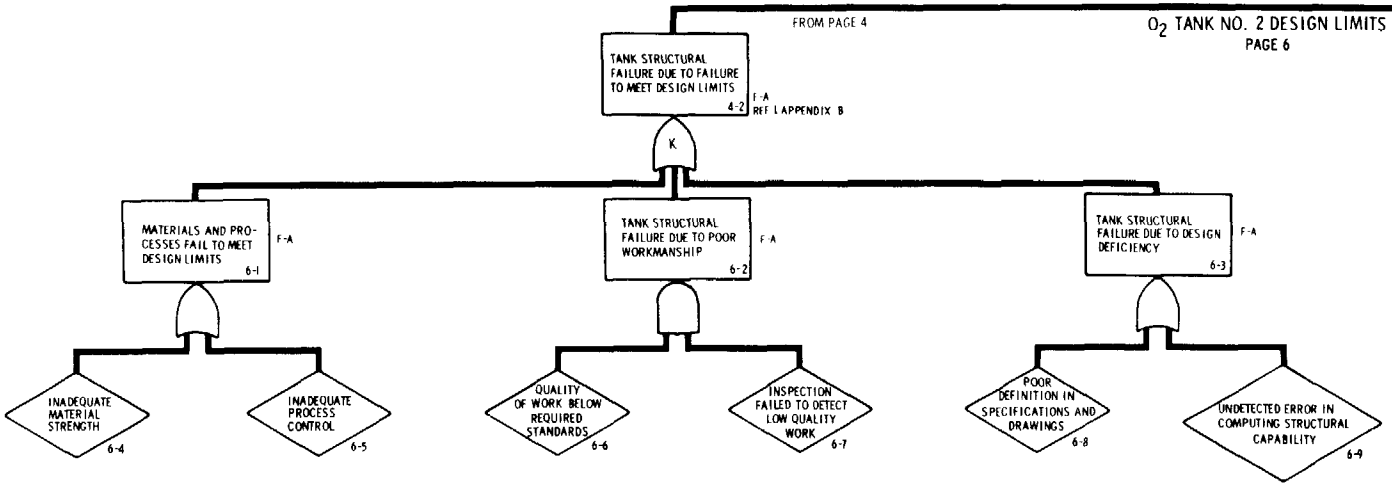

O_2 TANK NO. 2 DESIGN LIMITS
PAGE 6

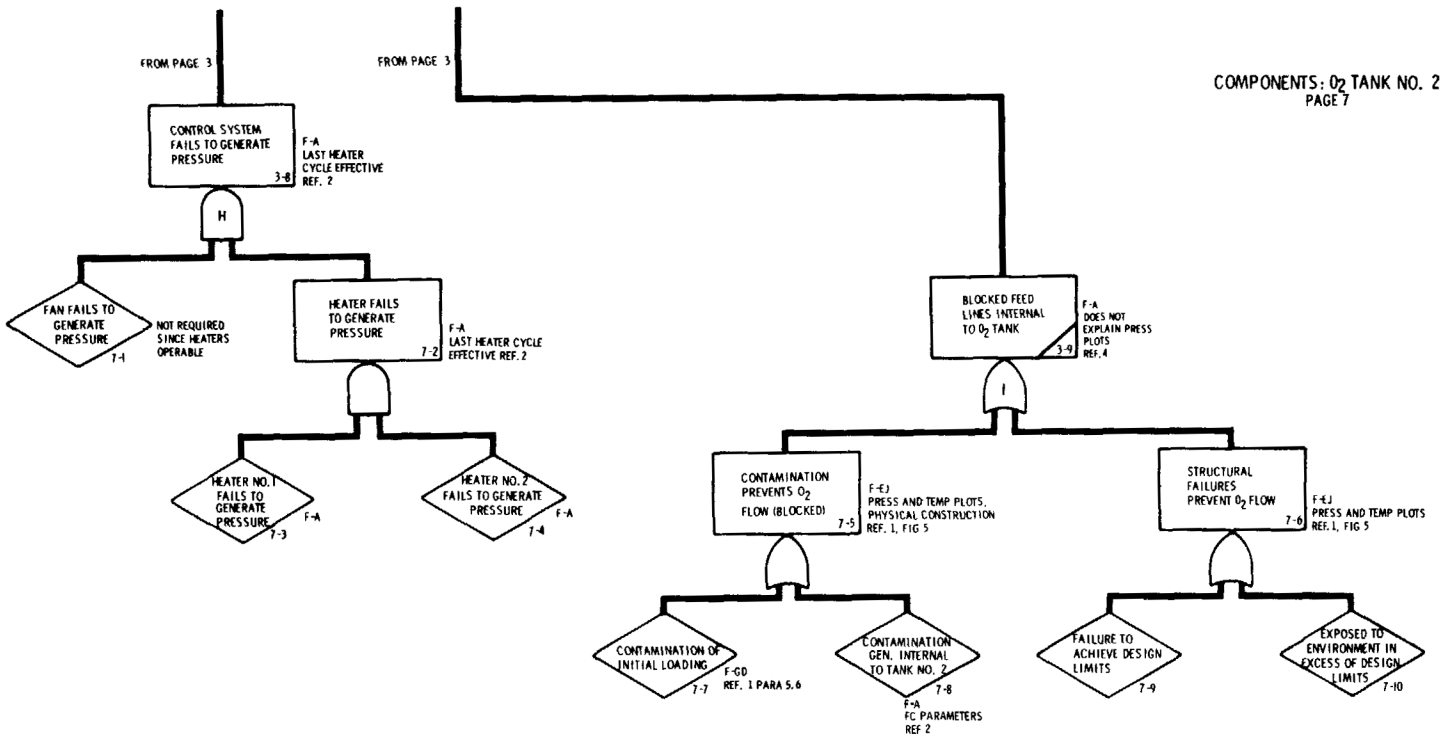
FROM PAGE 3
FROM PAGE 3
COMPONENTS: O_2 TANK NO. 2
PAGE 7
CONTROL SYSTEM FAILS TO GENERATE PRESSURE
3-8
F-A
LAST HEATER CYCLE EFFECTIVE
REF. 2
H
FAN FAILS TO GENERATE PRESSURE
7-1
NOT REQUIRED SINCE HEATERS OPERABLE
HEATER FAILS TO GENERATE PRESSURE
7-2
F-A
LAST HEATER CYCLE EFFECTIVE REF. 2
HEATER NO. 1 FAILS TO GENERATE PRESSURE
7-3
F-A
HEATER NO. 2 FAILS TO GENERATE PRESSURE
7-4
F-A
BLOCKED FEED LINES INTERNAL TO O_2 TANK
3-9
F-A
DOES NOT EXPLAIN PRESS PLOTS
REF. 4
I
CONTAMINATION PREVENTS O_2 FLOW (BLOCKED)
7-5
F-EJ
PRESS AND TEMP PLOTS, PHYSICAL CONSTRUCTION
REF. 1, FIG 5
STRUCTURAL FAILURES PREVENT O_2 FLOW
7-6
F-EJ
PRESS AND TEMP PLOTS
REF. 1, FIG 5
CONTAMINATION OF INITIAL LOADING
7-7
F-GD
REF. 1 PARA 5.6
CONTAMINATION GEN. INTERNAL TO TANK NO. 2
7-8
F-A
FC PARAMETERS
REF 2
FAILURE TO ACHIEVE DESIGN LIMITS
7-9
EXPOSED TO ENVIRONMENT IN EXCESS OF DESIGN LIMITS
7-10
COMPONENTS: O_2 TANK NO. 2
PAGE 7

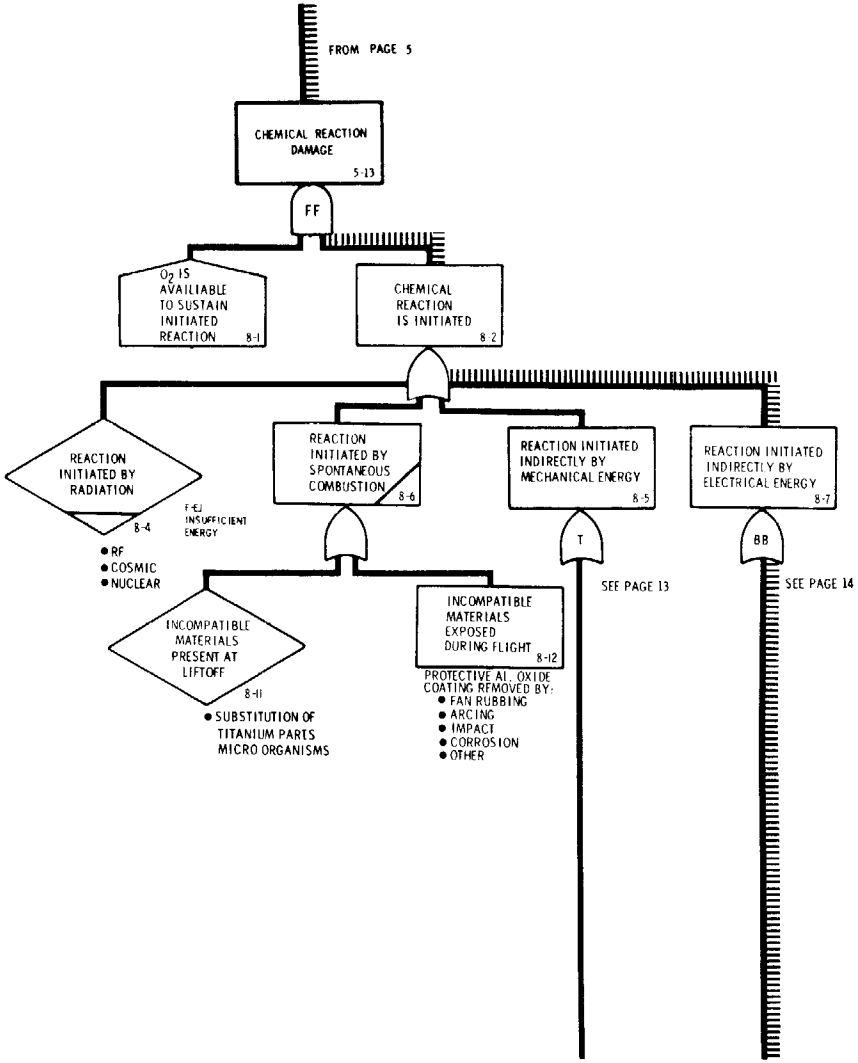

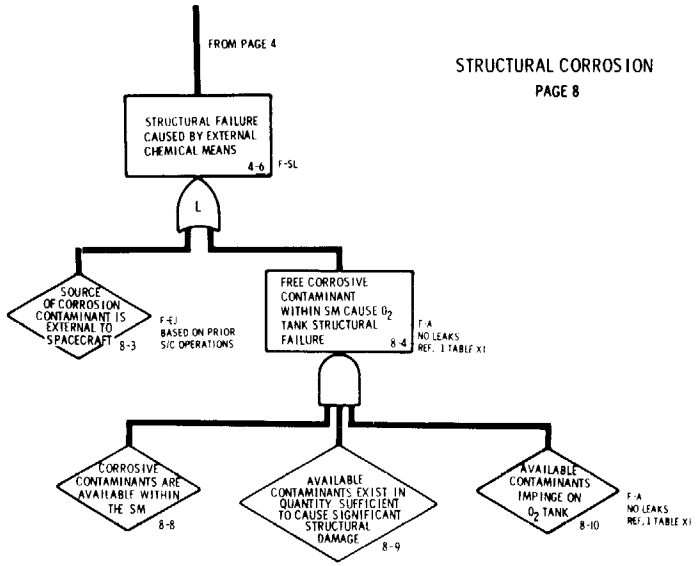

STRUCTURAL CORROSION
PAGE 8

STRUCTURAL CORROSION
PAGE 8

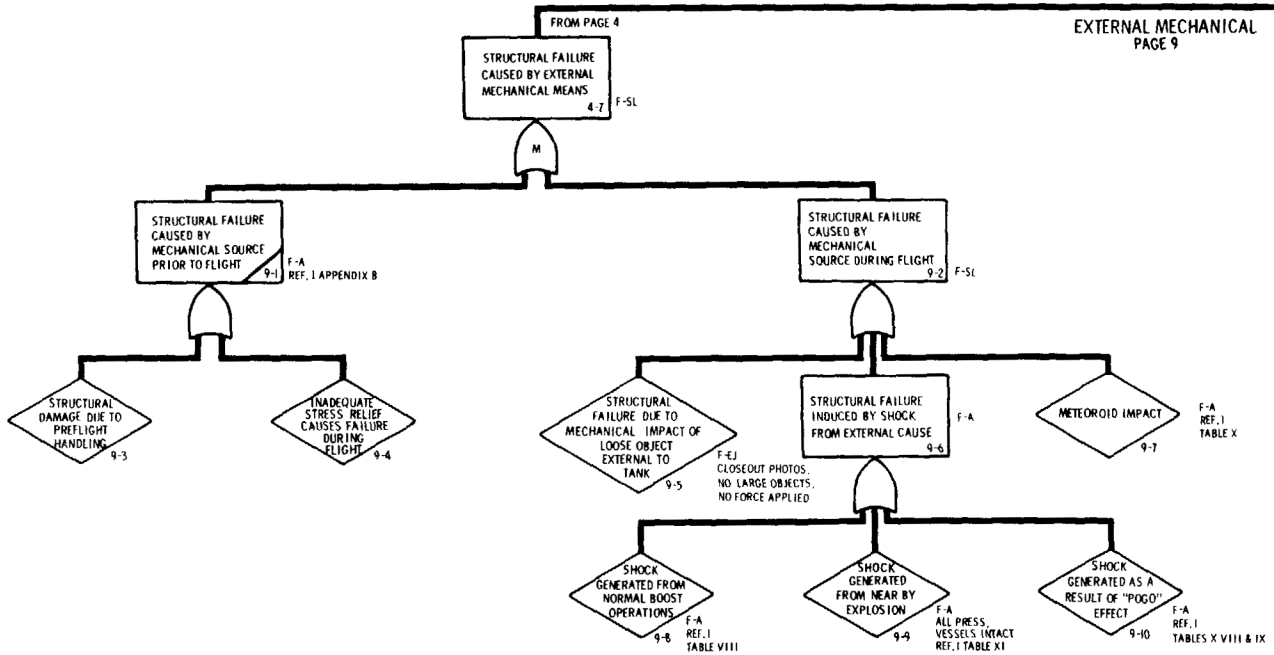

EXTERNAL MECHANICAL
PAGE 9

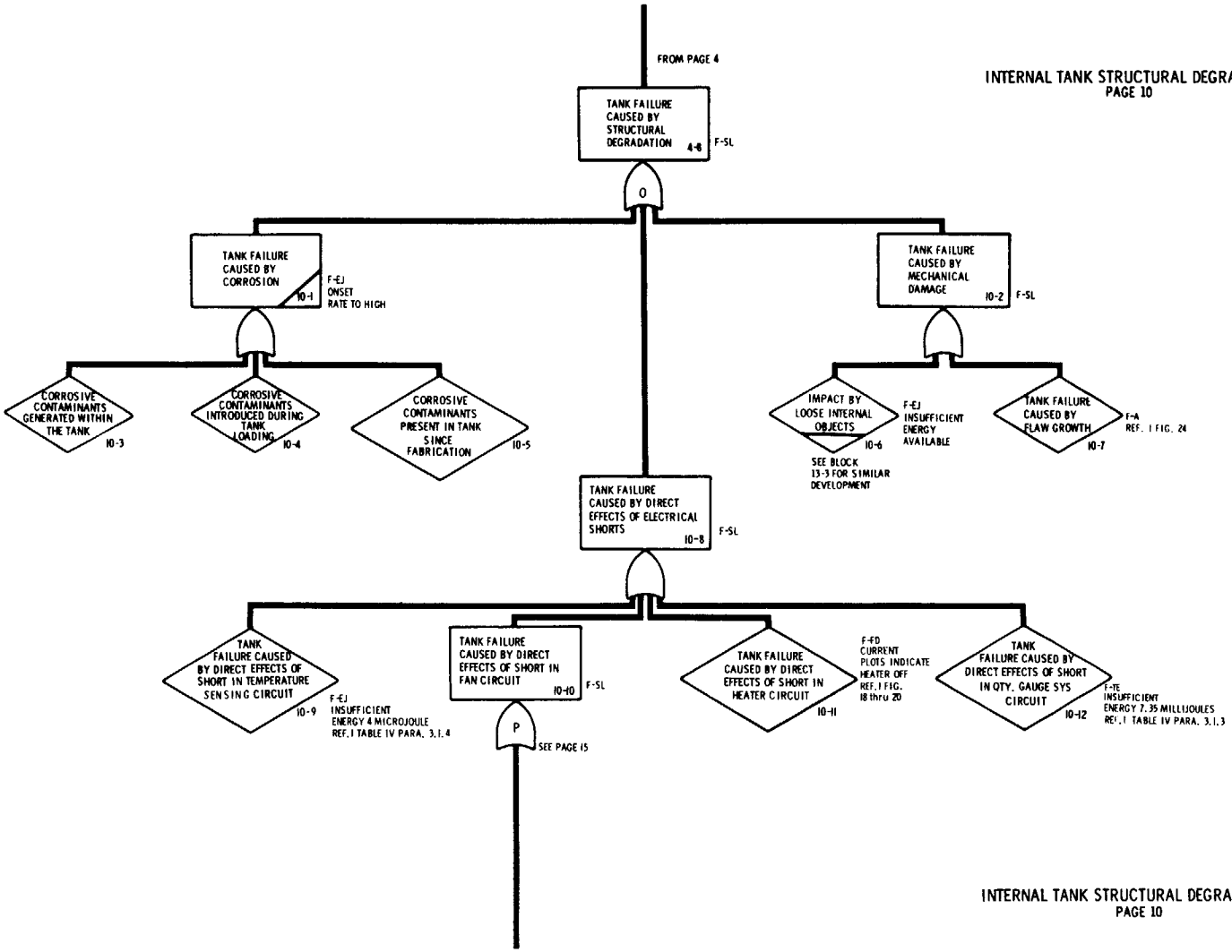

INTERNAL TANK STRUCTURAL DEGRADATION
PAGE 10

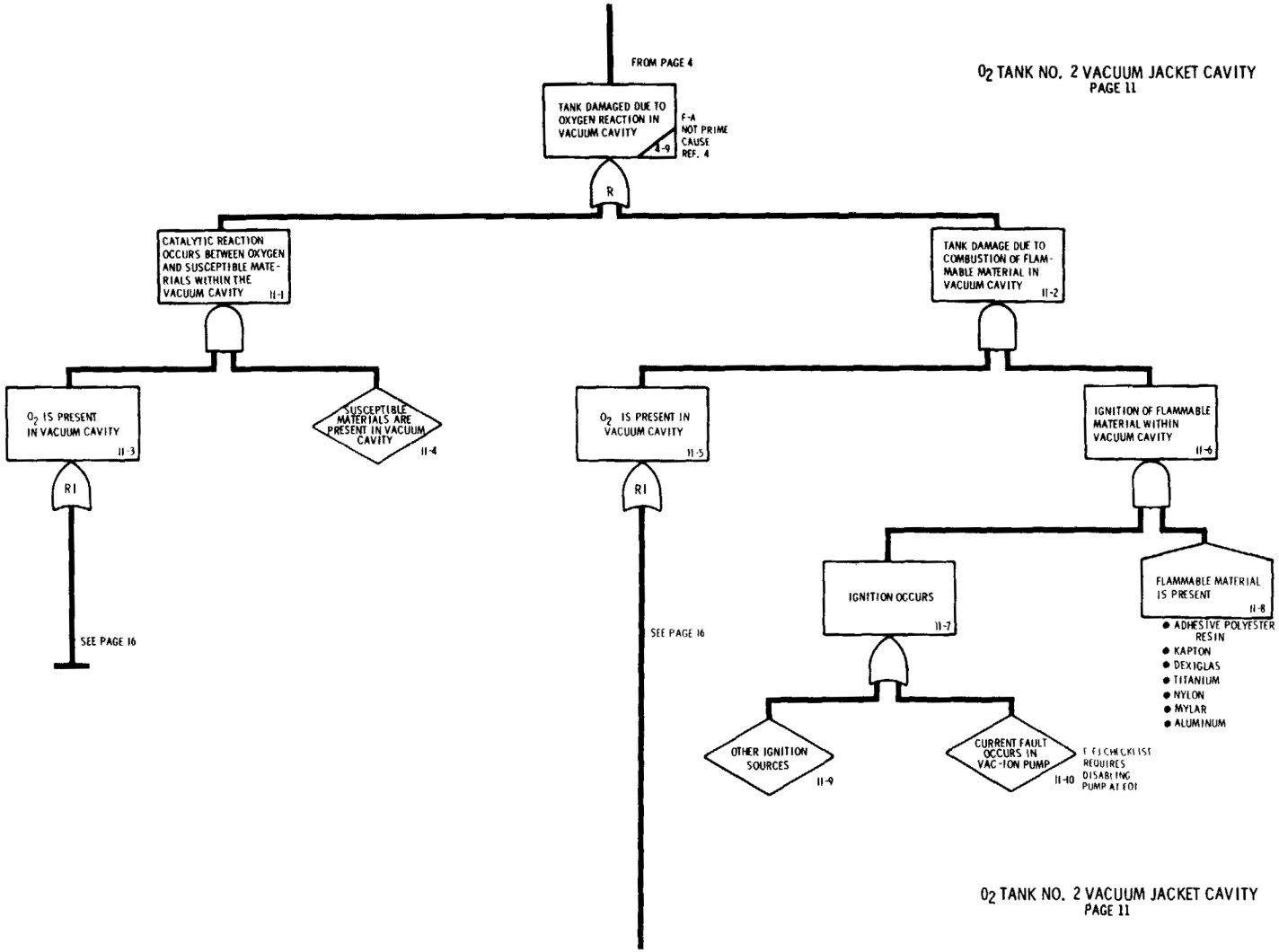
O_2 TANK NO. 2 VACUUM JACKET CAVITY
PAGE 11
FROM PAGE 4
TANK DAMAGED DUE TO OXYGEN REACTION IN VACUUM CAVITY
F-A
A-9
NOT PRIME CAUSE REF. 4
R
CATALYTIC REACTION OCCURS BETWEEN OXYGEN AND SUSCEPTIBLE MATERIALS WITHIN THE VACUUM CAVITY 11-1
TANK DAMAGE DUE TO COMBUSTION OF FLAMMABLE MATERIAL IN VACUUM CAVITY 11-2
O_2 IS PRESENT IN VACUUM CAVITY 11-3
SUSCEPTIBLE MATERIALS ARE PRESENT IN VACUUM CAVITY 11-4
O_2 IS PRESENT IN VACUUM CAVITY 11-5
IGNITION OF FLAMMABLE MATERIAL WITHIN VACUUM CAVITY 11-6
R1
R1
SEE PAGE 16
SEE PAGE 16
IGNITION OCCURS 11-7
FLAMMABLE MATERIAL IS PRESENT 11-8
ADHESIVE POLYESTER RESIN
KAPTON
DEXIGLAS
TITANIUM
NYLON
MYLAR
ALUMINUM
OTHER IGNITION SOURCES 11-9
CURRENT FAULT OCCURS IN VAC-ION PUMP 11-10
F F S CHECKLIST REQUIRES DISABLING PUMP AT EOI
O_2 TANK NO. 2 VACUUM JACKET CAVITY
PAGE 11

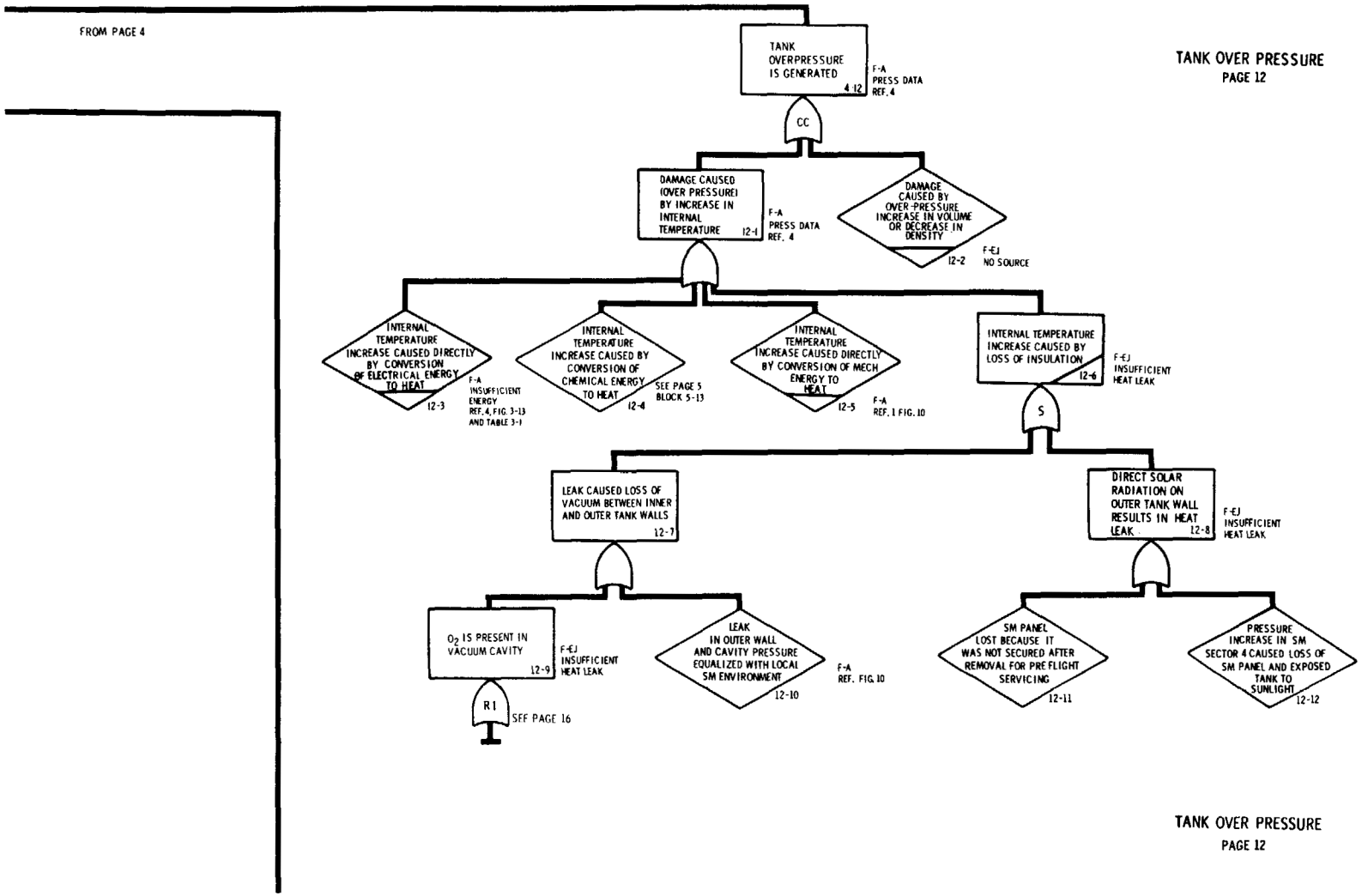

TANK OVER PRESSURE
PAGE 12

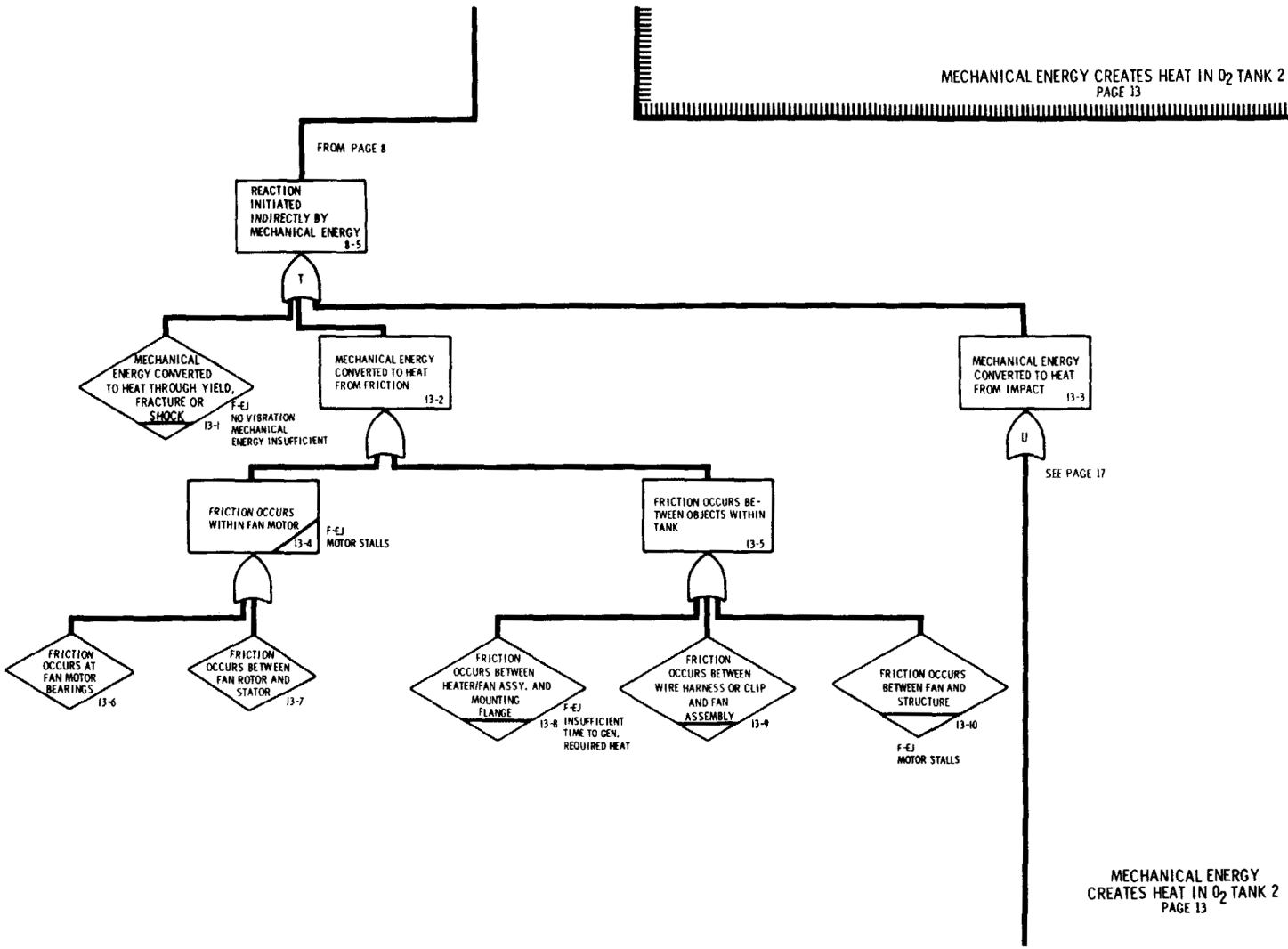

MECHANICAL ENERGY CREATES HEAT IN O_2 TANK 2
PAGE 13

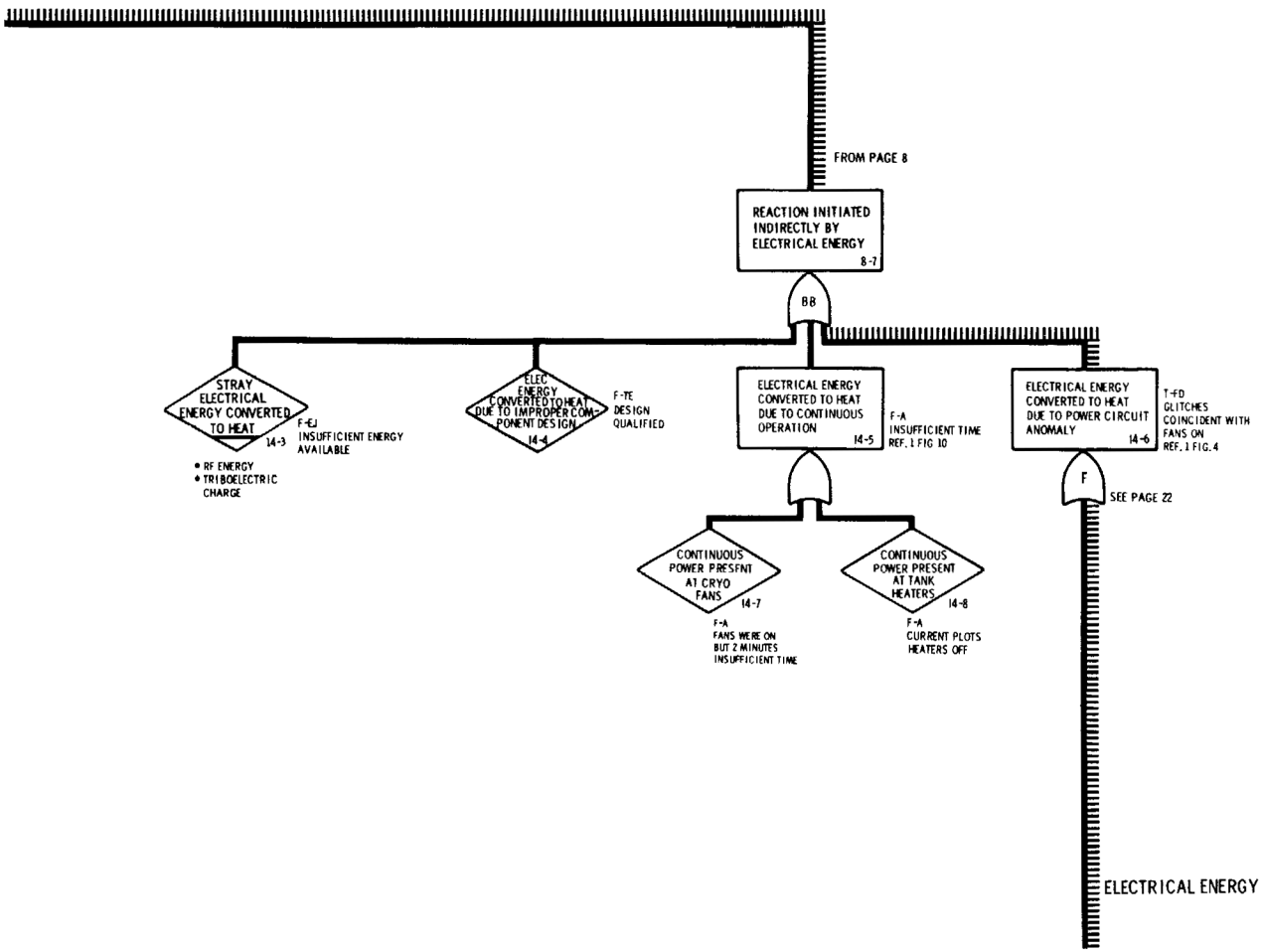
FROM PAGE 8
REACTION INITIATED INDIRECTLY BY ELECTRICAL ENERGY
8-7
BB
STRAY ELECTRICAL ENERGY CONVERTED TO HEAT
14-3
F-EJ
INSUFFICIENT ENERGY AVAILABLE
• RF ENERGY
• TRIBOELECTRIC CHARGE
ELEC ENERGY CONVERTED TO HEAT DUE TO IMPROPER COMPONENT DESIGN
14-4
F-TE
DESIGN QUALIFIED
ELECTRICAL ENERGY CONVERTED TO HEAT DUE TO CONTINUOUS OPERATION
14-5
F-A
INSUFFICIENT TIME
REF. 1 FIG 10
ELECTRICAL ENERGY CONVERTED TO HEAT DUE TO POWER CIRCUIT ANOMALY
14-6
T-FD
GLITCHES COINCIDENT WITH FANS ON
REF. 1 FIG. 4
F
SEE PAGE 22
CONTINUOUS POWER PRESENT AT CRYO FANS
14-7
F-A
FANS WERE ON BUT 2 MINUTES INSUFFICIENT TIME
CONTINUOUS POWER PRESENT AT TANK HEATERS
14-8
F-A
CURRENT PLOTS HEATERS OFF
ELECTRICAL ENERGY CREATES HEAT IN O_2 TANK NO. 2
PAGE 14

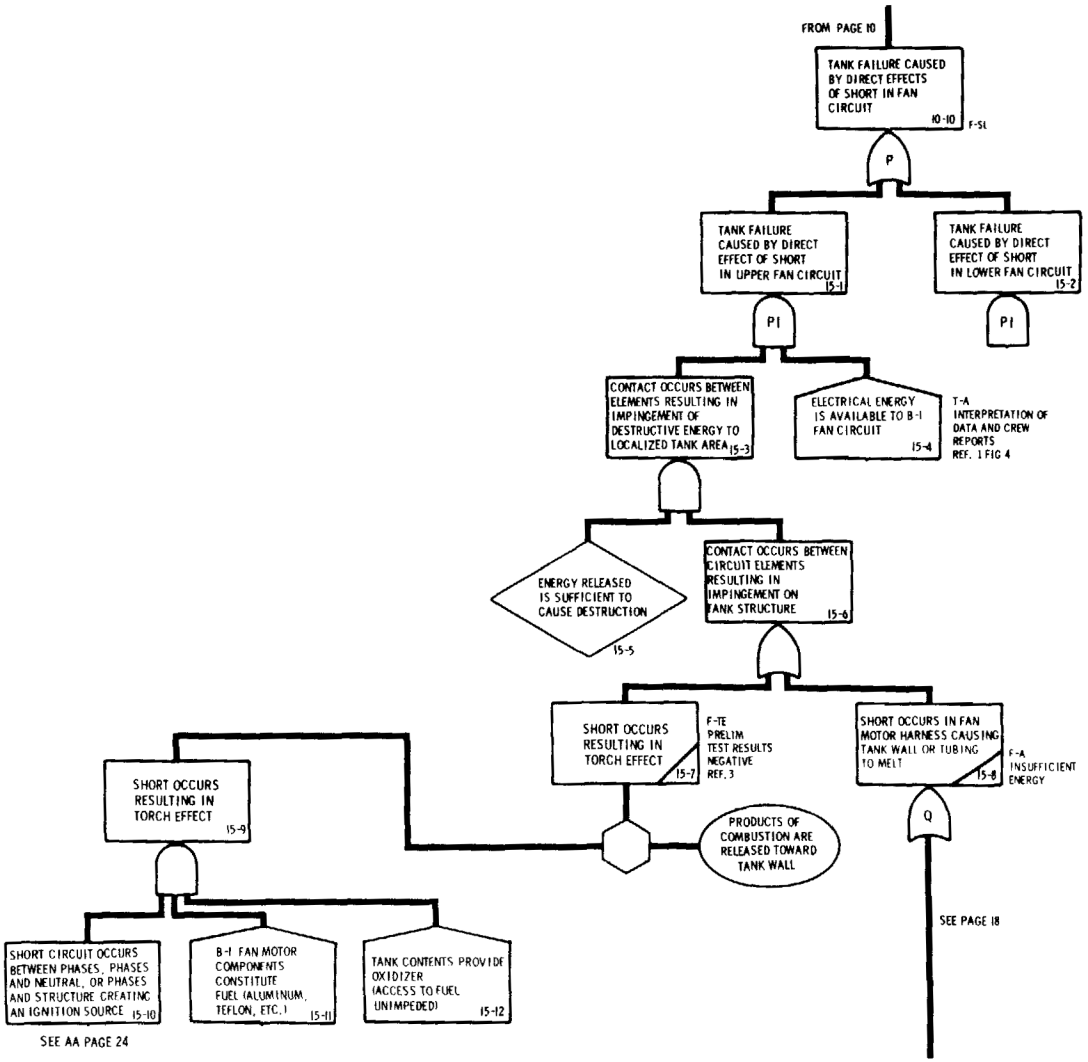

FANS MOTOR SHORT-TORCH EFFECT
PAGE 15

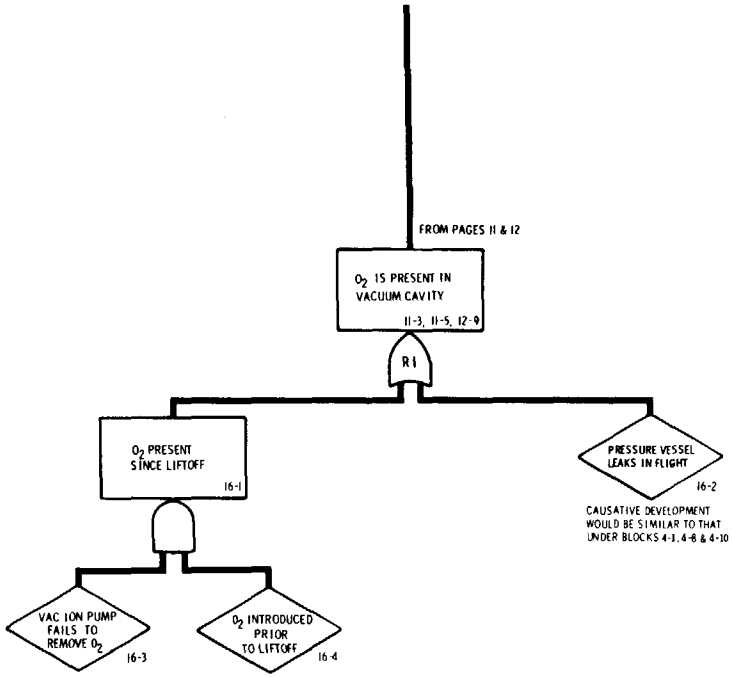

O_2 IN VACUUM CAVITY
PAGE 16

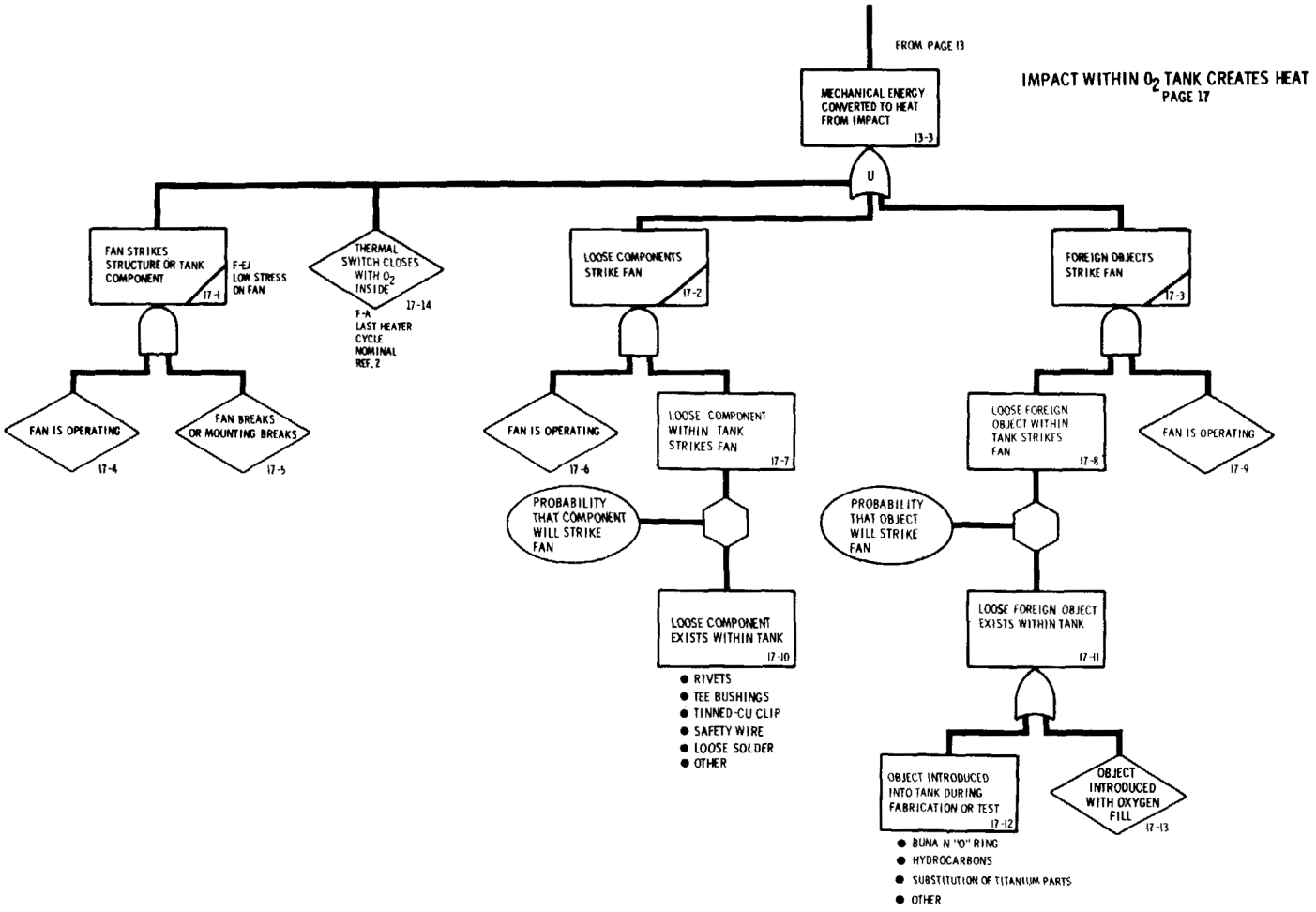
FROM PAGE 13
IMPACT WITHIN 0_2 TANK CREATES HEAT
PAGE 17
MECHANICAL ENERGY CONVERTED TO HEAT FROM IMPACT
13-3
U
FAN STRIKES STRUCTURE OR TANK COMPONENT
17-1
F-EJ LOW STRESS ON FAN
THERMAL SWITCH CLOSES WITH 0_2 INSIDE
17-14
F-A LAST HEATER CYCLE NOMINAL REF. 2
LOOSE COMPONENTS STRIKE FAN
17-2
FOREIGN OBJECTS STRIKE FAN
17-3
FAN IS OPERATING
17-4
FAN BREAKS OR MOUNTING BREAKS
17-5
FAN IS OPERATING
17-6
LOOSE COMPONENT WITHIN TANK STRIKES FAN
17-7
LOOSE FOREIGN OBJECT WITHIN TANK STRIKES FAN
17-8
FAN IS OPERATING
17-9
PROBABILITY THAT COMPONENT WILL STRIKE FAN
PROBABILITY THAT OBJECT WILL STRIKE FAN
LOOSE COMPONENT EXISTS WITHIN TANK
17-10
LOOSE FOREIGN OBJECT EXISTS WITHIN TANK
17-11
RIVETS
TEE BUSHINGS
TINNED-CU CLIP
SAFETY WIRE
LOOSE SOLDER
OTHER
OBJECT INTRODUCED INTO TANK DURING FABRICATION OR TEST
17-12
OBJECT INTRODUCED WITH OXYGEN FILL
17-13
BUNA N "O" RING
HYDROCARBONS
SUBSTITUTION OF TITANIUM PARTS
OTHER
IMPACT WITHIN 0_2 TANK CREATES HEAT
PAGE 17

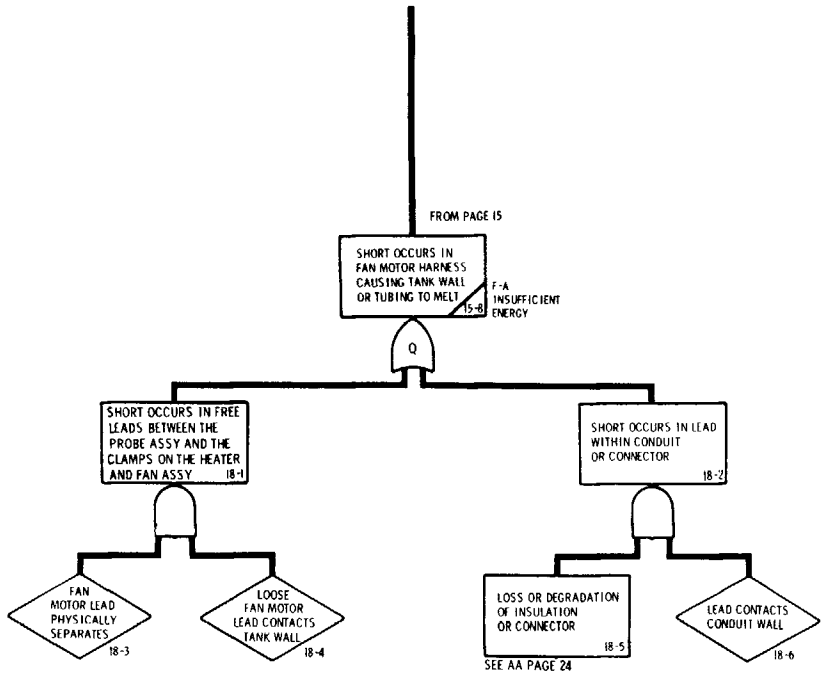

FAN CIRCUIT - TORCH EFFECT
PAGE 18

FUEL CELL NO. 1&3 POWER GENERATION
PAGE 19

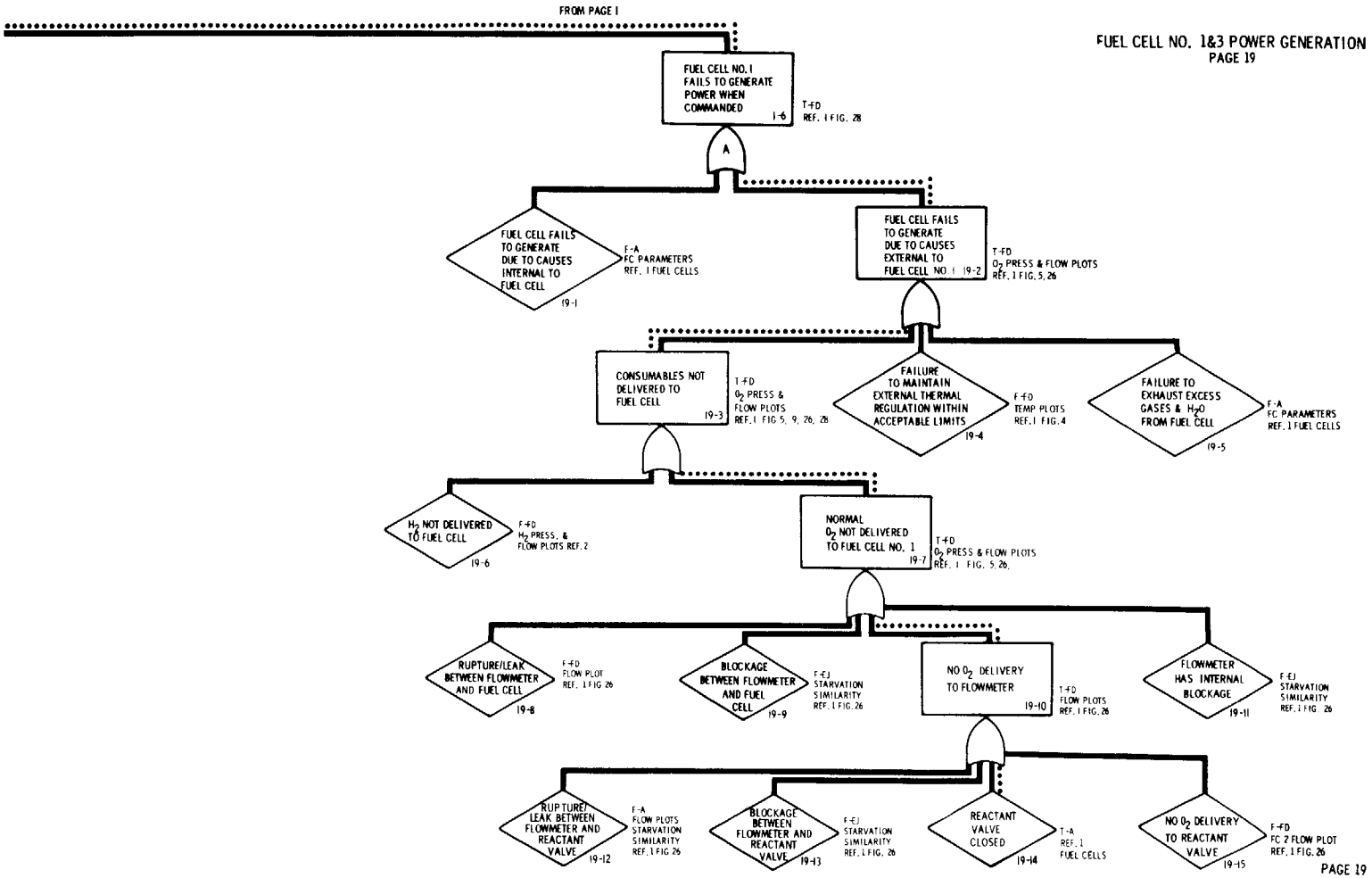

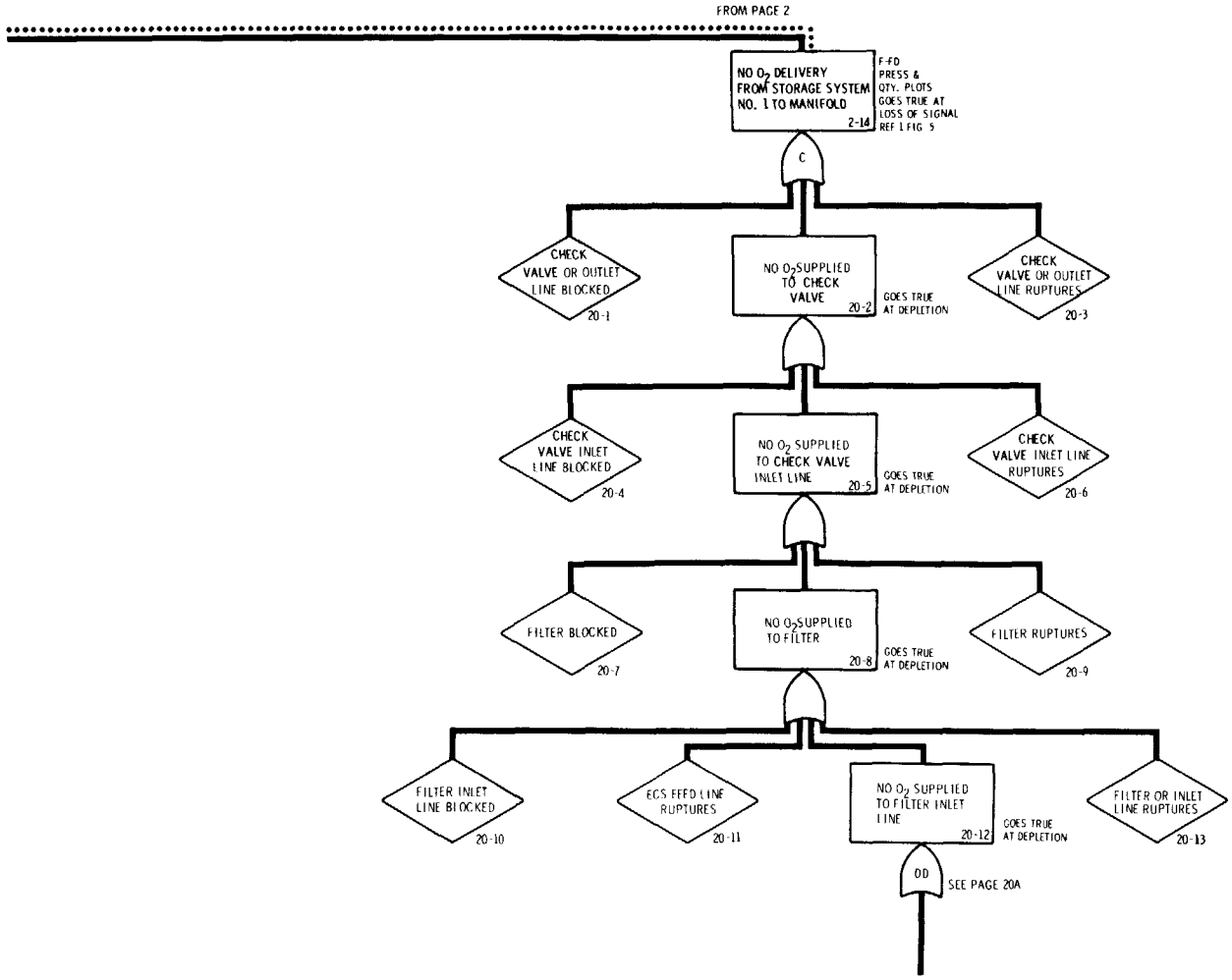
FROM PAGE 2
NO O_2 DELIVERY FROM STORAGE SYSTEM NO. 1 TO MANIFOLD
2-14
F-FD PRESS & QTY. PLOTS GOES TRUE AT LOSS OF SIGNAL REF 1 FIG 5
C
CHECK VALVE OR OUTLET LINE BLOCKED
20-1
NO O_2 SUPPLIED TO CHECK VALVE
20-2
GOES TRUE AT DEPLETION
CHECK VALVE OR OUTLET LINE RUPTURES
20-3
CHECK VALVE INLET LINE BLOCKED
20-4
NO O_2 SUPPLIED TO CHECK VALVE INLET LINE
20-5
GOES TRUE AT DEPLETION
CHECK VALVE INLET LINE RUPTURES
20-6
FILTER BLOCKED
20-7
NO O_2 SUPPLIED TO FILTER
20-8
GOES TRUE AT DEPLETION
FILTER RUPTURES
20-9
FILTER INLET LINE BLOCKED
20-10
ECS FEED LINE RUPTURES
20-11
NO O_2 SUPPLIED TO FILTER INLET LINE
20-12
GOES TRUE AT DEPLETION
FILTER OR INLET LINE RUPTURES
20-13
OD
SEE PAGE 20A

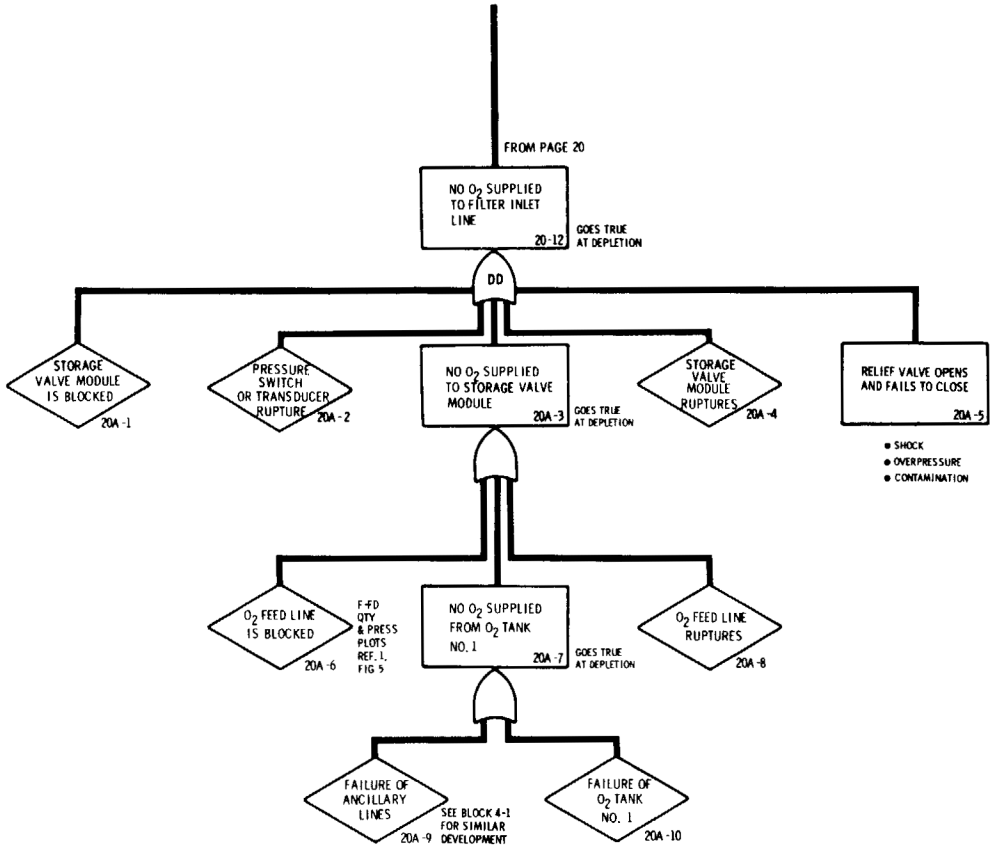

O_2STORAGE SYSTEM No. 1
& TANK NO. 1
PAGE 20A

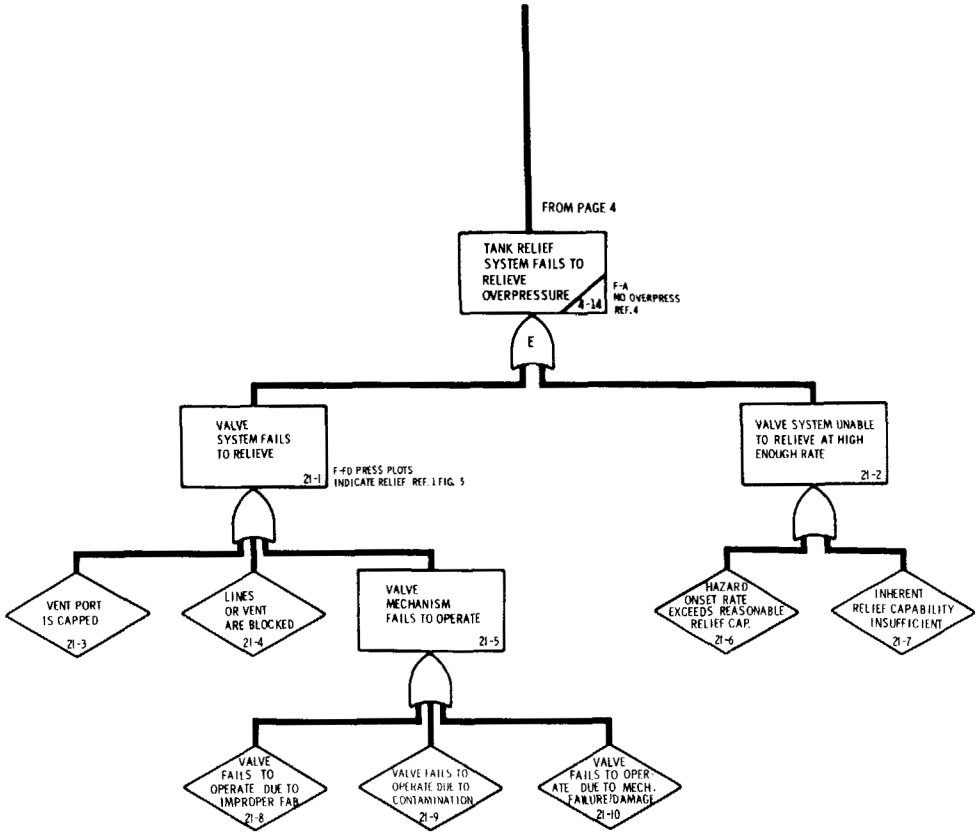

O_2 TANK NO. 2 PRESSURE RELIEF
PAGE 21

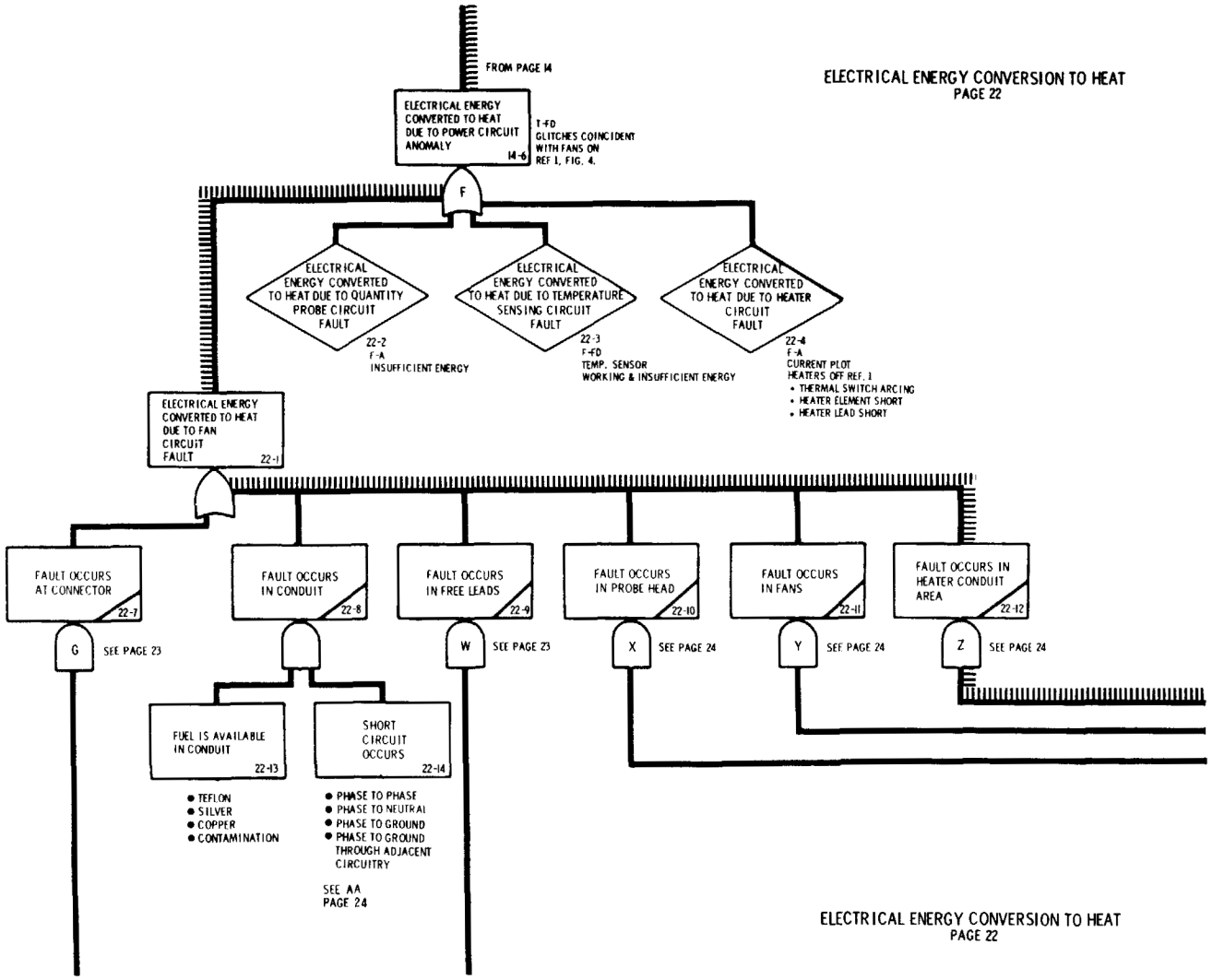

ELECTRICAL ENERGY CONVERSION TO HEAT
PAGE 22

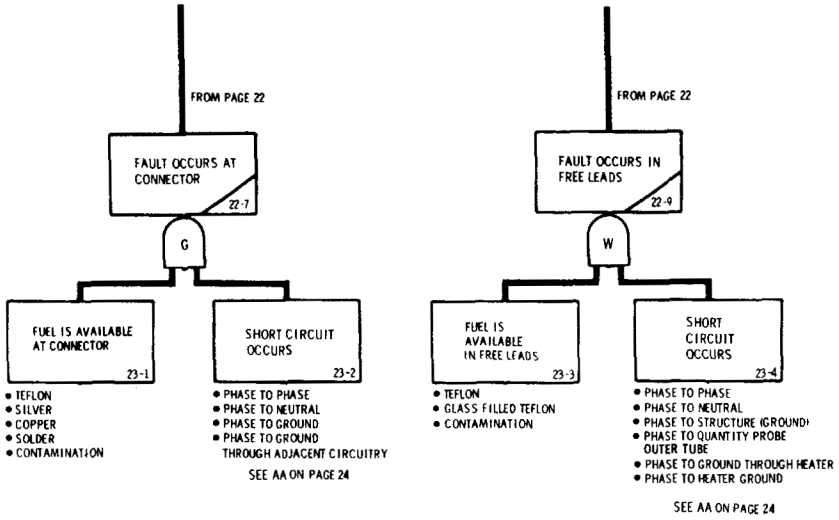

SHORT CIRCUIT REACTIONS
PAGE 23

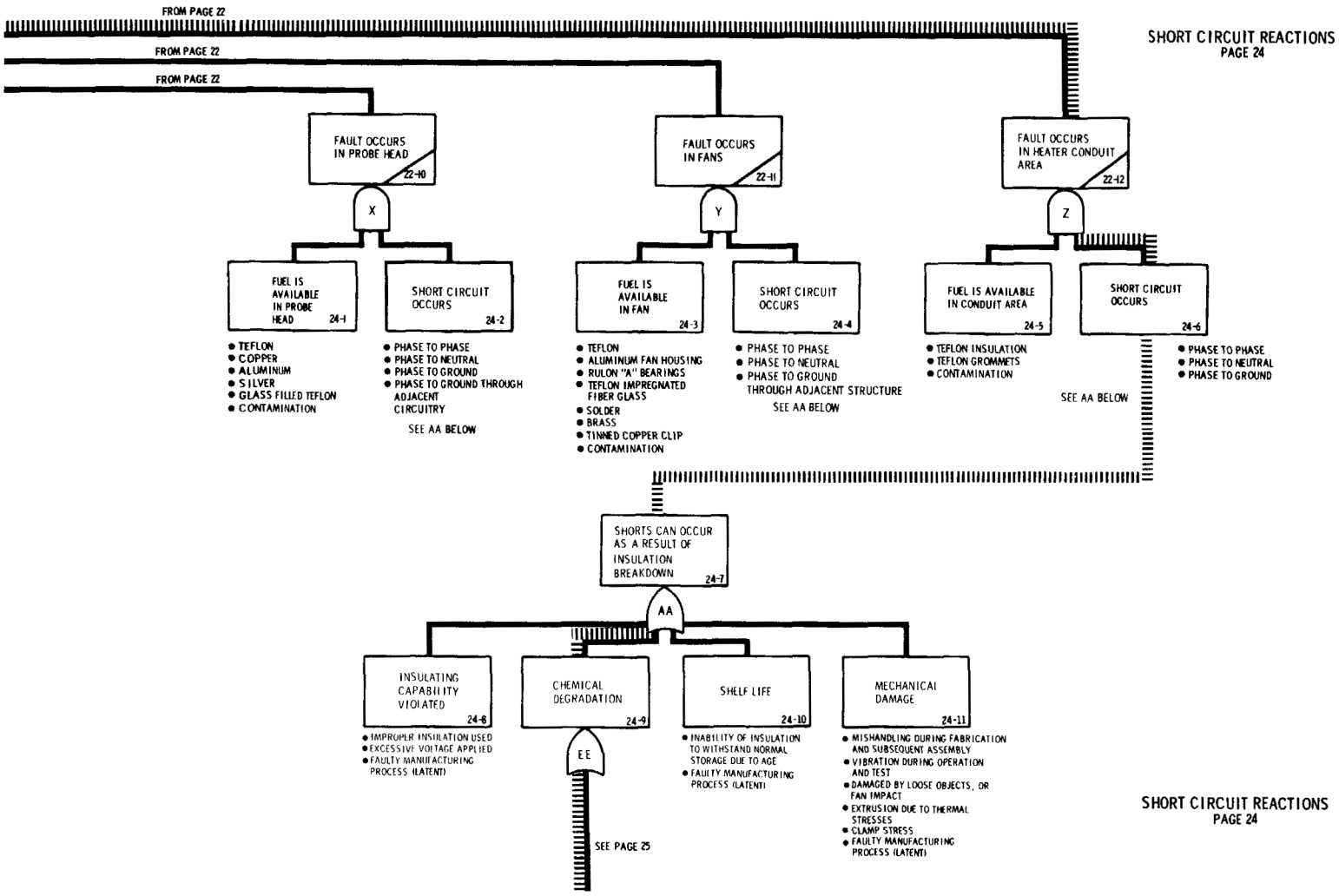
FROM PAGE 22
FROM PAGE 22
FROM PAGE 22
SHORT CIRCUIT REACTIONS
PAGE 24
FAULT OCCURS IN PROBE HEAD
22-10
FAULT OCCURS IN FANS
22-11
FAULT OCCURS IN HEATER CONDUIT AREA
22-12
X
Y
Z
FUEL IS AVAILABLE IN PROBE HEAD
24-1
SHORT CIRCUIT OCCURS
24-2
FUEL IS AVAILABLE IN FAN
24-3
SHORT CIRCUIT OCCURS
24-4
FUEL IS AVAILABLE IN CONDUIT AREA
24-5
SHORT CIRCUIT OCCURS
24-6
• TEFLON
• COPPER
• ALUMINUM
• SILVER
• GLASS FILLED TEFLON
• CONTAMINATION
• PHASE TO PHASE
• PHASE TO NEUTRAL
• PHASE TO GROUND
• PHASE TO GROUND THROUGH ADJACENT CIRCUITRY
SEE AA BELOW
• TEFLON
• ALUMINUM FAN HOUSING
• RULON "A" BEARINGS
• TEFLON IMPREGNATED FIBER GLASS
• SOLDER
• BRASS
• TINNED COPPER CLIP
• CONTAMINATION
• PHASE TO PHASE
• PHASE TO NEUTRAL
• PHASE TO GROUND THROUGH ADJACENT STRUCTURE
SEE AA BELOW
• TEFLON INSULATION
• TEFLON GROMMETS
• CONTAMINATION
SEE AA BELOW
• PHASE TO PHASE
• PHASE TO NEUTRAL
• PHASE TO GROUND
SHORTS CAN OCCUR AS A RESULT OF INSULATION BREAKDOWN
24-7
AA
INSULATING CAPABILITY VIOLATED
24-8
CHEMICAL DEGRADATION
24-9
SHELF LIFE
24-10
MECHANICAL DAMAGE
24-11
• IMPROPER INSULATION USED
• EXCESSIVE VOLTAGE APPLIED
• FAULTY MANUFACTURING PROCESS (LATENT)
EE
SEE PAGE 25
• INABILITY OF INSULATION TO WITHSTAND NORMAL STORAGE DUE TO AGE
• FAULTY MANUFACTURING PROCESS (LATENT)
• MISHANDLING DURING FABRICATION AND SUBSEQUENT ASSEMBLY
• VIBRATION DURING OPERATION AND TEST
• DAMAGED BY LOOSE OBJECTS, OR FAN IMPACT
• EXTRUSION DUE TO THERMAL STRESSES
• CLAMP STRESS
• FAULTY MANUFACTURING PROCESS (LATENT)
SHORT CIRCUIT REACTIONS
PAGE 24

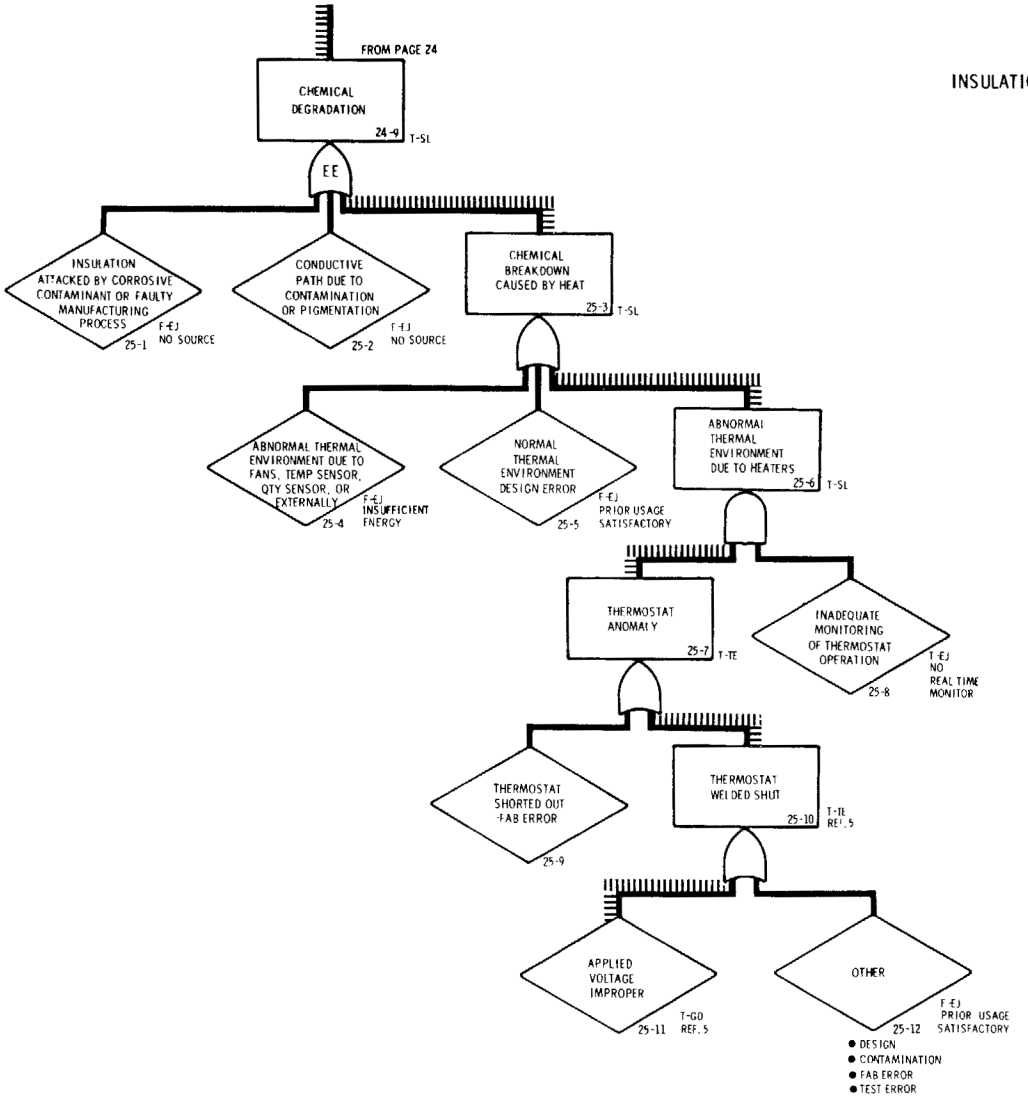

INSULATION
CHEMICAL DEGRADATION
PAGE 25

REFERENCES

1. Weber, Laurence A.: Thermodynamic and Related Properties of Oxygen from the Triple Point to 300° K at Pressures to 330 Atmospheres. Supplement A (British Units), NBS Report 9710A, August 29, 1968.

2. Stewart, Richard B.: The Thermodynamic Properties of Oxygen. PH.D. Thesis, Dept. of Mechanical Engineering, University of Iowa, June 1966.

3. Weber, Laurence A.: P-V-T, Thermodynamic and Related Properties of Oxygen from the Triple Point to 300 K at Pressures to 33 MN/m^2. Journal of Research of the National Bureau of Standards - A. Physics and Chemistry, Vol. 74A, No. 1, January-February 1970, pp. 93-129.